METAL ACETYLACETONATES AND THEIR PROPERTIES

By

EVRIM ARSLAN

A Dissertation submitted to the

Graduate School-Newark

Rutgers, The State University of New Jersey

In partial fulfillment of the requirements

for the degree of

Doctor of Philosophy

Graduate Program in Chemistry

written under the direction of

Professor Roger Lalancette

and approved by

_____

_____

_____

_____

Newark, New Jersey

October, 2019

ABSTRACT OF THE DISSERTATION

METAL ACETYLACETONATES AND THEIR PROPERTIES

By

Evrim Arslan

Dissertation Director: Professor Roger Lalancette

Metal acetylacetonates are significant since they were amongst the earliest metal compounds which were recognized as what later became known as coordination compounds. Additionally, they were significantly investigated during WWII as potentially useful in the separation of isotopes, especially of uranium because of their unexpected volatility. Consequently, much research was carried out over the years— a good deal of which was of suspect validity, which unfortunately cannot be checked because very little information was published on the syntheses and crystallization methods used in the preparation of the crystalline samples. Here, we report our efforts to clean the slate by reporting on those of Al(III), Mn(III), Co(III), Cr(III), Fe(III), V(III) and Ti(III). These studies were carried out with crystalline samples obtained from a wide variety of solvents and over the range 296-100K in attempts to reproduce, verify, and correct, at times, the claims made in print. Our results, covering over 100 samples, are detailed in this thesis. We have also made crystallographic measurements at temperatures other than 100K and 296K for crystals of $Al(acac)_3$ and $Mn(acac)_3$ guided by their thermochemical information using DSC and Cp measurements. The very small energy changes found by DSC and Cp measurements (of the order of 5-50 cal/mol)

cannot be associated with 1st-order transitions, nor even of rotational barriers. We believe that this is a case of librations brought about by the higher temperatures.

In addition, we have explored the interaction of $[(acac)_2V=O]$(acac = 2,4-pentanedione) with a series of nitrogenous ligands which were chosen because of their ability to attach themselves onto the sixth (axial) position of such bis-acetylacetonates and because they have the capability of linking pairs of $[(acac)_2V=O]$ molecules, thus creating magnetically-coupled substances whose coupling would be interesting to document by electron spin resonance as well as by magnetic susceptibility vs. T. The results are rather surprising in that unexpected chemical reactions occurred which had not been envisioned, nor have been previously observed in preceding studies.

Acknowledgements

First, I would like to express my sincere appreciation for my advisor and mentor, Dr. Roger Lalancette for his endless support and guidance. He has had a tremendous effect in my research and has given me the freedom to work on my project. Dr. Lalancette had a very important impact on my decision to pursue a Ph.D. in Chemistry. He was my undergraduate General Chemistry professor who made me love the subject. For his invaluable impact, I will forever be grateful. His love for teaching and research inspires me.

I would like to thank the rest of my thesis committee: Dr. Sergiu Gorun, Dr. John Sheridan, and Dr. Frieder Jaekle, for their encouragement, insightful help, and constructive comments about my thesis.

Additionally, I would like to thank Dr. Ivan Bernal for his insight, encouragement, and support throughout my graduate career. He was always present with his guidance whenever I needed it.

This work would not be possible without the numerous collaborations. I would like to thank Dr. Janusz Grebowicz from the University of Houston, Dr. Miroslaw Pluta from Centre of Molecular and Macromolecular Studies of Polish Academy of Sciences, and also Dr. Francesc Lloret from the University of Valencia in Spain. I would also like to thank Dr. Trevor Tyson of New Jersey Institute of Technology.

I would like to acknowledge undergraduates Monica Soliman and Salma Harfouche for their help towards this research.

I would like to thank my brothers for being wonderful, amazing, and supportive towards my goals. They have blessed me with endless support. I have dragged them to

school with me as my guards on weekends and late nights. Thanks for always being there for me. Thank you for believing in me and encouraging me.

I would also like to thank my parents for their endless love and support. I would never be able to do any of this without their love. I feel very blessed to have them as my parents. Their selfless love and support have always been my drive to strive any accomplishment in life. This thesis and Ph.D. is the product of their hard work just as much as it is mine. I appreciate everything they have done.

Lastly, I would like to thank my boyfriend Patrick De Bella Jr. for his love and encouragement. Thank you for believing in me and supporting me. I feel very lucky and blessed to have your love and presence in my life. I am happy and thankful that you are part of this experience. I am looking forward to many more life experiences with you.

Table of Contents

List of Figures

List of Schemes

List of Tables

Introduction

Metal tris-acetylacetonates

It has long been known that an atom, usually a metal, surrounded by six monoatomic species, can be *asymmetric*, like tetrahedral carbon is, under similar conditions. Such information has been known since the 19th century by the work of Pasteur. If a central atom is surrounded by six monodentate ligands such as A, B, C, D, E, F, *the central atom is said to be asymmetric*, because its mirror image cannot be superimposed on it. They do not match in the sense that not all atoms in the new image will fall on others of their kind. That such is the case is illustrated by the entity shown in Figure 1.

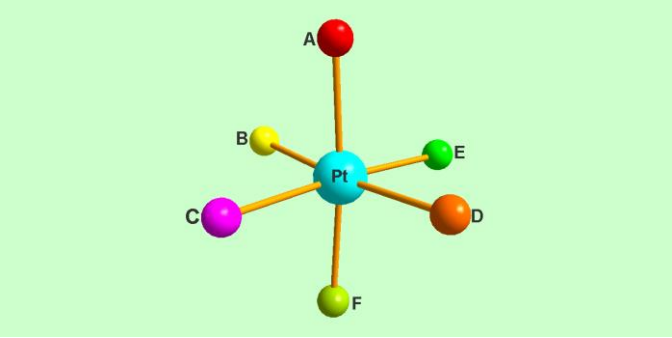

Fig. 1. Here, Pt is surrounded by species such as fluoride, chloride, bromide, hydroxide… The image derived by any mirror operation cannot be super-imposed on the original. The metal is, then, a chiral center, and will be capable of rotating the plane of polarized light.

If such a species were to be made by a non-stereospecific reaction, the resulting mixture would consist of isomers obtained by exchanging each of the ligands shown with

all the other ones. Then, A can be exchanged with the other five, B with the remaining four, etc…. So, the total would be 5 + 4 + 3 + 2 + 1 = 15 isomers, and the central atom (Pt in this case) would be a chiral center; therefore, each isomer would rotate the plane of polarized light. That is the most asymmetric species ever made, or so was claimed by a Russian chemist.[1] As of now, no one has repeated such a synthetic feat, and not even the authors claimed to have isolated all the components. However, the basic argument is correct and remains a major challenge in stereochemistry.

By contrast, a six-bonded metal atom (or ion) can be bonded in a similar manner, but by ligands able to provide two binding points; e, g. bidentate ligands. An example of such a species is acetylacetone – subject of the study in this thesis. In such species, the central atom is no longer an asymmetric center; yet, it still can be chiral. Such an entity is referred to as *dis*symmetric; and, referring to these, the terms Delta and Lambda are frequently used to identify the enantiomers we are discussing, as seen in Figure 2.

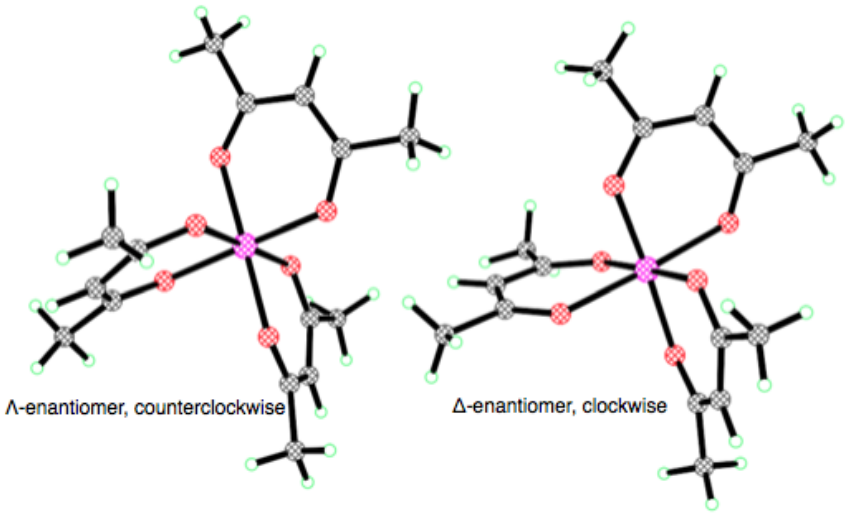

Fig. 2: Acetylacetone anion forms a 6-membered ring with Mn(III). Mn1, on the left, has stereochemistry of Λ while the other, on the right, is Δ. Pink atoms are Mn, red are O, gray are C, and green are H atoms.

Acetylacetone (2,4-pentanedione), $CH_3COCH_2COCH_3$, is a *β*-diketone that exists in an equilibrium mixture of tautomeric keto and enol forms. In pure acetylacetone, the diketo form is in equilibrium with the cyclic enol-like form (Scheme 3).

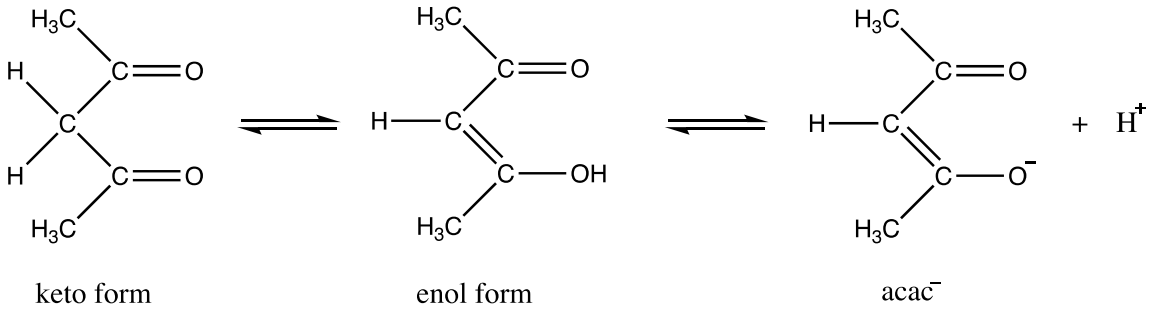

Scheme. 1: Keto and enol forms of acetylacetone.

In Scheme 2, the resonance forms of acac anion are shown.

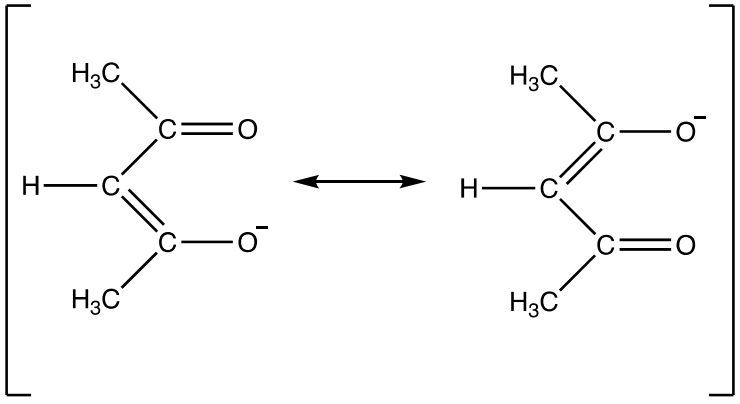

Scheme 2: Resonance forms of acac anion.

In basic solution, this organic compound is deprotonated to form the acac or acetylacetonate anion (Scheme 3).

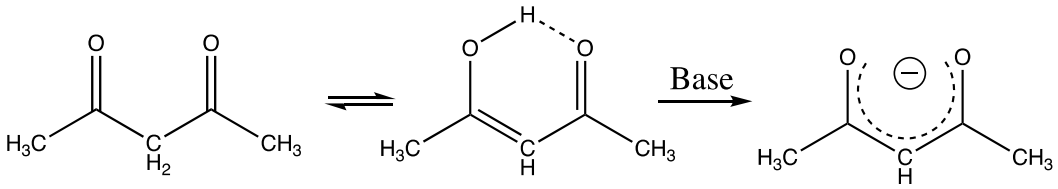

Scheme 3: Keto-enol tautomerism in acetylacetone and formation of the acetylacetonate anion.

The acac anion can act as a ligand towards metal ions, forming complexes in which the ligand is bonded to the metal through both oxygen atoms, forming a six membered ring (Scheme 4).

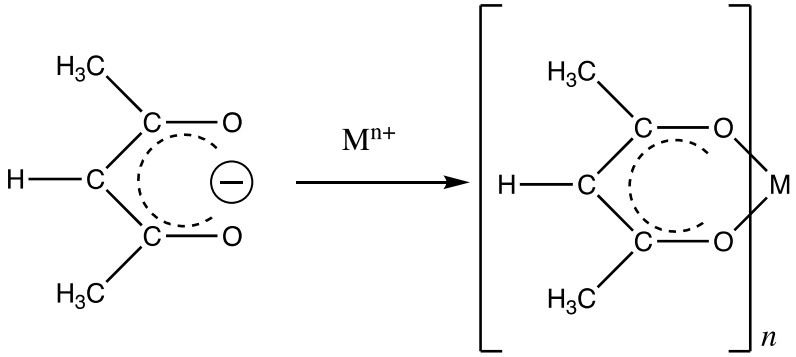

Scheme 4: Acetylacetone forms a 6-membered ring with the metal

Metal acetylacetonates were studied in the early days of coordination chemistry because of the ease of extraction of their natural complexes into organic solvents.[2] Additionally, they can be modified by substitution of the $–CH_3$ moiety on either end which affects the properties of the products, such as solubility and volatility. Because of the unexpected volatility of the actinide acetylacetonates, they were of high interest

during the Manhattan Project as potentially important in the purification of uranium.[2] They were supplanted by the discovery of the more volatile hexafluorides.[3] Because of this interest, many metal acetylacetonates were studied during World War II and during the Cold War, including their crystal structures.[3] Interestingly and probably because of classification of scientific data of importance to the military, the earliest structural description of an uranium acetylacetonate appearing in the Cambridge Structural Database (CSD) occurred in 1970 and it is from Scandinavia.[4,5] Acetylacetonates of other metals, and their X-ray structures, appeared over the years. Unfortunately, these studies were collected by film, various manual, semi-automated, and automated diffractometers which, at times gave poor results. Also, prior to 1990, almost all datasets were done at room temperature and were incomplete.

The CSD collection revealed that, prior to the late 1990's, the only space groups reported for these complexes were $P2_1/c$ and Pbca.[4] It also appeared that occurrence of one or the other of these space groups seemed to be associated with the solvent the crystals were obtained from. This issue was not very clear since reporting of such information was often omitted; and, when reported, it was rather brief, including omission of details of crystallization, such as whether the solvent was allowed to evaporate or the crystals were obtained by cooling of the solutions in a refrigerator. In the absence of such information, it was difficult to ascertain why there were, or were not, variations in the crystallization mode(s). In essence, the provenance of the crystals was not given.

The first reported studies of metal tris-acetylacetonates were on the Ga(III) and Sc(III) derivatives which appeared in 1926, reporting both of them as crystallizing in

space group $Pnm2_1$.[6] This is remarkable since it indicates that Astbury and Morgan clearly understood the concept of systematic absences in X-ray diffraction as early as 1926.[6] More likely, their crystals really belonged in space group Pbca given that, since then, no one has ever reported the appearance of crystals of any $M(acac)_3$ species in space group $Pnm2_1$; however, those two space groups share a large number of systematic absences, and the X-ray equipment then available must have been extremely primitive. We also note that Astbury was one the pioneers of X-ray diffraction and an early editor of the International Tables for X-Ray Crystallography. Interestingly, this apparently odd choice of metals was, no doubt, determined by the need to obtain information of those two relatively new metals. In 1871, Dmitri Mendeleyev predicted gallium to exist, and it was discovered in 1875. It is a liquid above 29.76ºC and, therefore, much of the work used in characterizing it was done with compounds thereof, this being one of them. As for scandium, it was discovered shortly after gallium, in 1879, after also being postulated to exist by Dmitri Mendeleyev, who named it ekaboron; and, by contrast, its melting point is 1541ºC. Both substances were, therefore, historically and scientifically interesting to characterize as much as possible at that time.

Consequently, much research was carried out over the years— a good deal of which was of suspect validity, which unfortunately cannot be checked because very little information was published on the syntheses and crystallization methods used in the preparation of the crystalline samples. In chapters 1 and 2, we report single X-ray crystal structures of metal tris-acetylacetonates of Al(III), Mn(III), Co(III), Cr(III), Fe(III), V(III) and Ti(III), and the thermochemical information specifically for Al(III) and Mn(III). These studies were carried out with crystalline samples obtained from a wide

variety of solvents and over the range 296-100 K in attempts to reproduce, verify, and correct, at times, the claims made in print.

We also wanted to synthesize and characterize adducts of vanadyl bis-acetylacetonate, seen in Figure 3, in which the sixth position around the metal is occupied by a good electron donor, with the *proviso* that such moiety could function as an electron donor to the metal center.

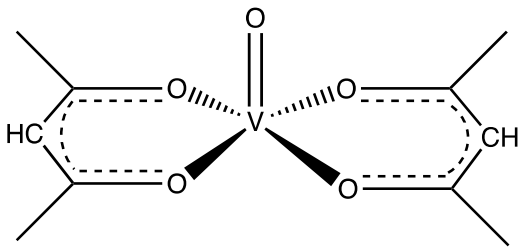

Fig. 3: Vanadyl bis-acetylacetonate

Thus, depending on the ligand, one could obtain mono-, di- and tri-metallic species, which could be magnetically coupled or not, depending on their composition and stereochemical properties. These results are outlined in Chapter 3.

The general goal of this research is to better understand crystal formation, structural differences, and its effect on the properties of its products in metal bis-acetylacetonates and tris-acetylacetonates. This will also help understand whether magnetic coupling occurs in these complexes or not.

Notes and References

1. (a) Essen, L.N.; Zakharova, F. A.; and Gel'man, A. D., *Zhur. Neorg. Khim.*,**1956**, *1*, 2475; (b) N. Essen, F. A. Zakharova and A. D. Gel'man, *Zhur. Neorg. Khim.,* **1958**, *3*, 2654.
2. Werner, A.; Vilmos, A. Z.; *Anorg Chem.,* **1899**, *21*, 145-158.
3. National Academy of Sciences, National Research Council. Nuclear Science Series, Document NAS-NS 3050, 360 pages. Issued in March of 1962. "*The Radiochemistry of Uranium"* gives a massive description of the preparation and solvent extraction of a multitude of acetylacetonates of uranium and related elements, as well as data on many derivatives of the transition elements. The document does not give any structural information, even though by that time some studies had been carried out; however, most of this material was classified during the WWII conflict and subsequent years of the Cold War.
4. CSD = Cambridge Crystallographic Structural Database CCSD, Cambridge Crystallographic Data Centre, 12 Union Road, Cambridge CB2 1EZ, UK, release 1.19 (2017). They can be contacted at http://www.ccdc.cam.ac.uk.
5. Titze, H., *Acta Chem Scand.* **1970**, *24*, 405-414. Interestingly, this entry has the following notation: "Brta C2/c". However, no further information was provided.
6. Astbury, W.T.; Morgan, G.T.; *Proc. R. Soc. London*, **1926**, Ser A, *112*, 448-467.

Chapter 1

Properties of Metal(III) Tris-Acetylacetonates

Introduction

Note: Our search of the literature runs through April 2016, as was present in CSD Version 1.18.

The older studies on metal acetylacetonates were carried out by researchers with different interests, backgrounds and facilities. Their results vary because some of the described structural data are collected by film, others by various manual and semi-automated diffractometers, and by completely automated diffractometers. Also, some of these data were collected over very limited ranges of 2θ, some with Cu radiation, others with Mo and Fe radiation. The following problems were seen in historical data published on metal acetylacetonates:

a) Mostly, they did not report the provenance of the crystal, given that the same compound was reported in differing space groups;
b) Both the synthetic methods used and the origin and the purity of the reagents were frequently omitted. This point is crucial since it is known that impurities can affect the crystallization behavior of tris-metal acetylacetonates;
c) The solvent used for crystal growth was not mentioned. We now know that the solvent, as well as the temperature of crystallization, can affect the outcome of the structure.[1,2]

Appendix B is an EXCEL file report of tris-acetylacetonates compiled from CSD.[3] It includes the space groups of these species depending on the M(III) cation used, and some of them exhibit solvent and thermal polymorphism information.[3] We studied the 3d trivalent metal complexes and also $Al(^{3+})$ by DSC (differential scanning calorimetry), TG (thermogravimetric analysis), mass spectrometry, and the single crystal X-ray diffraction in the temperature range 300-100K. Also, the temperature-dependent magnetic susceptibility of the complexes with unpaired electrons was examined to attempt to answer the following questions:

a) For a given metal, do the structures differ as the solvent is varied?
b) For a given metal and solvent, are the complexes thermally polymorphic?
c) If some are polymorphic, but others are not, what crystallographic and/or structural changes occur?
d) How many crystallographic phases exist between 100K and room temperature?
e) What are the structural details of those molecules in the different phases?
f) Is there a difference in crystalline behavior between transition metal compounds (V, Ti, Fe, Mn, Co, Cr, Fe) and the main group element Al(III)?
g) Is the crystalline behavior dependent on the electronic configuration of the transition metal cations? If so, how?
h) From the scant information available, depending on the metal, there seems to be a solvent of crystallization dependence on the crystalline phase obtained; can we verify this?
i) Finally, do crystals of a given compound, belonging to a space group by virtue of its crystallization solvent, interconvert thermally into the crystalline phase(s) of

that same substance obtained from other solvents? Below, we present the results of our investigations.

In the literature, there are several studies published of the behavior of mixed tris-acetylacetonates such as Al(III) + Co(III) and Cr(III) + Ga(III).[2,4] We never studied these types of structures because they constitute an entirely different problem which is extensive enough in scope as to be a major enterprise on its own. Here, we solely concentrate on pure metal complexes of tris-acetylacetonates and their crystalline behavior.

The first fully described structures of $M(acac)_3$ compounds began appearing in the literature during 1950s. These were: the Cr(III) derivative (ACACCR06) the aluminum(III) (ALACAC17), and the iron(III) (FEACAC04), all of which were published in 1956.[5,6]

At the end of 2015, there were 266 structural reports in CSD describing the structures of metal tris-acetylacetonates. We attempted, vainly, to systematize all of this information – a fact not surprising, given the information we have summarized in Appendix B.

The older structural data available in the literature had been collected mostly at room temperature, ca. 300 K. Therefore, no information was available on potential temperature-induced polymorphism. These studies showed that certain metal derivatives crystallized exclusively in $P2_1/c$ from certain solvents while others did so in Pbca, always with one molecule in the asymmetric unit.

Space groups $P2_1/c$ and Pbca have in common the following positions:

$P2_1/c$: x, y, z -x, -y, -z, -x, ½ + y, ½ - z x, ½ - y, ½ + z

Pbca has, in addition, the following four symmetry positions:

½+x, ½ - y, -z ½ - x, -y, ½ + z ½- x, ½ + y, z ½+x, y, ½ - z, which are related to the above by additional mirrors and simple translations of ½. For example, ½+x, ½ - y, -z is obtained from -x, -y, -z by a mirror normal to the **a**-axis, followed by a translation of ½ in **a** and ½ in **b**. Thus, the orthorhombic cell doubles in size compared to the monoclinic one.

It was, therefore, of interest to us to discover that there were some contradictory claims in the literature, namely: (1) a change in space group from the centrosymmetric Pbca to the Sohncke $P2_12_12_1$ in the case of $Fe(acac)_3$. This claim could be legitimate because $P2_12_12_1$ is a valid sub-group of Pbca, and phase transitions obtained by cooling normally result in lowering the symmetry of a crystalline lattice.

These claims were made in an entry of CSD labeled FEACAC02, which seemed fairly realistic in that they were from data collected with a diffractometer and the R-factor reported as 3.80%.[3,7] Unfortunately, none of the current tests for Sohncke space groups available today were used then. However, a very telling factor was evident from the position of the atoms in the published list; namely, that the "center of mass" of their asymmetric unit was located at 0.5790, 0.5000, 0.5000.[7] Given that, in order to fix the origin in space group $P2_12_12_1$, one has to arbitrarily select and fix one coordinate, **x** could be 0.5000 as well. That means that there is (possibly) an inversion center in the so-called $P2_12_12_1$ space group. Since this is unlikely, we believe that the space group for this complex is, indeed, Pbca.

There is, however, an interesting *caveat* here: this could be a case of a thermally-induced polymorphic transition of the type labeled kryptoracemic crystallization. Such a phenomenon was first described in 1995 and reviewed in 2015.[8,9] If this were the case here, it was not recognized by the authors since the existence of the phenomenon had not yet been published.[7] If this is what happened, the asymmetric unit recorded for FEACAC02 had to contain two enantiomerically-related molecules, and this is precisely the case, as shown in Figure 1.1.[7]

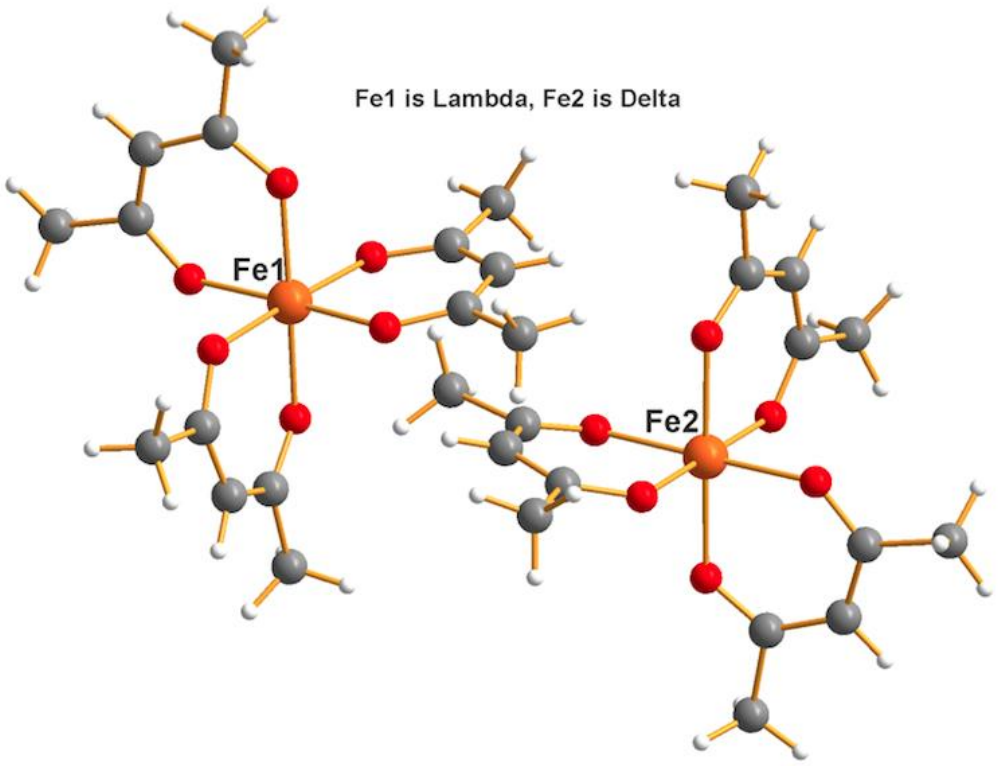

Fig. 1.1. Fe(1) appears on the left and Fe(2) on the right, in the pair shown. The former is Λ and the latter Δ, as required by the enantiomeric pairs expected in a kryptoracemic crystal.

The “center of mass” of the asymmetric unit is located at 0.5000, 0.5000, 0.5000. We tested experimentally whether this report is correct and the results are described below.

2) A second claim that challenged the status quo was that described in the case of $Mn(acac)_3$ which had been reported in the older literature as crystallizing in space group $P2_1/c$, with Z’ = 1.0 until 2005 and again in 2008, when it was claimed that new phases with space groups $P2_1$ and $P2_1/n$ were observed.[10,11] The synthesis and preparation of the crystals were well-documented in the case of ACACMN23; in the latter case, no crystallization information was provided at all.[10,11]

The results for ACACMN23 and ACACMN24 are in complete agreement with each other and report the space group at 293 K and 223 K, respectively, as being $P2_1$ with Z = 8 and Z’ = 4, implying that the space group remains constant throughout that thermal range.[10,11] The packing of the molecules within the crystal in the structure derived from ACACMN23, is shown in Figure 1.2 below.

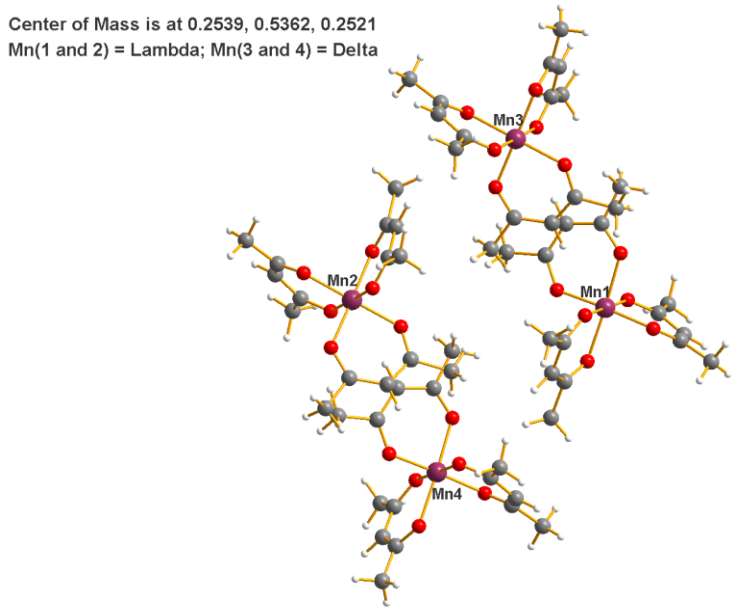

Fig. 1.2. There are four molecules in the asymmetric unit of ACACMN23 (shown above). They occur as two pairs of enantiomers such that Mn(1 & 2) are Λ, while Mn(3 & 4) are Δ. In this case, the center of mass for the pattern shown above is located at 0.2539, 0.5362, 0.2521. It is important to note that those numbers are derived from the refinement of the positions of atoms which were assumed to be independent of one another. Nonetheless, that center of mass is quite close to the special position ¼, ½, ¼, and the structure could also be a case of kryptoracemic crystallization, or incorrect space group assignment (the space group most probably is $P2_1/c$, with a center of symmetry between Mn1 & Mn2 as well as between Mn3 & Mn4). The reduced cell from ACACMN24 is the same as that of ACACMN23 (Niggli matrix) and, since the Flack parameter from ACACMN24 is 0.528(16), these two structures must be both centrosymmetric, as also implied by the center of mass of each pair. Despite many attempts in various solvents to reproduce this material, we were never able to get the space group to be $P2_1$.

The claims made for Fe(III) and Mn(III) in the above-cited references could very well be correct, except for the fact that an analysis of the Niggli matrix in the case of FEACAC02 reveals that the reported unit cell constants belong to crystals in space group Pbca, as was commonly reported previously.[7, 9-11] In the case of Mn(III), it seems that both are correct in the sense that the Niggli analysis indicates the space group is primitive and monoclinic, as claimed.[9-11] It was part of our studies to examine these claims in more detail.

Finally, in relatively more recent times, there were other poorly-documented, but interesting claims that Cr(III) (see ACACCR08) crystallizes in space group $P2_1/c$, as always published before, but with six molecules in the asymmetric unit ($Z' = 6$), instead of the normal one ($Z' = 1$), and the remark that there is a thermally-induced phase transition between 150 and 110 K.[12] The structure derived from this report is given in Figure 1.3.

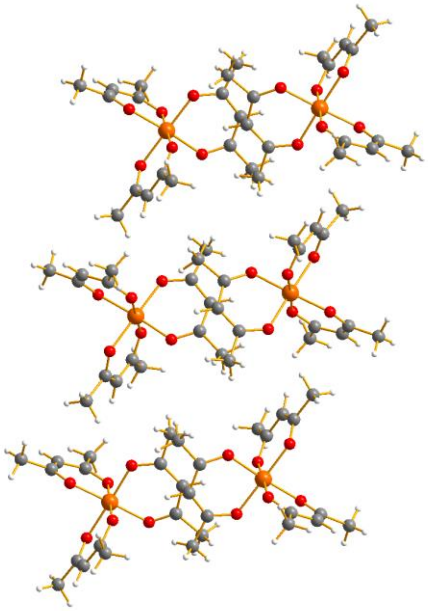

Fig. 1.3. The six molecules in the asymmetric unit (Z' = 6) described in ACACCR08. Each of the three horizontal rows consists of a pair of enantiomers. For example, the left one on the upper row is Δ, while the one on the right is Λ. The rows alternate throughout the entire lattice as a result of the two-fold screw axis. Thus, in the middle row, the left one is Λ while right one is Δ, and so forth. Therefore, the contents of each row consist of an enantiomeric pair, which is enantiomeric with the pair in the row above and/or below it, *at infinitum*. Consequently, the contents of row 3 are the same as those on row 1, etc. Finally, by translation(s), the asymmetric unit shown above can be extended, infinitely to the left and to the right, and above and below. The Niggli matrix obtained from the cell constants listed indicates the reported cell needs not be modified; however, we note that the cell depicted in Figure 1.4 is nothing but two times the identical cell one would get from a monoclinic cell with Z' = 1.0, including the inversion center between any adjacent pair of molecules as observed in Figure 1.3. An identical observation is true for the

molecules depicted in Figure 1.5, whose contents are simply three times that shown in Figure 1.3. Furthermore, we note that the value of the b-axis is identical, within a few standard deviations, in all three cells, implying that they merely constitute different slices from a common grid – a fact verified by their sharing identical reduced cells.

To our knowledge, the literature available in CSD though the release 1.18 of April 2016 has no additional surprises; therefore, we now report our findings on the syntheses and crystallization behavior as a function of solvent, using a common procedure for all our samples, as well as the thermal behavior of our crystals as studied by DSC, TGA, magnetic susceptibility, and X-ray diffraction studies, all as a function of temperature.

Results and Discussion

Description of the Structures

Below is a description of only one of the many structures for each individual metal for each solvent system investigated [see Appendix C for a complete list]. When the dataset at room temperature was a better overall structure than the one at 100K (only occasionally), that is the one being reported here. In all cases, for each different metal, the best structure was selected irrespective of solvent and/or temperature at which the dataset was taken for that particular complex. However, when the space group was different at different temperatures for a particular metal complex, then both of the structures are presented.

1. Aluminum Acetylacetonate From Acetone at 296K:

The description of the structure of the aluminum derivative appears in Figure 1.4.

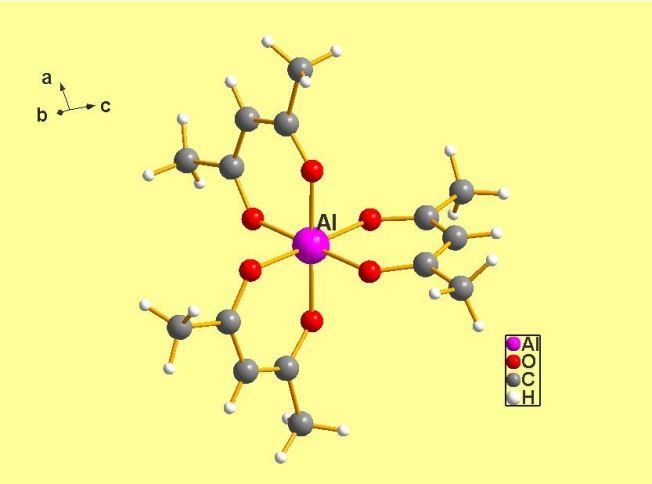

Fig. 1.4. $Al(acac)_3$

The space group in the case of $Al(acac)_3$ is invariant as far as solvent (12 different ones studied) and temperature: it is <u>always</u> $P2_1/c$. The absolute configuration of the complex as shown above is Λ; however, in $P2_1/c$, there exists also the racemic molecule Δ, across the center of symmetry. Also, all of the H atoms were found in electron-density difference maps and they are fully ordered. The average Al-O distance is 1.882(3) Å. The average O-Al-O angle is 90.88˚(7). All of the bonding parameters for this substance are available in the CIF file submitted to CSD [1484898]. This structure contrasts with many previously-published reports of various space groups ($P2_1/c$, Pnam, $Pna2_1$), as well as various numbers of molecules in the cell: Z = 4, 12, 16; and, a number of solid-state phase changes between 150K and 110 K (ALACAC18, ALALAC19, ALALAC10).[13-15] As far as these previous reports [See Appendix I], we have not found any examples in the 12 different solvents from which we have crystallized this complex, nor any effect due to

temperature variation, to corroborate their reports. Since we do not know the provenance of the crystals from previous reports (but we do know the provenance of all of our crystals), we believe that this is the definitive structure of this complex at least at 100K and room temperature.

As seen in Table 1, our studies show that no matter what solvent is used to crystallize the complex (polar aprotic through polar protic through non-polar), $Al(acac)_3$ always crystallizes in the space group $P2_1/c$. . The data in these previous reports are inconsistent with our findings.

Polar Aprotic	Acetone	$P2_1/c$, Z'=1
	Acetonitrile	$P2_1/c$, Z'=1
	Dimethyl formamide	$P2_1/c$, Z'=1
	Ethyl acetate	$P2_1/c$, Z'=1
	2,4-pentanedione	$P2_1/c$, Z'=1
Polar Protic	Ethanol	$P2_1/c$, Z'=1
	Methanol	$P2_1/c$, Z'=1
	Isopropanol	$P2_1/c$, Z'=1
	Water	$P2_1/c$, Z'=1
Non-Polar	Benzene	$P2_1/c$, Z'=1
	Cyclohexane	$P2_1/c$, Z'=1
	Diethyl ether	$P2_1/c$, Z'=1

Table 1: Summary of $Al(acac)_3$ crystallographic structures from polar aprotic, polar protic, and non-polar solvents.

2. Manganese Acetylacetonate:

2a. Manganese Acetylacetonate From Acetonitrile at 100K:

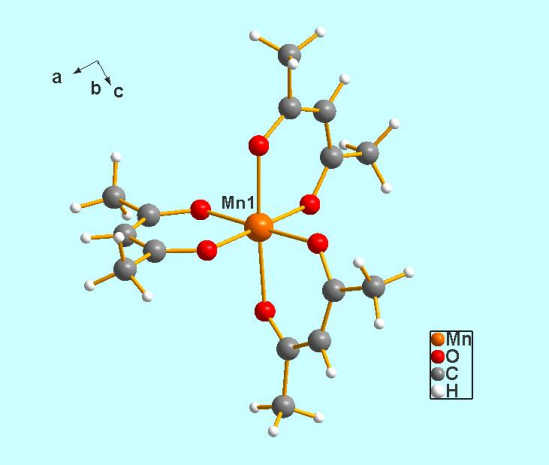

Fig. 1.5. $Mn(acac)_3$

The space group in the case of $Mn(acac)_3$ is Pbca from acetonitrile; it also is invariant as a function of temperature. The absolute configuration of the molecule as shown above is Δ. Also, all of the H atoms are fully ordered. The average Mn-O distance is 1.999(2) Å. However, it is clear from the structure that the Jahn-Teller effect is readily observable in this structure, given the fact that the axial distances are 2.127(1) and 2.152(1) Å, whereas the equatorial distances are 1.926(1), 1.9355(9), 1.926(1), and 1.9240(9) Å, with an average of 1.9287(19) Å.[16] The average O-Mn-O angle is 89.24(7)˚. A complete description of all the bonding parameters for this substance is available in the CIF file submitted to CSD [1484899].

2b. Manganese Acetylacetonate From Ethyl Acetate at 100K:

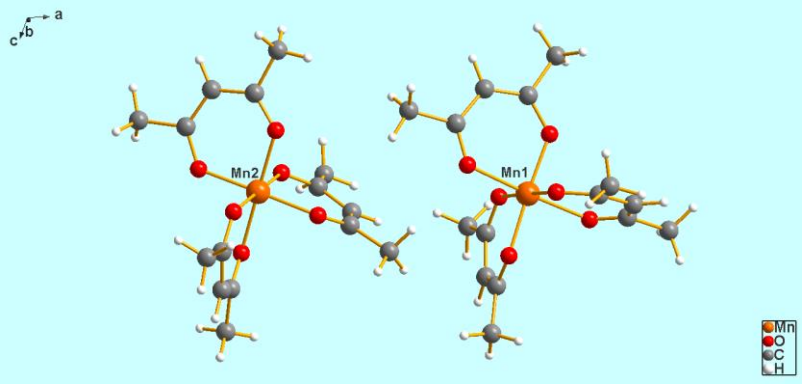

Fig. 1.6. $Mn(acac)_3$

Contrasting with the structure from acetonitrile presented above in Figure 1.5, the space group for $Mn(acac)_3$ from ethyl acetate at 100K is $P2_1/c$, with Z' = 2 (as shown in Figure 1.6 above); in this space group, Z = 8 in the cell. On the left, Mn2 is Λ while the one on the right, Mn1, is Δ. Also, all of the H atoms, including those of the terminal methyl groups, are fully ordered. For Mn1, the average Mn1-O distance is 1.999(3) Å. The average O-Mn1-O angle is 89.60(9)˚. For Mn2, the average Mn2-O distance is 1.996(3) Å, and the average O-Mn2-O angle is 89.40(9)˚. However, it is clear that the Jahn-Teller effect is observable in both molecules given the fact that the axial distances are 2.1122(12) and 2.1079(13) Å for Mn1 and 2.0706(14) and 2.0770(14) Å for Mn2, whereas the equatorial distances are 1.8981(12), 1.9660(13), 1.9305(13), and 1.9768(13) Å, with an average of 1.943(2) Å for Mn1. These same equatorial distances are 1.9207(12), 1.9929(14), 1.9293(13), and 1.9860(15) Å, with an average of 1.957(2) Å for Mn2. A complete description of all the bonding parameters for this substance is available in the CIF file submitted to CSD [1484900].

2c. Manganese Acetylacetonate From Ethyl Acetate at 296K:

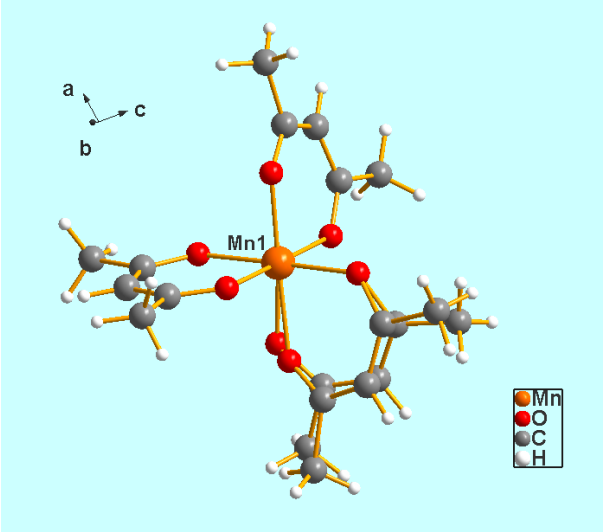

Fig. 1.7. $Mn(acac)_3$

At 296K, the space group for $Mn(acac)_3$ is invariant at $P2_1/c$ (like the one above at 100K, shown in Figure 1.6); however, Z = 4 and Z' = 1, and the molecule is partially disordered. As shown above, two of the rings are fully ordered, whereas the third one occupies two positions with ca. 50:50 distribution. Because of the presence of disorder, we feel that giving information for the entire molecule is not warranted. Inasmuch as the exact same disorder situation exists in all crystals obtained from all of the remaining solvents used in this study at RT (benzene/diethyl ether, MeOH, 2-propyl alcohol, acetone, acetonitrile) for $Mn(acac)_3$, we feel it is not necessary to show additional pictures of the remaining Mn derivatives. A complete description of all the bonding parameters for this substance is available in the relevant CIF file submitted to CSD [1484901].

Table 2 refers to the summary of $Mn(acac)_3$ structures from various solvents. Crystals from acetonitrile <u>always</u> give Pbca as the space group regardless of the temperature. <u>All</u> the other solvents always crystallize in the space group $P2_1/c$. At 100K,

Z'=2 while at RT it is always Z'=1. As mentioned above, there is also always disorder in one of the acetylacetone rings at RT for all the solvents except for acetonitrile.

Polar Aprotic	Acetone	$P2_1/c$
	Acetonitrile	Pbca, Z'=1
	Ethyl acetate	$P2_1/c$
Polar Protic	Methanol	$P2_1/c$
	Isopropanol	$P2_1/c$
Non-Polar	Benzene	$P2_1/c$

Table 2: Summary of $Mn(acac)_3$ crystallographic structures from polar aprotic, polar protic, and non-polar solvents.

3. Cobalt Acetylacetonate From Ethyl Acetate at 100K:

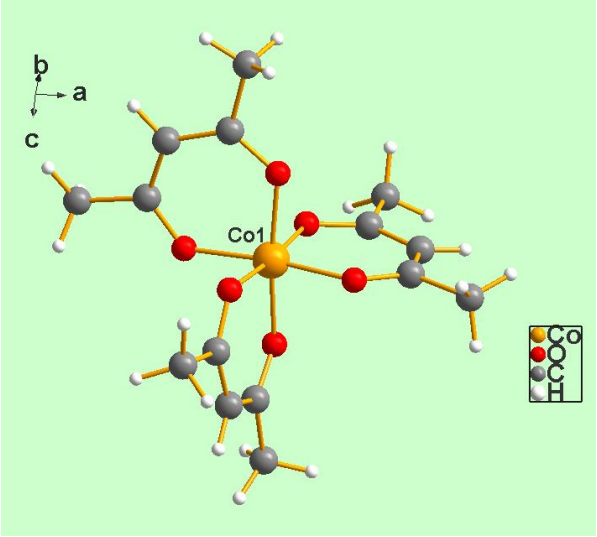

Fig. 1.8. $Co(acac)_3$

The space group in the case of $Co(acac)_3$ from ethyl acetate, as well as in crystals from all the other solvents studied (acetone, acetonitrile, hexane/benzene, MeOH, 2,4-pentanedione, 2-propyl alcohol, and water), at all temperatures, is $P2_1/c$. Table 3 summaries all of the structures crystallized from all the different solvents. The absolute configuration of cobalt shown in Figure 1.8 is Λ. Also, all of the H atoms are fully ordered. The average Co-O distance is 1.886(2)Å, and the average O-Co-O angle is 90.17(7)˚. In all eight solvents used (see Appendix C), the molecules are always ordered and the average value of all the geometrical parameters are very similar, as expected for a very stereochemically-rigid Co(III) cation. A complete description of all the bonding parameters for this substance is available in the CIF file submitted to CSD [1499759].

Polar Aprotic	Acetone	$P2_1/c$, Z'=1
	Acetonitrile	$P2_1/c$, Z'=1
	Ethyl acetate	$P2_1/c$, Z'=1
	2,4-pentanedione	$P2_1/c$, Z'=1
Polar Protic	Methanol	$P2_1/c$, Z'=1
	Isopropanol	$P2_1/c$, Z'=1
	Water	$P2_1/c$, Z'=1
Non-Polar	Hexane	$P2_1/c$, Z'=1

Table 3: Summary of $Co(acac)_3$ crystallographic structures from polar aprotic, polar protic, and non-polar solvents

4. Chromium Acetylacetonate from Acetone at 100K:

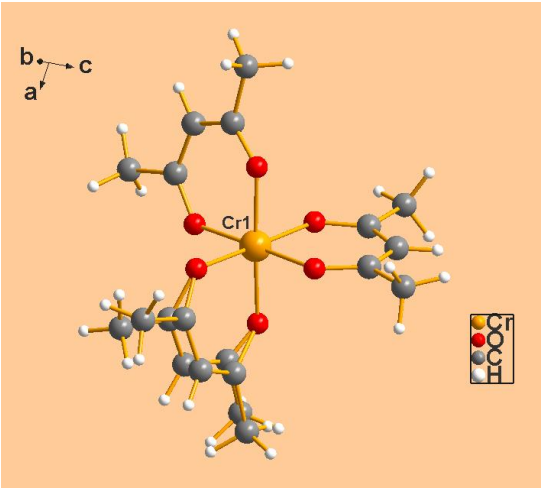

Fig. 1.9. $Cr(acac)_3$

The space group for $Cr(acac)_3$ is invariant as far as solvent and temperature for this metal: it is always $P2_1/c$. This is summarized in Table 4 which lists results of crystallographic structures from polar aprotic, polar protic, and non-polar solvents. As

shown above from acetone at 100K, two of the rings are fully ordered, whereas the third one occupies two positions with ca. 50:50 distribution. Because of the presence of disorder, we feel that giving information for the entire molecule is not warranted. Inasmuch as the exact same situation exists in crystals obtained from all the remaining solvents used in this study both at RT and at 100K (acetonitrile, cyclohexane, DMF, EtOH, ethyl acetate, heptane, hexane/benzene, 2-propyl alcohol, toluene, and water), we feel it is not necessary to show additional pictures of the remaining Cr derivatives. A complete description of all the bonding parameters for this substance is available in the relevant CIF file submitted to CSD [1484903].

Polar Aprotic	Acetone	$P2_1/c$, Z'=1
	Acetonitrile	$P2_1/c$, Z'=1
	Dimethyl formamide	$P2_1/c$, Z'=1
	Ethyl acetate	$P2_1/c$, Z'=1
Polar Protic	Ethanol	$P2_1/c$, Z'=1
	Isopropanol	$P2_1/c$, Z'=1
	Water	$P2_1/c$, Z'=1
Non-Polar	Cyclohexane	$P2_1/c$, Z'=1
	Heptane	$P2_1/c$, Z'=1
	Hexane	$P2_1/c$, Z'=1
	Toluene	$P2_1/c$, Z'=1

Table 4: Summary of $Cr(acac)_3$ crystallographic structures from polar aprotic, polar protic, and non-polar solvents.

5. Iron Acetylacetonate from Methanol at 100K:

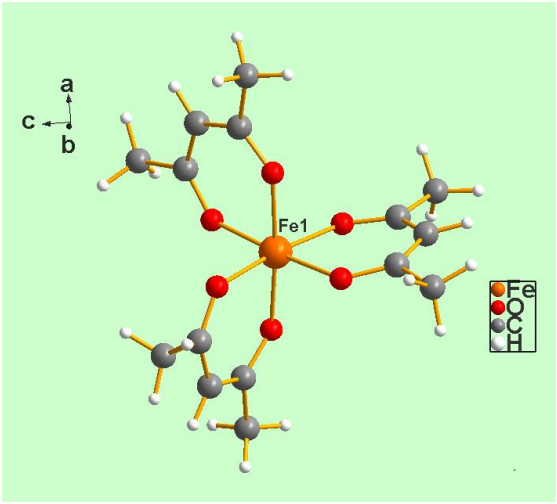

Fig. 1.10. $Fe(acac)_3$

As seen in Table 5, for $Fe(acac)_3$, the space group is always Pbca at all temperatures. This is invariant in all crystals studied from all the various solvents (MeOH, acetone, acetonitrile, benzene, DMF, diethyl ether, ethyl acetate, 2-propyl alcohol, and water). The absolute configuration of iron, as shown above, is Λ. All of the H atoms, including those of the terminal methyl groups, are fully ordered. The average Fe-O distance is 1.998(2) Å, and the average O-Fe-O angle is 90.07(9)˚. In all of the solvents studied, the molecules are always ordered and the average value of all the geometrical parameters are very similar, as expected for a stereochemically rigid Fe(III) cation. A complete description of all the bonding parameters for this substance is available in the CIF file submitted to CSD [1484904]. There was one previous study which gave the space group as $P2_12_1\ 2_1$ (see Appendix B). We believe this report to be in error.

Polar Aprotic	Acetone	Pbca, Z'=1
	Acetonitrile	Pbca, Z'=1
	Dimethyl formamide	Pbca, Z'=1
	Ethyl acetate	Pbca, Z'=1
Polar Protic	Methanol	Pbca, Z'=1
	Isopropanol	Pbca, Z'=1
	Water	Pbca, Z'=1
Non-Polar	Benzene	Pbca, Z'=1
	Diethyl ether	Pbca, Z'=1

Table 5: Summary of $Fe(acac)_3$ crystallographic structures from polar aprotic, polar protic, and non-polar solvents.

6. Vanadium Acetylacetonate:

6a. Vanadium Acetylacetonate from Methanol at 100K:

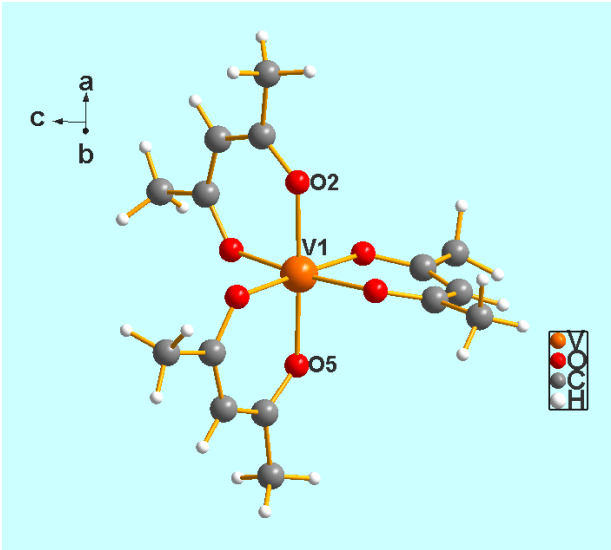

Fig. 1.11. $V(acac)_3$

The space group in this case is Pbca, with Z = 8, and Z' = 1. The absolute configuration of vanadium as shown is Λ. All of the H atoms, including those of the terminal methyl groups, are fully ordered. The average V-O distance is 1.987(2) Å, and the average O-V-O angle is 87.95(7)˚. The average V-O axial distance is 2.0076(13) Å while the average equatorial distance is 1.9764(19) Å [the difference being 0.021 Å while the V-O distance esds for all six bonds is 0.001 Å (see CIF file), implying that the difference is 21 times esd, which is acceptably above the significance level.] Thus, the Jahn-Teller effect is very clearly observed in this case, as expected. A complete description of all the bonding parameters for this substance is available in the CIF file submitted to CSD [1484905]. One other report at 150K [VAACAC15, see Appendix B] gives the space group as $P2_1/c$; we do not know the provenance of these crystals, and have never found this space group in our studies.

6b. Vanadium Acetylacetonate from THF at 100K:

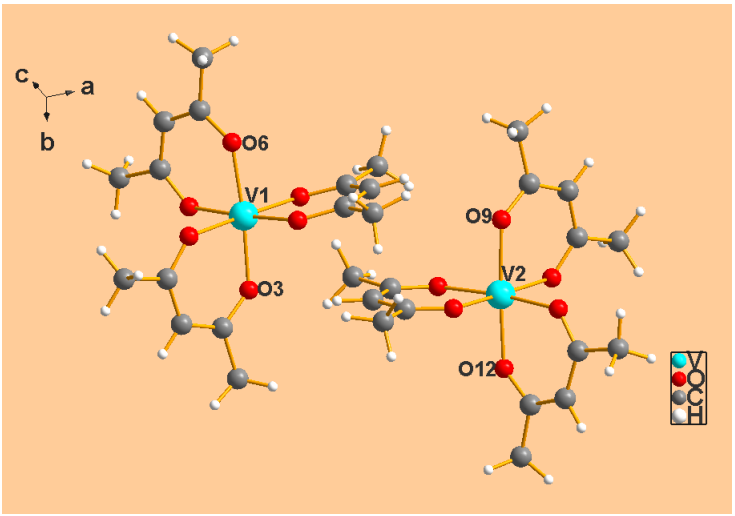

Fig. 1.12. $V(acac)_3$

The space group in this case is $P2_1/c$, but with Z = 8 and Z' = 2. The absolute configuration of V1 in this particular diagram is Λ while that of V2 is Δ. All of the H atoms are fully ordered. The average V1-O distance is 2.003(3) Å while the average V2-O distance is 2.002(3) Å. The average O-V1-O angle is 90.02(1)˚ and the average O-V2-O is 90.06(1)˚. The average V1-O axial distance is 2.000(3) Å while the average equatorial distance is 2.005(2)Å (the difference being -0.005 Å, implying that there is a negative Jahn-Teller effect (i.e., an equatorial expansion) at a significant level since the standard deviation for all six V1-O bonds is 0.002 Å. The average V2-O axial distance is 2.005(2) Å while the average equatorial distance is 2.001(3)Å [the difference being 0.004 Å], the result being significant inasmuch as standard deviation for all six V2-O distances is 0.002 Å (see CIF file) implying that the difference is 2 times esd which is "acceptable."] Thus, the Jahn-Teller effect is observed in this case, as expected. A complete description of all the bonding parameters for this substance is available in the CIF file submitted to CSD [1484906].

6c. Vanadium Acetylacetonate from THF at 296K:

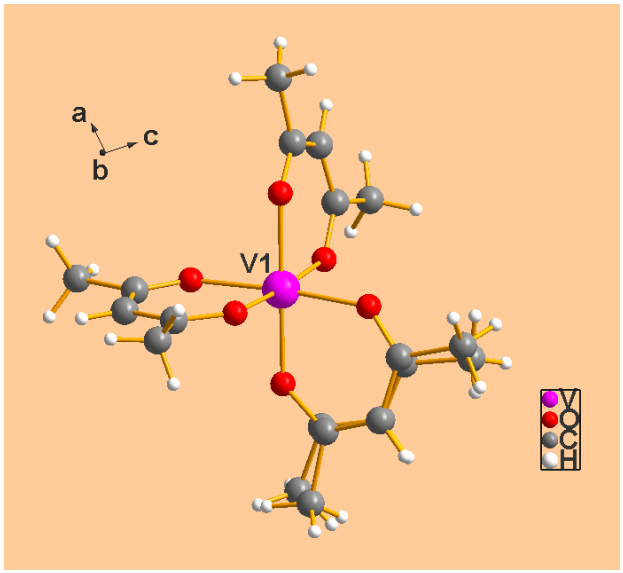

Fig. 1.13. $V(acac)_3$

The space group in this case is also $P2_1/c$, but with Z = 4 and Z' = 1. As shown in this figure, in this solvent, at 296K, two of the acac rings are fully ordered whereas the third one occupies two positions with ca. 53:47 distribution. Because of the presence of disorder, we feel that giving information for the entire molecule is not warranted. Inasmuch as the exact same situation exists in all of the crystals for this complex obtained from other solvents (methyl alcohol, toluene, see Appendix C), we feel that it is not necessary to show additional pictures of the remaining V derivatives. A complete description of all the bonding parameters for this substance is available in the relevant CIF file submitted to CSD [1484907].

Table 6 shows the overall results for $V(acac)_3$. The space group for $V(acac)_3$ from methanol at 100K is Pbca, with Z = 8, and Z' = 1. However, from THF at 100K, the

space group changes to $P2_1/c$ with Z = 8 and Z' = 2. $V(acac)_3$ from THF at room temperature has space group $P2_1/c$ with Z = 4 and Z' = 1. Two of the rings are fully ordered whereas the third one occupies two positions with 53:47(2)% distribution. Crystals from toluene always give $P2_1/c$ with Z = 4 and Z' = 1 as the space group regardless of the temperature. Also, one of the acetylacetone rings has disorder at both RT and 100K.

Polar Aprotic	Tetrahydrofuran	$P2_1/c$
Polar Protic	Methanol	Pbca, Z'=1
Non-Polar	Toluene	$P2_1/c$, Z'=1

Table 6: Summary of $V(acac)_3$ crystallographic structures from polar aprotic, polar protic, and non-polar solvents.

7. Titanium Acetylacetonate:

7a. Titanium Acetylacetonate from Dichloromethane at 100K:

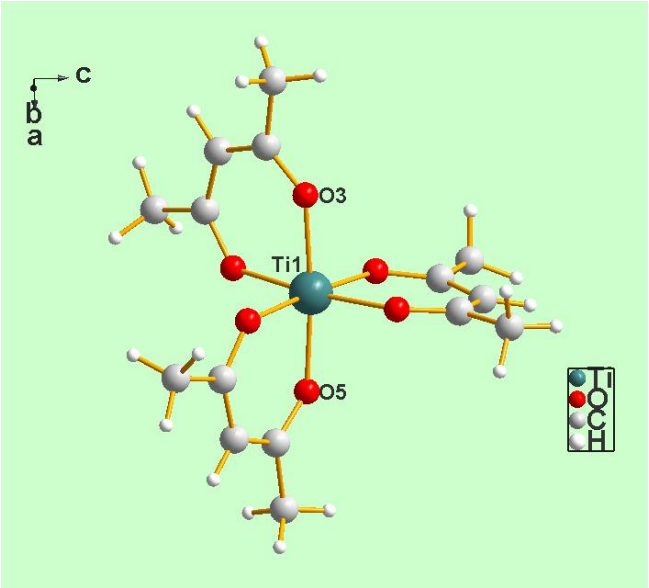

Fig. 1.14. $Ti(acac)_3$

The space group in this case is Pbca. The absolute configuration of the titanium in this particular figure (Figure 1.14) is Λ, as shown above. Also, all of the H atoms, including those of the terminal methyl groups, are fully ordered. The average Ti-O distance is 2.013(2) Å. The average O-Ti-O angle is 90.09(7)˚. The average Ti-O axial distance is 2.010(2) Å while the average equatorial distance is 2.0198(15) Å [the difference being 0.004 Å while the Ti-O distance esds for all six bonds is 0.001 Å (see CIF file), implying that the difference is 4 times esd, which is acceptable above the significance level. Thus, the Jahn-Teller effect is also observed in this case, as expected,

although small. A complete description of all the bonding parameters for this substance is available in the CIF file submitted to CSD [1484908].

7b. Titanium Acetylacetonate from 2,4-Pentanedione at 100K:

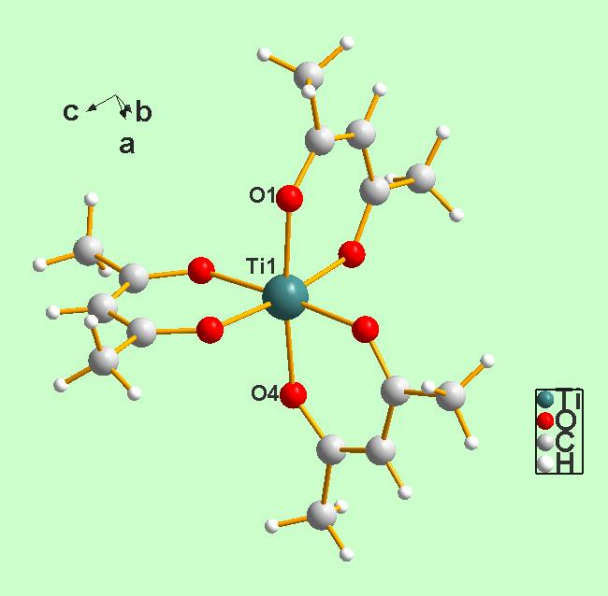

Fig. 1.15. $Ti(acac)_3$

The space group in this case is $P2_1/n$. The absolute configuration of titanium, as shown, is Δ. All of the H atoms, including those of the terminal methyl groups, are fully ordered. The average Ti-O distance for all is 2.018(2) Å. The average O-Ti-O angle is 90.10(7)˚. The average Ti-O axial distance is 2.0265(15) Å while the average equatorial distance is 2.013(2) Å [the difference being 0.010 Å while the Ti-O distance esds for all six bonds is 0.001 Å (see CIF file), implying that the difference is 10 times esd.] Thus, the Jahn-Teller effect is clearly observed in this case, also as expected. A complete

description of all the bonding parameters for this substance is available in the CIF file submitted to CSD [1484909].

Titanium tris-acetylacetonate from dichloromethane has the space group Pbca with Z = 8, and Z' = 1, regardless of temperature. Crystals from 2,4-pentanedione at 100K and at 296K always crystallize in space group $P2_1/n$ with Z = 4, and Z' = 1. In addition, crystals from toluene always crystallize in space group $P2_1/n$ with Z = 4, and Z' = 1, regardless of temperature.

Polar Aprotic	2,4-pentanedione	$P2_1/n$, Z'=1
Non-Polar	Toluene	$P2_1/c$, Z'=1
	Dichloromethane	Pbca, Z'=1

Table 7: Summary of $Ti(acac)_3$ crystallographic structures from polar aprotic, polar protic, and non-polar solvents.

Jahn-Teller Effect in $M(acac)_3$

The physical and chemical properties of metals depend on the distribution of the electrons within the five *d*-orbitals of the metal ion. In the presence of ligands ($acac^-$ in this case), the *d* orbitals are split into groups of different energies. The extent of splitting depends on the nature of the ligands. Both magnetic properties and electronic spectra reflect the splitting of *d* orbitals. Below is Figure 1.16, describing the splitting of the *d* orbitals in an octahedral crystal field.[17]

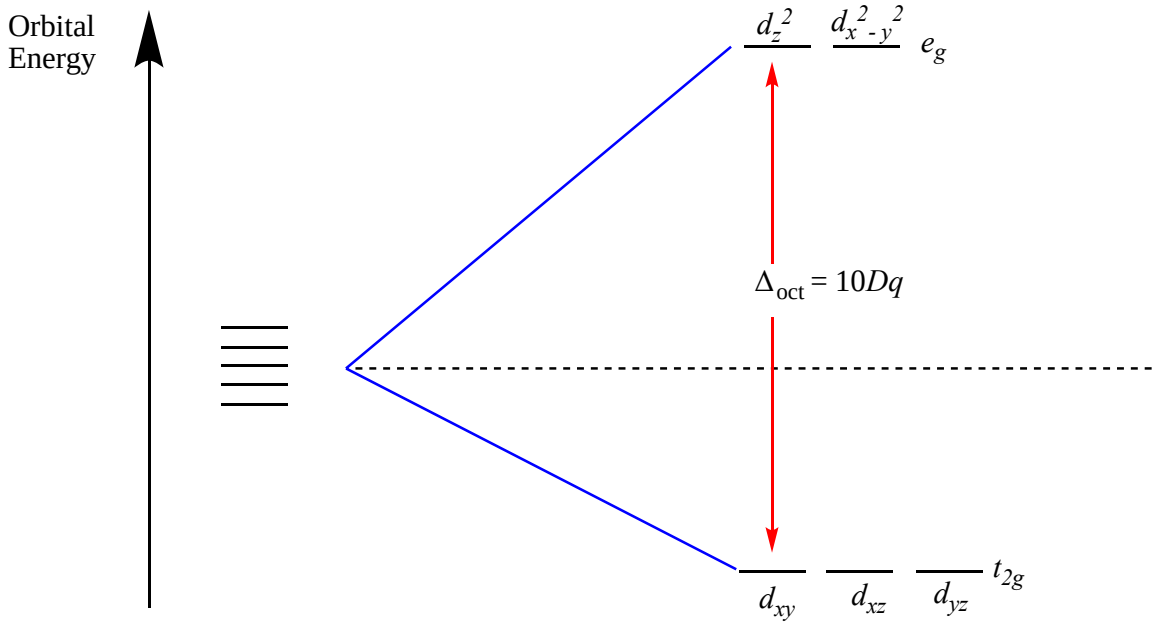

Fig. 1.16: Splitting of the *d* orbitals in an octahedral crystal field, with the energy changes measured with respect to baricenter, the energy level shown by the hashed line.

The observed tetragonal distortion of an octahedral complex is accompanied by a change in symmetry (O_h to D_{4h}) and a splitting of the e_g and t_{2g} sets of orbitals. Elongation of the complex is accompanied by stabilization of each *d* orbital that has a *z* component, while the d_{xy} and $d_{x^2-y^2}$ orbitals are destabilized.

For octahedral complexes of d^4, d^5, and d^6 configurations, there are two possible ways that electrons can be placed in the *d*-orbitals, as seen in Figures 17 through Figure 22 below. If more energy is required to pair up two electrons than to move up one to the unoccupied e_g orbital, the electrons each occupy one individual orbital which leads to a 'high-spin' electronic configuration. On the other hand, if more energy is required to

move an electron to an e_g orbital than to pair it up in a t_{2g} orbital, then the electrons will be in the t_{2g} orbital resulting in the 'low-spin' electronic configuration.

Octahedral complexes of d^9 and high spin d^4 [$Mn(acac)_3$ in our study] ions are often distorted so that two metal ligand bonds (axial) are different lengths from the remaining four (equatorial). For a high-spin d^4 ion, one of the e_g orbitals contains one electron while the other is vacant. If the singly occupied orbital is the d_z^2, most of the electron density in this orbital will be concentrated between the cation and the two ligands on the *z* axis. Thus, there will be greater electrostatic repulsion associated with these ligands than with the other four and the complex suffers elongation along the z axis. Conversely, occupation of the $d_{x^2-y^2}$ orbital will lead to elongation along the *x* and *y* axes. This is caused by the Jahn-Teller effect. The Jahn Teller theorem states that any non-linear molecular system in a degenerate electronic state will be unstable and will undergo distortion to form a system of lower symmetry and lower energy, therefore, removing the degeneracy.

$Ti(acac)_3$

The Ti^{3+} ion has one unpaired electron. It is located in one of the d_{xy}, d_{xz}, d_{yz} orbital as shown below. It shows the Jahn-Teller effect in the excited state, $t_{2g}^0\ e_g^1$. Single occupancy of the e_g level results in a lowering of the degeneracy, although the resultant energy separation between the two orbitals is small. This corresponds to our results that show very small Jahn-Teller distortion and small ground state in $Ti(acac)_3$.

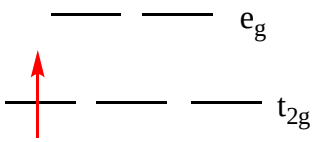

Fig. 1.17: Electronic configuration for the Ti^{3+} ion

V(acac)$_3$

The V^{3+} ion has two unpaired electrons. They are located in the two degerate d_{xy}, d_{xz}, or d_{yz} orbitals as shown below. Since the t_{2g} orbital is unevenly occupied, there is a weak Jahn-Teller distortion seen in V(acac)$_3$, which is consistent with our results. or

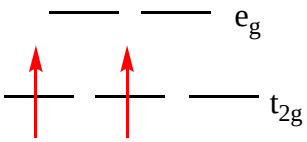

Fig. 1.18: Electronic configuration for the V^{3+} ion

Cr(acac)$_3$

The Cr^{3+} ion has three unpaired electrons located in the d_{xy}, d_{xz}, d_{yz} orbitals as shown in Figure 1.19. Here, there is no Jahn-Teller effect observed since all the t_{2g} orbitals are evenly filled.

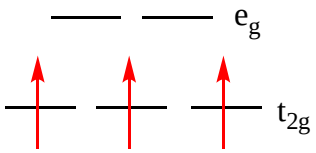

Fig. 1.19: Electronic configuration for the Cr^{3+} ion

Mn(acac)$_3$

The Mn^{3+} ion has four unpaired electron which show two possible electron configurations: high-spin (left) and low-spin (right), as shown below in Figure 1.20. Both the high-spin complex and the low-spin complex have unpaired electrons and, therefore, they are paramagnetic.

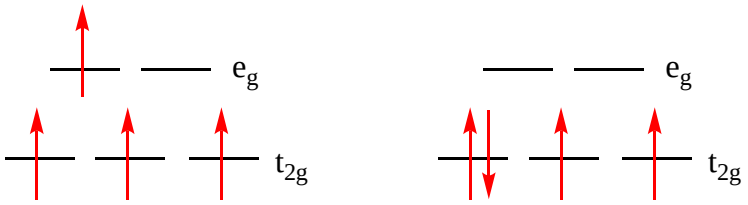

Fig. 1.20: High spin (left) and low spin (right) electronic configurations for the Mn^{3+} ion.

High spin Mn(acac)$_3$ has a ^5E_g ground state which has an imbalance in the filling of the electrons in orbitals that point directly at ligands as follows:

$$(t_{2g})^3 (d_{x^2-y^2})^1 (d_{z^2})^0 \text{ or } (t_{2g})^3 (d_{x^2-y^2})^0 (d_{z^2})^1$$

This results in significant distortion from the ideal octahedral symmetry. Either elongating or shortening two trans-related positions, relative to the four remaining equal positions in a plane, will form the distortions. This is in agreement with our results which show elongation of the two ligands for Mn(acac)$_3$ as it is the only complex with a degenerate occupancy in the e_g set; hence, the strongest Jahn-Teller effect has been seen.

Fe(acac)$_3$

The Fe^{3+} ion has five unpaired electrons which show two possible electron configurations, high-spin (left) and low-spin (right) as shown in Figure 1.21. Both the high-spin complex and the low-spin complex have unpaired electrons and therefore, are paramagnetic. Since the $acac^-$ is a π-donor ligand, the high-spin complex is preferred over the low-spin complex. Specifically, the energy required to pair electrons in the t_{2g} orbitals is larger. Any anionic oxygen donor will not be enough to overcome the energy needed to generate low-spin Fe(III) complexes. Since all the t_{2g} and e_g orbitals are evenly filled, we do not see the Jahn-Teller effect here.

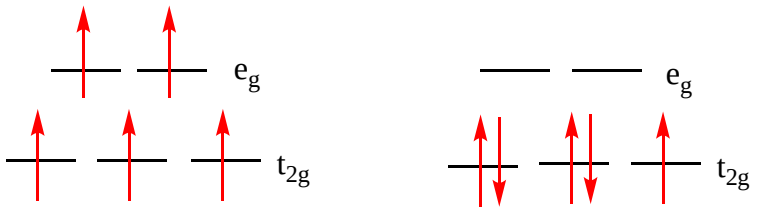

Fig. 1.21: High-spin (left) and low-spin (right) electronic configurations for the Fe^{3+} ion.

Co(acac)$_3$

The Co^{3+} ion has six unpaired electrons which show two possible electron configurations, high-spin (left) and low-spin (right) as shown in Figure 1.22. The high-spin complex has four unpaired electrons and is paramagnetic. The low-spin complex has no unpaired electrons, and is diamagnetic. Hence, the cobalt complex prefers a low-spin configuration.

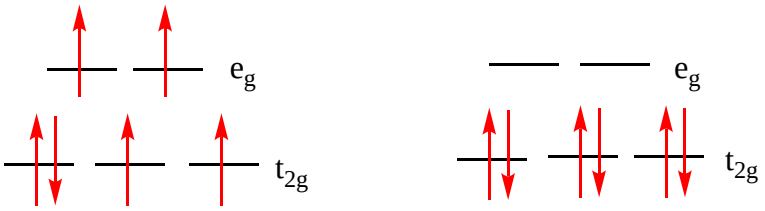

Fig. 1.22: High-spin (left) and low-spin (right) electronic configurations for the Co^{3+} ion.

Since all the t_{2g} orbitals for the low-spin complex are evenly filled, we do not see a Jahn Teller distortion or elongation for $Co(acac)_3$.

Conclusions

Tris acetylacetonates of Al(III), Mn(III), Co(III), Cr(III), Fe(III), V(III), and Ti(III) were crystallized in as many as twelve different solvents (for the Al complex), and the resulting crystals were analyzed by DSC, TGA, magnetic susceptibility, and single-crystal X-ray diffraction. In the case of the X-ray studies, this amounted to the determination of the space group and cell constants of hundreds of crystals, and then the determination of the structure of hundreds of these. Once a crystal structure was determined both at RT and at 100 K for an individual solvent system, if additional crystals gave the same space group and cell constants for that same solvent, the latter data were recorded, but no additional X-ray data were collected.

Our results indicate that many of the older published data [see Appendix B] were correct in space group, cell constants, and general description of the molecular structure. However, whereas the older data were almost always only determined at RT, and always with very limited data sets, our data were always determined at both RT and 100K, and

always with a full sphere of data, using CuKα radiation [compare Appendix C (our new data) to Appendix B (the original data)].

By studying the various metal(III) complexes crystallized from different solvents, we have concluded that for $Al(acac)_3$, $Co(acac)_3$, $Cr(acac)_3$, and $Fe(acac)_3$ regardless of what solvent is used, the space group does not change, Table 8.

		$Al(acac)_3$	$Mn(acac)_3$	$Co(acac)_3$	$Cr(acac)_3$	$Fe(acac)_3$	$V(acac)_3$	$Ti(acac)_3$
Polar Aprotic	Acetone	P21/c, Z'=1	P21/c*	P21/c, Z'=1	P21/c, Z'=1	Pbca, Z'=1		
	Acetonitrile	P21/c, Z'=1	Pbca, Z'=1	P21/c, Z'=1	P21/c, Z'=1	Pbca, Z'=1		
	Dimethylformamide	P21/c, Z'=1			P21/c, Z'=1	Pbca, Z'=1		
	Ethylacetate	P21/c, Z'=1	P21/c*	P21/c, Z'=1	P21/c, Z'=1	Pbca, Z'=1		
	2,4-pentanedione	P21/c, Z'=1		P21/c, Z'=1				P21/n, Z'=1
	Tetrahydrofuran						P21/c*	
Polar Protic	Ethanol	P21/c, Z'=1			P21/c, Z'=1			
	Methanol	P21/c, Z'=1	P21/c*	P21/c, Z'=1		Pbca, Z'=1	Pbca, Z'=1	
	Isopropanol	P21/c, Z'=1	P21/c*	P21/c, Z'=1	P21/c, Z'=1	Pbca, Z'=1		
	Water	P21/c, Z'=1		P21/c, Z'=1	P21/c, Z'=1	Pbca, Z'=1		
Non-Polar	Benzene	P21/c, Z'=1	P21/c*			Pbca, Z'=1		
	Cyclohexane	P21/c, Z'=1			P21/c, Z'=1			
	Diethylether	P21/c, Z'=1				Pbca, Z'=1		
	Heptane				P21/c, Z'=1			
	Hexane			P21/c, Z'=1	P21/c, Z'=1			
	Toluene				P21/c, Z'=1		P21/c, Z'=1	P21/c, Z'=1
	Dicholoromethane							Pbca, Z'=1

Table 8. Summary of different solvents used for the $M(acac)_3$. Red indicates disorder in one of the acac rings. *The number of molecules in the asymmetric unit (Z' above) for all of the Mn complexes (except for the one from acetonitrile) and for the V complex from THF changes as a function of temperature.

For $Mn(acac)_3$, the space group changes only for acetonitrile. Also, there is always disorder in one of the acac rings at room temperature, except for acetonitrile. $V(acac)_3$ gives a different space group for methanol (polar protic) than it does for the

polar aprotic or non-polar solvents. On the other hand, $Ti(acac)_3$ gives a different space group for every type of solvent the crystals are grown from. The reason why different results are seen for Mn(III), Ti(III), and V(III) tris-acetylacetonates could be associated with the Jahn-Teller effect. Of all the metals studied here, these three are the only ones that show the Jahn-Teller effect. Tables 9-11 show the axial and equatorial distances of the Jahn-Teller effect seen in Mn(III), V(III), and Ti(III), but it excludes information for structures with disorder in one of the acac rings.

$Mn(acac)_3$		Axial Distance Average	Equatorial Distance Average
Acetone 100K	Mn1	2.106(±3)	1.944(±4)
	Mn2	2.065(±3)	1.961(±4)
Acetonitrile 296K	Mn1	2.026(±3)	1.972(±4)
	–	–	–
Acetonitrile 100K	Mn1	2.1393(±14)	1.9287(±19)
	–	–	–
Ethyl Acetate 100K	Mn1	2.1101(±18)	1.943(±3)
	Mn2	2.074(±2)	1.957(±3)
Methanol 100K	Mn1	2.106(±3)	1.942(±4)
	Mn2	2.066(±3)	1.961(±4)
Isopropanol 100K	Mn1	2.108(±2)	1.942(±3)
	Mn2	2.070(±2)	1.958(±3)
Benzene:Diethyl ether (1:1) 100K	Mn1	2.108(±2)	1.942(±3)
	Mn2	2.074(±2)	1.957(±3)

Table 9. The axial and equatorial distances of the Jahn-Teller effect of Mn(III). The table does not include those structures with disorder in one of the rings.

$V(acac)_3$		Axial Distance Average	Equatorial Distance Average
Methanol 100K	V1	2.0076(±13)	1.9764(±19)
	–	–	–
Methanol 296K	V1	2.008(±3)	1.976(±4)
	–	–	–
Tetrahydrofuran 100K	V1	2.012(±2)	1.999(±3)
	V2	2.009(±2)	1.998(±3)

Table 10. The axial and equatorial distances of the Jahn-Teller effect of V(III). The table does not include those structures with disorder in one of the rings.

$Ti(acac)_3$		Axial Distance Average	Equatorial Distance Average
Dichloromethane 100K	Ti1	2.0198(±15)	2.010(±2)
	–	–	–
Dichloromethane 296K	Ti1	2.016(±2)	2.005(±3)
	–	–	–
2,4-Pentanedione 100K	Ti1	2.0265(±15)	2.013(±2)
	–	–	–
2,4-Pentanedione 296K	Ti1	2.0240(±17)	2.013(±2)
	–	–	–
Toluene 100K	Ti1	2.021(±2)	2.004(±4)
	–	–	–
Toluene 296K	Ti1	2.017(±3)	2.008(±5)
	–	–	–

Table 11. The axial and equatorial distances of the Jahn-Teller effect of Ti(III). The table does not include those structures with disorder in one of the rings.

We found that there were (a) phase changes caused by changes of solvent(s) [see Appendix C, specifically $Mn(acac)_3$], (b) there were thermally-induced phase transitions as well [see Appendix C, specifically, $Mn(acac)_3$ & $V(acac)_3$]. More important, though, is the fact that we were unable to verify the existence of some of the phase transitions described in some of the previous work (i.e., ALACAC20, ALACAC21, ALACAC22, ALACAC23, ALACAC24, ACACMN22, ACACMN23, ACACCR07, and ACACCR08), even in the case of those in which we crystallized our samples from the same solvent as specified in the published reports. This was possible only in a few cases inasmuch as the majority of the data available was rarely explicit concerning the provenance of their crystals.

In a few cases, we are certain that the samples said to be new polymorphic forms are incorrect since the space groups reported are incorrect by the following information: (a) the Niggli matrix of the reported reduced cell(s) belong to higher symmetry space groups (such as we found) and (b) the center of mass of the contents of the asymmetric unit of those reported in Sohncke space groups correspond precisely at special positions such as 0,0,0, ¼, ¼, ½, etc., clearly indicating that the space group was incorrectly described as belonging in the Sohncke class.

Finally, we have seen evidence that the crystals of Ti(III), V(III) and Mn(III) display the expected Jahn-Teller distortions of those having an electronic degenerate ground state. This is clearer in some cases than in others, as presented above in Tables 9-11. That, no doubt, is the result of the quality of the crystal used because the effect is

rather subtle and small, in terms of differences in bond lengths (in some instances) and is also dependent on the magnitude of the esd's. However, it was observed at the level of 21 esds in one case and 10 esds in another. Thus, we feel vindicated in saying that we recorded the Jahn-Teller effect in the appropriate cases.

Experimental

1. Synthetic Procedures

Note: Full details of the data reported herein are given in the attached Excel file [Appendix C]. In that document, we give the following information: name of the compound, solvent from which crystals were obtained for X-ray diffraction and DSC measurements, temperature for X-ray measurements, cell dimensions, volume, Z and Z', space group, R-factor, the known CCDC numbers and some comments; therefore, those details are omitted below.

1.1 The syntheses of $M(acac)_3$:

The metal acetylacetonates were either purchased or synthesized (see below). The synthesized metal acetylacetonates (Al, Co, Cr & Fe) were prepared according to the procedures in "Inorganic Experiments", Chap. 3.1, by C. Glidewell, p. 109-123 without any modifications.[18] However, the titanium(III) complex was prepared in-house in a glove box (see procedure below). The $V(III)(acac)_3$ and $Mn(acac)_3$ complexes were purchased from Alfa Aesar.

1.1a. Aluminum Acetylacetonate: Al(III)(acac)$_3$:

To prepare the ammonia acetylacetone solution: pipet 3mL of acetylacetone (Alfa Aesar) into a 100mL flask. Add 40mL of distilled water to this, followed by 7mL of 6M of ammonia solution (NH_4OH). Into a 250mL beaker, weigh out 3 grams of aluminum sulfate [$Al_2(SO_4)_3$]•$16H_2O$] (Fisher Scientific) and dissolve in 30mL of cold distilled water with stirring. To this last solution, slowly add the ammoniated acetylacetone solution. Check the pH using blue litmus paper to make sure it is neutral to litmus. If not, add more of the ammonia acetylacetone solution until it is neutral. Let the neutral solution sit for at least 20 minutes. A very light yellow product forms. Filter this product, and rinse it with 100mL of cold distilled water. Dry this product under vacuum.

For this study, we used crystals of the aluminum compound grown from acetone, acetonitrile, benzene, cyclohexane, dimethyl formamide (DMF), ethyl alcohol (EtOH), ethyl acetate, diethyl ether, methyl alcohol (MeOH), 2,4-pentanedione, 2-propyl alcohol, and water.

The reaction equation for this experiment is as follows:

$Al_2(SO_4)_3$•$16H_2O + 6CH_3COCH_2COCH_3 + 6NH_4OH \rightarrow 2Al(CH_3COCHCOCH_3)_3 + 3(NH_4)_2SO_4 + 22H_2O$

1.1b. Manganese Acetylacetonate: Mn(III)(acac)$_3$:

This complex was purchased from Alfa Aesar and was dissolved and crystallized from acetone, acetonitrile, benzene/diethyl ether (1:1 v/v), ethyl acetate, MeOH, and 2-propyl alcohol.

1.1c. Cobalt Acetylacetonate: Co(III)(acac)$_3$:

Weigh 2.5g of cobalt carbonate (Fisher Scientific) into a 250mL beaker. Add 20mL of acetylacetone (Alfa Aesar). Heat this solution to 90°C. Slowly add 30mL of 10% hydrogen peroxide over 30 minutes. Between each addition of hydrogen peroxide, cover the beaker with a watch glass. After the H_2O_2 addition is complete, leave the solution stirring for another 15 minutes. A dark green crystalline product precipitates. After it cools to room temperature, place the beaker in ice water bath for at least 30 minutes. Filter this product on glass-frit filter, and let this product dry in the filter funnel.

For this study, we used crystals of the compound grown from acetone, acetonitrile, ethyl acetate, hexane/benzene (10:1 v/v), MeOH, 2,4-pentanedione, 2-propyl alcohol, and water.

$2\ CoCO_3 + H_2O_2 + 6\ CH_3COCH_2COCH_3 \rightarrow 2\ CO_2 + 4\ H_2O + 2\ Co(CH_3COCHCOCH_3)_3$

1.1d. Chromium Acetylacetonate: Cr(III)(acac)$_3$:

Weigh 1.4g of chromium chloride [$CrCl_3 \cdot 6H_2O$] (Fisher Scientific) into a 250mL beaker. Dissolve this in 50mL of distilled water with stirring. Weigh out 10g of urea and

add to the solution in small portions. To this dark green solution, add 3mL of acetylacetone (Alfa Aesar). Cover with a watch glass. Bring the temperature up to 80°C and heat it for 1.5 hours. Deep maroon crystals will form. Cool and filter the product.

Acetone, acetonitrile, cyclohexane, DMF, EtOH, ethyl acetate, heptane, hexane/benzene (1:1 v/v), 2-propyl alcohol, toluene, and water were the solvents used to crystallize this complex.

$CrCl_3 \cdot 6H_2O + 3CH_3COCH_2COCH_3 + H_2O + CH_4N_2O \rightarrow CO_2 + HCl +$

$Cr(CH_3COCHCOCH_3)_3 + 2NH_4Cl + 6H_2O$

1.1e. Iron Acetylacetonate: Fe(III)(acac)$_3$:

Weigh 3.3g of iron chloride [$FeCl_3 \cdot 6H_2O$] (Fisher Scientific) into a 250mL beaker. Dissolve this in 25mL of distilled water with stirring. In a separate 50mL beaker, add 4mL of acetylacetone and 10mL of methanol. Add this to the iron chloride solution over a period of 15 minutes. A red solution forms. To this, add a solution of 5.1g of sodium acetate in 15mL of distilled water. Bring the temperature up to 80°C and heat it for 15 minutes. A red crystalline product will precipitate. After it cools to room temperature, place the beaker in an ice water bath for at least 10 minutes. Filter this product on a glass-frit filter, and rinse it with 100mL of cold distilled water. Let the product dry under vacuum.

The iron complex was crystallized from acetone, acetonitrile, benzene, DMF, diethyl ether, ethyl acetate, MeOH, 2-propyl alcohol, and water.

$FeCl_3 \cdot 6H_2O + 3CH_3COCH_2COCH_3 + 3CH_3COONa \rightarrow Fe(CH_3COCHCOCH_3)_3 + 3CH_3COOH + 6H_2O + 3NaCl$

1.1f. Vanadium Acetylacetonate: V(III)(acac)$_3$:

This complex was purchased from Alfa Aesar and was dissolved and crystallized (all inside a glove box), from dry MeOH, dry tetrahydrofuran (THF), and dry toluene.

1.1g. Titanium Acetylacetonate: Ti(III)(acac)$_3$:

In a dry box, 82mL of $TiCl_3$, 20% w/w in 2N HCl (purchased from Fisher Scientific), and 50mL of acetylacetonate were placed in a 200 mL glass bomb. To this solution, ammonium carbonate was added to destroy the HCl (until effervescence stopped). After sealing the reaction vessel, it was heated to 80°C for 1 hour, whereupon a dark blue crystalline product precipitated, which was dissolved and crystallized from dry dichloromethane (DCM), dry 2,4-pentanedione, and dry toluene.

$TiCl_3 / HCl + 3CH_3COCH_2COCH_3 + (NH_4)_2CO_3 \rightarrow Ti(CH_3COCHCOCH_3)_3 + 2NH_4Cl + CO_2(g) + H_2O$

2. Crystallization Procedures

The crystals used in this study were prepared as follows: 0.30 grams of each compound were dissolved in 25mL of a specific solvent (various) and placed in a sealed glass bomb, which was then placed in a silicone oil bath for one hour at 80°C, with magnetic stirring. After it cooled back to room temperature, the mixture was filtered

through a fine glass-frit filter and divided into a number of 20-mL vials, which were covered with Parafilm through which a number of small holes were pierced; these vials were left to evaporate at room temperature until crystals appeared. The V(III)$(acac)_3$ and Ti(III) $(acac)_3$ [light- and/or air- sensitive] were each dissolved in various "dry" solvents in a glove-box, placed in a glass bomb, sealed, heated and cooled as above, then allowed to evaporate in vials in the glove box. The crystals of each compound were examined under a microscope in order to establish whether or not morphological differences appeared, which oftentimes are indicative of polymorphism, as suggested by previously published information. We have never observed such an occurrence.

3. DSC Studies, TGA and Magnetic Susceptibility Studies

On the basis of DSC (differential scanning calorimetry) and TGA (thermogravimetric analyses), carried out in the same instrument, measured from room temperature down to -150 ^{o}C, we have found no evidence of thermally-induced transitions, at least for the following metals: Al(III), Mn(III), Co(III), Cr(III), Fe(III), V(III) and Ti(III), irrespective of the solvent from whence our crystals came. Those studies were carried out in collaboration with Professor J. Grebowicz of the University of Houston; and, because the samples were derived from crystallizations in many different solvents, and with different metals, they constitute a massive study which must be reported in detail elsewhere. If any of the readers of this report wish to have detailed information on any, or all, of these studies, we are willing to provide answers to specific questions addressed to us. Since it is literally impossible to tell the nature of those

species mentioned above (as reported by others), and how they were obtained (their provenance), we can only rely on our own observations.

In some of the previously-reported thermal phase transitions, the starting material was reported as having the same space group and reduced cell dimensions as ours, at room temperature. Nonetheless, we have not been able to observe their reported phase transition(s) upon lowering the temperature(s). Efforts to obtain additional information from the authors of those reports have either (a) not been answered or (b) we received a reply to the effect that such a long time has elapsed that they cannot reconstruct the events of the past.

As for the magnetic susceptibility measurements of the Mn(III), Cr(III), Fe(III), V(III) and Ti(III) compounds, they are under study and analysis at the laboratory of Professor Fransesc Lloret of the University of Valencia. Again, this is also a massive study carried out to 4K, and which examines all polymorphic forms we obtained (as described above). In summary, they behave, as expected, as isolated paramagnetic species with small antiferromagnetic components observed at the lower temperatures; and, in the case of the Mn(III) derivative, a small impurity of a Mn(II) species was detected by both the susceptibility measurements and by solid-state esr spectroscopy. We, therefore, recrystallized many times freshly-prepared material and removed whatever impurity was present (the same applies to the thermal studies described above). This study is, once more, a very large enterprise, which must be published separately, especially since, as above, the reports will be addressing the specialists in those fields.

4. X-Ray Diffraction Studies

Single Crystal X-ray Analyses. A suitable crystal of each compound was mounted on a Bruker-AXS SMART APEX II CCD diffractometer at 100(1)K. The cell dimensions and intensities were all collected with CuKα radiation (λ = 1.54178 Å). Data processing, Lorentz-polarization, and face-indexed numerical absorption corrections were performed using SAINT, APEX, and SADABS computer programs.[19-21] The structures were solved by direct methods and refined by full-matrix least-squares methods on F^2, using the SHELXTL V6.14 program package.[22,23] All non-hydrogen atoms were refined anisotropically. All H atoms were found in electron-density difference maps, and then allowed to ride on their respective C atoms. The methyl H atoms were placed in ideally staggered positions with C---H distances of 0.98 *Å* and $U_{iso}(H) = 1.5U_{eq}(C)$. The methine H atoms were placed in geometrically-idealized positions and constrained to ride on their parent C atoms with C---H distance 0.95 *Å* and $U_{iso}(H) = 1.2U_{eq}(C)$. For all structures, the numbers in parentheses are the errors in the least significant digit (see REFCODES for each individual structure as shown in Appendix C). Each crystal was allowed to warm up to room temperature (or a new one mounted), and the cell dimensions and a new dataset were collected to verify that the material was invariant at the different temperatures.

X-ray crystallographic files in CIF format have been deposited with the Cambridge Structural Database and their numbers are associated with each individual compound (See Appendix C). These materials can be obtained, free of charge, on

application to CCDC, 12 Union Road, Cambridge CB2 1EZ, UK. (fax: +44 1223 336033 or e-mail: deposit@ccdc.cam.ac.uk).

References

1. Von Dreele, R.B.; Fay, R.C., *J Am Chem Soc*, **1971**, *93*, 4936-4938.
2. Kannan Raghavan, M.; Jaiswal, P.; Sundaram, N.; Shivashankar, S.A., *Polyhedron*, **2014**, *70*, 188-193.
3. CSD = Cambridge Crystallographic Structural Database CCSD, Cambridge Crystallographic Data Centre, 12 Union Road, Cambridge CB2 1EZ, UK, release 1.19 (2017). They can be contacted at http://www.ccdc.cam.ac.uk.
4. Astbury, W.T.; Morgan, G.T., *Proc. R. Soc. London*, **1926**, Ser A, *112*, 448-467.
5. Shugam, E.A.; Shkolnikova, L.M., *Kristallografiya (Russ.)(Crystallogr Rep)*, **1956**, *1*, 478-82.
6. Roof, R.B., *Acta Crystallogr*, **1956**, *9*, 781-786.
7. Kabak, M.; Elmali, A.; Ozbey, S.; Atakol, O.; Kenar, A., *Z Kristallogr*, **1996**, 211, 831-832.
8. Bernal, I., *American Crystallographic Association Annual Meeting*, 23–28 July 1995, **1995**, Montreal, Quebec, Canada. Abstract 4a.1.e.
9. Bernal, I.; Watkins, S.F., *Acta Crystallogr*, **2015**, *C71*, 216-221.
10. Geremia, S.; Demitri, N., *J Chem Educ*, **2005**, 82, 460-465.
11. Frohlich, R.; Milan, R.; Yadava, S., *Private Communication to CSD*, **2008**.
12. von Chrzanowski, L.S.; Lutz, M.; Spek, A.L., *Acta Crystallogr*, **2007**, *C63***,** 377-382.
13. Shkol'nikova, L. M, *Kristallografiya*, **1959**, *4*, 419-410.
14. von Chrzanowski, L.S.; Lutz, M.; Spek, A.L., *Acta Crystallogr*, **2006**, *E62*, 3318-3320.
15. McClelland, B.R., *Acta Crystallogr*, **1975**, *B31*, 2496-2498.
16. Teller, J. H., *Stability of Polyatomic Molecules in Degenerate Electronic States. I. Orbital Degeneracy*, *P R Soc A*, **1937**, *161*, 905, 220–235. Bibcode:1937RSPSA.161.220J.doi:10.1098/rspa.1937.0142
17. Housecroft, C.; Sharpe, A., "Inorganic Chemistry", Third Edition, Pearson Education Limited, **2008**, Chapter 21, 637-685
18. Glidewell, C., in "*Inorganic Experiments*", Edited by J. Derek Woollins, 3rd Revised Edition, Wiley-VCH Verlag GmbH & Co., KGaA, **2010**, Chap. 3.2, 109-123.
19. Bruker, *SAINT*, **2009**, Version 7.23a. Bruker AXS Inc., Madison, Wisconsin, USA.
20. Bruker, *APEX 2*, **2009**, Version 2.0-2. Bruker AXS Inc., Madison, Wisconsin, USA.
21. Sheldrick, G.M., *SHELXTL, Acta Crystallogr*, **2008**, A-64, 112-122.
22. Sheldrick, G.M., *SHELXT, Acta Crystallogr*, **2015**, A71, 3-8.
23. Sheldrick, G.M., *SHELXL2014, Acta Crystallogr*, **2015**, C71, 3-8.

Chapter 2

The Thermochemistry and Crystallography of $Al(acac)_3$ and $Mn(acac)_3$

Introduction

We were interested in whether both Al(III) and Mn(III) exhibited polymorphism and were interested in the thermochemistry and crystallography of these substances. If Al(III) and Mn(III) exhibit polymorphism, is it induced by (a) changes in solvent of crystallization, (b) changes in temperature of the crystalline samples derived from various solvents, and (c) if any phase changes were observed by changing solvents, did they interconvert by temperature changes?

In Chapter 1 of this thesis, crystals of Al(III) and Mn(III) were mounted on the X-ray diffractometer in a cryo-nitrogen stream set for 100K, and complete spheres of data collected. Then, the temperature was slowly allowed to rise to 296K and a new sphere of data collected. However, no measurements were made at temperatures in between. In this chapter, we have made crystallographic measurements at temperatures other than 100 and 296K, guided by thermochemical information provided by three separate institutions, using samples from the same batches used in the crystallographic studies. DSC measurements were carried out in laboratories in the University of Houston-Downtown and at the Centre of Molecular and Macromolecular Studies (CBMM), Polish Academy of Science, Lodz. Calorimetric measurements were carried out, as well, at New Jersey Institute of Technology on the Mn(III) sample.

Historical data on $M(acac)_3$ gave disparate sets of reports which described structural data collected by film, various manual, semi-automated, and fully-automated

diffractometers using different radiation wavelengths (absorption and fluorescence problems), etc. Also, the older structural data available in the literature for the $M(acac)_3$ compounds were limited exclusively to room temperature; and it was not until the late 1990s that lower temperature information began appearing; thus, with respect to thermally-induced phase transitions, the older results are of no importance.

And, most frustrating about the historical data is that:

a) Mostly, they did not report the provenance of the crystal, given that the same compound was reported in differing space groups.

b) Both the synthetic methods used and the origin and the purity of the reagents were frequently omitted. This point is crucial since it is known that impurities can affect the crystallization behavior of the tris-metal acetylacetonates.[1]

c) The solvent used for crystal growth was not mentioned. We now know that the solvent, as well as the temperature of crystallization, can affect the outcome of the structure.[1-3]

As mentioned in Chapter 1, a scan of the Cambridge Crystallographic Database (CSD) collection revealed that, prior to the late 1990's, the only space groups reported for M(acac)3 were $P2_1/c$ (or its variants) and Pbca.[4] It also appeared that occurrence of one or the other seemed to be associated with changes in the solvent that the crystals were obtained from, since those inconsistent claims were from studies performed at the same temperature (see below example). The reporting of crystal growth information was often omitted completely, irrespective of the length of the paper. In the absence of such information, it was difficult to ascertain why there were, or were not, variations in the

crystallization mode(s) reported. Good examples of such confusion are the two reports appearing in CSD as ALACAC19 and ALACAC24.[4-6] These studies were carried out, at the same temperature, 110K, by the same authors a number of years apart; however, there is no information on the former as to the provenance of the crystal, which is described as "colorless, block cut from needle and polymorph gamma". The latter is described as "crystallized from ethyl acetate, colorless, hexagonal prism, polymorph delta." Moreover, the former is described as crystallizing in the orthorhombic space group $Pna2_1$, while the latter was assigned to the monoclinic space group $P2_1/c$. Hence, changes in space group were reported by the same group, for the same temperature, with minimal information on the provenance of the crystal.

Some of the structures reporting questionable results may be due to incorrect assignment of space groups resulting in erroneous claims of polymorphism. A fine example of that is the $P2_12_12_1$ assignment to a "polymorph" of $Fe(acac)_3$ in FEACAC02.[7] The Niggli matrix for the reported cell indicates that, indeed, it is primitive orthorhombic; but PLATON's examination of CheckCIF indicates with 100% certainty that (a) there is an inversion center in the reported data, and (b) that it contains a, b, and c glide planes.[8] Thus, the space group for that dataset is truly Pbca, as we have reported in our previous work and publication.[3]

When we began this project, it was our belief that the phase transitions associated with the claims in CSD for metal(III)$(acac)_3$ were of the order of multi-Kcal·mole^{-1}.[4] For example, that is the magnitude of the enthalpy change that occurs with a change of space

group in IKERUL, [Co(tren)cis(N_3)$_2$] I.[9] The magnitude of the enthalpy change reported in this paper is of the order of kJ/mole.[9] There, the space group changed from P2$_1$/n at 293K to P21 at 120K and is a reversible (no hysteresis) first-order transition. In the process, the cell constants changed from: a = 7.3779(7), b = 11.5028(9), c = 16.4145(13) Å, β = 90.930(7)^o to a = 7.2891(5), b = 11.5321(11), c = 16.1555(8) Å, β = 91.727(6)^o, which kept the volume nearly constant; but this complex had a number of solid-state phase transitions (three of them) which had large values of ΔH in the kJ mol-1 range. Therefore, we assumed that the phase transitions for our acetylacetonates would also be in the kJ/mole range.

Unfortunately, this turned out to be massively incorrect. Therefore, it is not surprising that our initial DSC measurements appeared to show absolutely no phase transitions, which is what we reported in our previous publication.[3] In the early study, the DSC instrument was set for detection of changes in the kJ mol^{-1} range, and the results are shown in Figure 2.1 below.

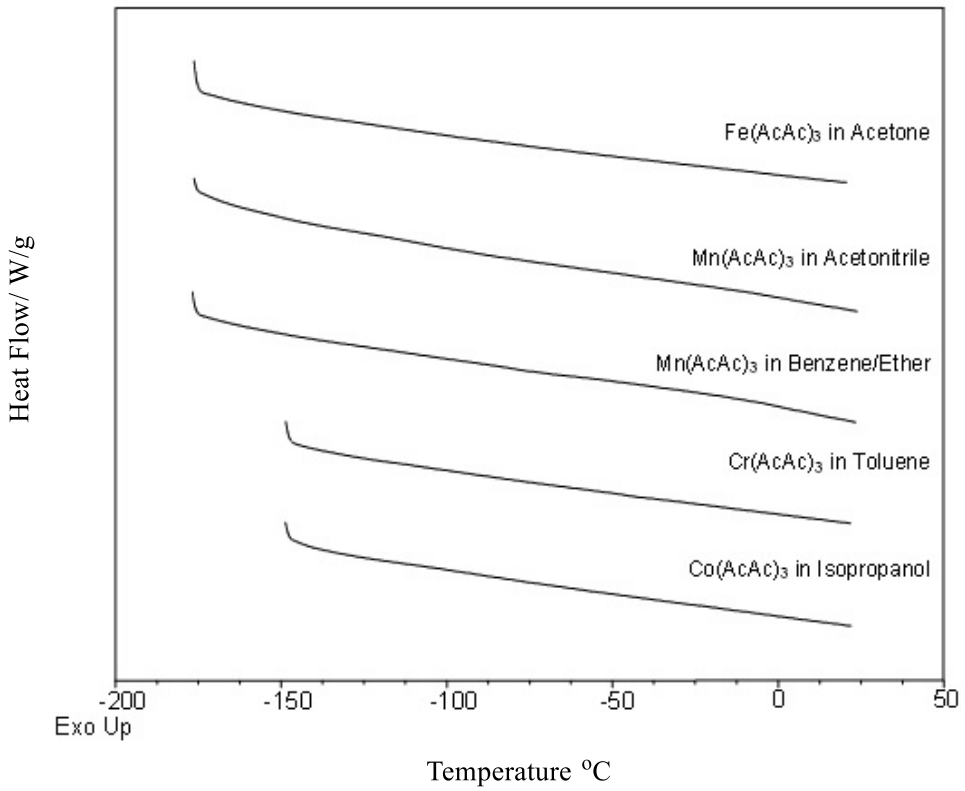

Fig. 2.1. DSC curves recorded on heating from -150°C/123.2K or -180°C/93.2K to room temperature. No first-order thermal phase transitions were observed for any of these samples, irrespective of solvent used for the crystallization. The solvent used in the case of each metal is specified; for the space group of each of the above samples, see Appendix C.[4]

Among concerns of the magnitude of the energetics associated with polymorphic changes is the example of the aluminum derivative ALACAC23, $P2_1/c$ at 150K, and that which the same authors give in ALACAC24 ($P2_1/c$ at 110K), whose cell constants were listed, respectively, as: a = 13.796(<1), b = 7.440(<1), c = 16.149(<1) Å, β = 98.91(<1)° at 150K and a = 22.742(1), b = 7.447(<1), c = 29.617(1) Å, β = 103.22(<1)° (at 110K).[6]

Given the massive change in cell constants in the two above examples, we assumed that in our project we were looking for a ΔH of magnitude comparable with that

for IKERUL (kJ mol^{-1}) which should have easily been detected. That turned out to be incorrect because the magnitude of the transition we found, at 141K, is orders of magnitude less than that observed in IKERUL.

Results and discussion

Observed Motion of the Methyl Groups in the Aluminum(acac)$_3$ Complex Between 100-296K

Initially, our crystallographic and DSC studies did not detect polymorphism; however, more precise DSC measurements guided new crystallographic studies in the thermal regions identified.[3] The crystal structures of the Al(III) and Mn(III) derivatives were first selected because they seemed to display the new features more prominently. Below are our results for the aluminum samples grown from DMF (see Figure 2.2).

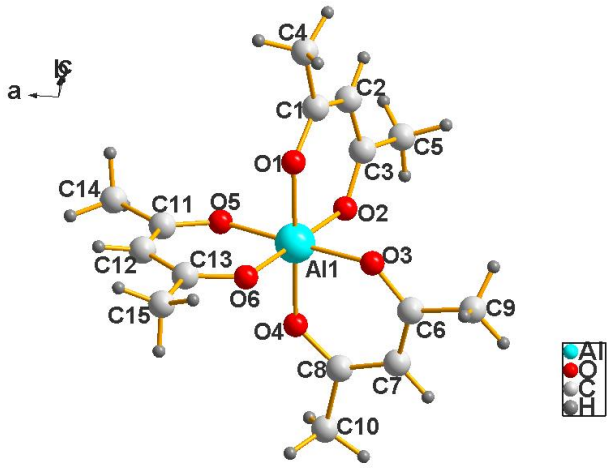

Fig. 2.2. Structure of Al(acac)$_3$ at 100K.[4] Note that the hydrogens are rigidly held in positions found experimentally and optimized subsequently, as described in the crystallographic section. The structure was determined at various higher temperatures as described and shown in Figures 2.3-2.5 below.

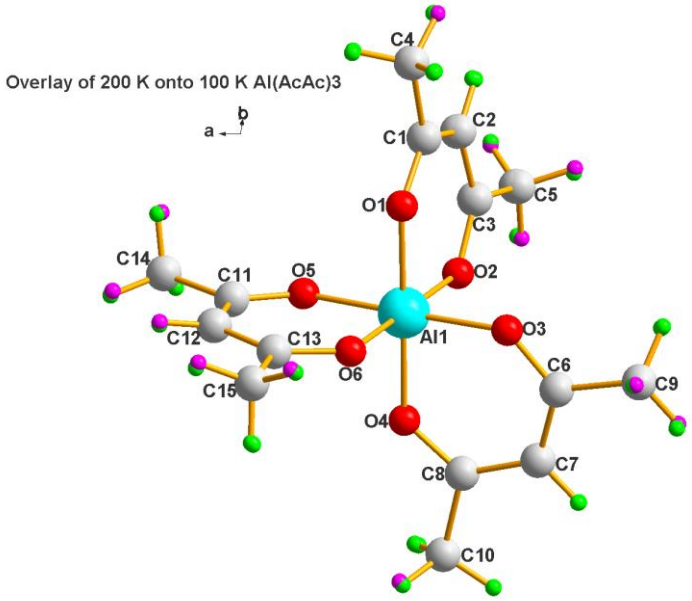

Fig. 2.3. Structure overlay of $Al(acac)_3$ at 200K on top of that at 100K. Lilac and green colors are used to emphasize the changes. Note that the difference in the hydrogens is minimal, even to those of the methyl groups. Those that remain green only are so because we could not see the other one in this projection.[3-4]

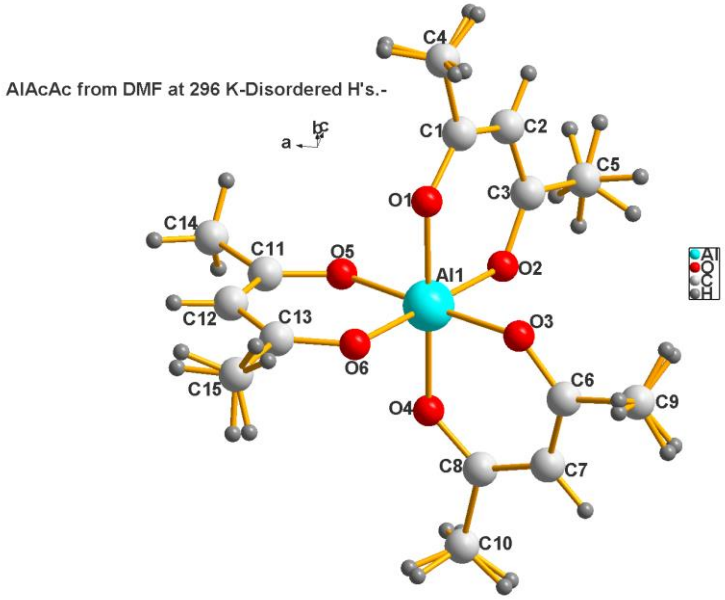

Fig. 2.4. Structure at 296K.[3] Rotational changes are anisotropic, which is an important observation with regards to the structure observed in the DSC recordings as well as in the heat capacity measurements. However, the hydrogens are positioned where they were found in difference maps and idealized as per above.

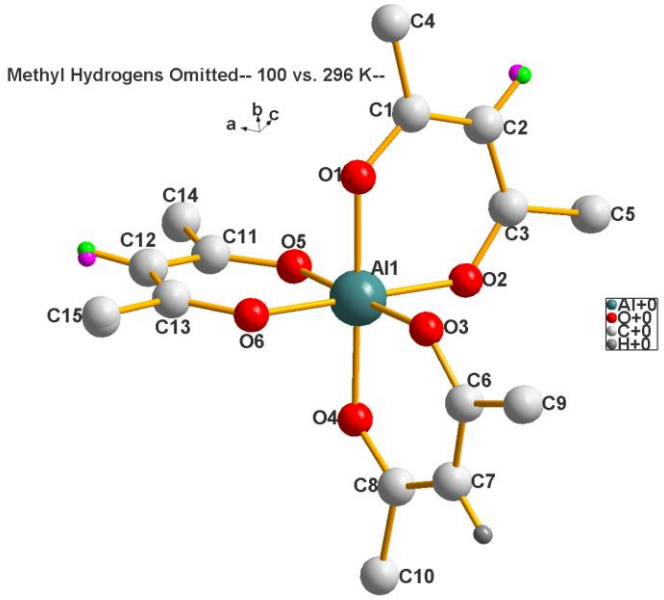

Fig. 2.5. Superposition diagram of the 296K data on top of that at 100K. The methyl hydrogens were left out to emphasize the near perfect match, including the methylene hydrogens. C7 hydrogen match is perfect and those for C2 and C12 are nearly so. It seems "heavier atoms" (metal, oxygen & carbon, and even the methylene hydrogen atoms) move insignificantly during the thermal events associated from increasing the temperature from 100K to 296K and give rise exclusively to the torsional motion of the terminal methyl groups.

Historical Notes Concerning the Rotation of Methyl Groups

In 1929, Kathleen Lonsdale determined the structure of hexamethylbenzene.[10] This was a momentous achievement; but, given the data collection equipment and mathematical methods of data processing, it is not surprising the methyl group hydrogens were not found experimentally; especially, as was later found, they were disordered at room temperature and even at lower temperatures.

The barrier to rotation of methyl groups has been estimated since then; for example:

1. The methyl group rotation and the low temperature transition in hexamethylbenzene was estimated at 2100 J mol^{-1} (502 cal mol^{-1}) using neutron diffraction data.[11]

2. A neutron scattering study of hindered rotations in a series of methylbenzenes, gave the following estimates:[12]

Compound	Barrier to Rotation (Kcal/mol)
1,2-Dimethlybenzene	1.96 ± 0.14
1,2,3-Trimethylbenzene	2.23 ± 0.17
1,2,4,5-Tetramethylbenzene	2.03 ± 0.16
1,2,3,4-Tetramethylbenzene	1.92 ± 0.18
Hexamethybenzene (Phase II)	1.07 ± 0.09
Hexamethybenzene (Phase III)	1.35 ± 0.10

Table 2.1: Note the size of the barrier to rotation is of the order of 1-2.5 Kcal/mol (~200-600 J/mol), and NOT the 20-70 J/mol we found in the Al complex.

3. Nelson & Pierce measured the rotational barrier in acetone to be 778 cal/mol.[13]

All measured and/or calculated values of the methyl group barriers to rotation are in the thousands of calories (or Joules), suggesting that the results we observed do NOT correspond to a rotational barrier phenomenon.

Conclusion

A second set of DSC results (run at very high resolution by expanding the y-axis to be able to be converted into J/mol rather than in kJ/mol) revealed very small thermal events: a) the slight variations detected by the X-ray diffraction corresponded to thermal

events in the DSC experiments; b) they occurred in the expected thermal region; c) they show structure, which implies anisotropy, as we found in the diffraction studies.

For $Mn(acac)_3$, the heat capacity results as a function of temperature match that of DSC and complement what we found by X-ray diffraction. It shows very small energy changes associated with the phase transitions at 175K and 225K.

We now think that the energy that we are measuring is so small as to not be associated with the methyl group rotations, but with librations of the methyl groups themselves.

The very small energy changes found by DSC and Cp measurements (of the order of 5-50 cal/mol) cannot be associated with 1^{st}-order transitions, nor even of rotational barriers. We believe that this is a case of librations brought about by the higher temperatures.

As discussed in Chapter 1, there is a difference in the behavior of Ti(III), V(III) and Mn(III) since, upon lowering the temperature, we appear to see distortions of the molecule due to the Jahn-Teller effect. As expected, the effect is small for Ti(III) and V(III) and more pronounced for Mn(III). For those three elements, there are clear differences because there is no Jahn-Teller effect in Main Group elements. For that matter, there is no Jahn-Teller Effect in closed shell (or closed half-shell) situations, such as in the Cr(III), Fe(III) and Co(III) derivatives.

Experimental

Differential Scanning Calorimetric Measurements

Samples of $Al(acac)_3$ and $Mn(acac)_3$ were synthesized and crystallized from a variety of solvents.[3] DSC measurements were carried out in laboratories in the University of Houston-Downtown and at the Centre of Molecular and Macromolecular Studies (CBMM), Polish Academy of Science, Lodz. Calorimetric measurements were carried out at New Jersey Institute of Technology on the manganese(III) sample only.

Both the Al and Mn acetylacetonates were analyzed with differential scanning calorimetry (DSC) in sub-ambient temperature range to gather evidence of any thermally-induced phase transitions in these compounds. To make certain the results were reproducible, they were carried out with samples from the same batch, at two different laboratories: namely, at UH-Downtown and at PAS Lodz. We also carried out additional crystallographic studies at any temperature between 296K and 100K at which there was a suspicion of any crystalline change since the crystallographic results reported earlier were carried out exclusively at 296K and at 100K.[3] DSC analyses were carried out using a TA Instruments Q20 series DSC equipped with a liquid nitrogen cooling system.

Thermal Analysis for $Al(acac)_3$

DSC thermograms of $Al(acac)_3$, obtained from temperature cycles to both -150^{o}C/123.2K and -180^{o}C/ 93.2K, displayed weak exothermic transitions upon cooling at around -134.80^{o}C/138.4K and a corresponding endothermic transition at

-132.13ºC/141.0K during heating (see Figure 2.6). The averaged transition enthalpies for the two cooling and heating curves are 0.069 J g^{-1} (22.2 J mol^{-1}) and 0.211 J g^{-1} (68.5 J mol^{-1}), respectively. The presence of that signal was confirmed on successive runs when cooling to -180ºC/93.2K**.**

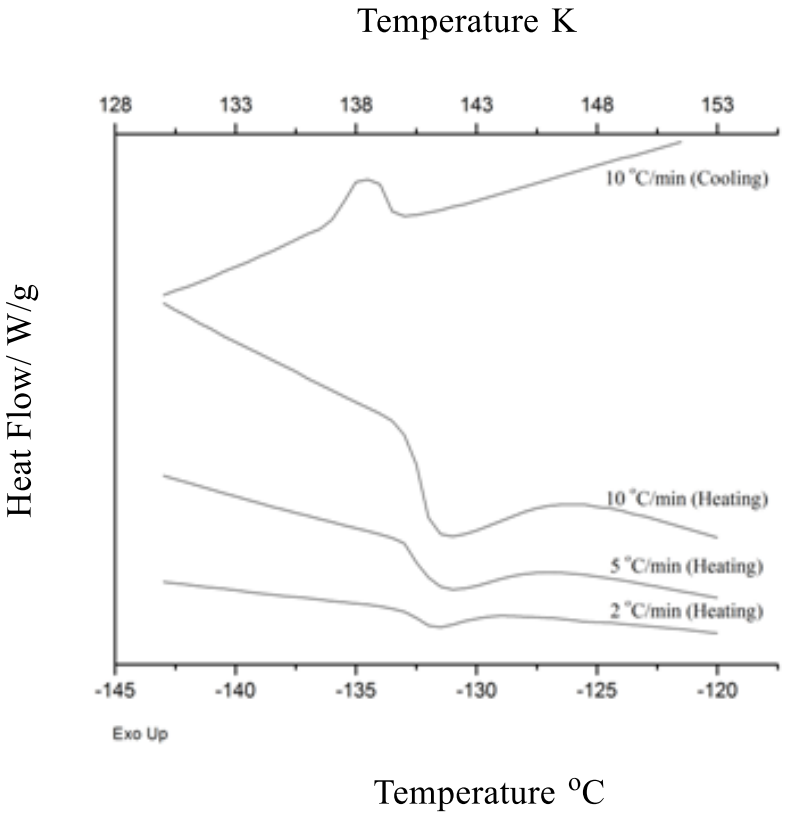

Fig. 2.6. DSC curves recorded for the Al(III) complex. Small peaks are observed upon cooling and heating at around -133ºC/140.2K. This transition has been confirmed with multiple runs, with different samples of different masses and with different heating rates.

Data from these thermograms are summarized in Table 2.2.

Table 2.2. Peak temperatures and enthalpies for the two heating and cooling DSC runs for the aluminum(III) complex recorded at 10, 5 and 2K min^{-1} rate.

Cycle/number	Peak Temp/°C/K	ΔH/J mol^{-1}	ΔS/J $K^{-1}mol^{-1}$	Rate/°C min^{-1}
Cool/1	-134.8/138.4	20.3	0.2	10
Cool/2	-134.8/138.4	24.2	0.2	10
Heat/1	-131.4/141.7	68.3	0.5	10
Heat/2	-131.6/141.6	68.8	0.5	10
Heat	-131.2/141.0	55.4	0.4	5
Heat	-131.7/141.5	37.5	0.3	2

Duplicate analyses were performed with two samples of different weights, 16.4 mg and 8.65 mg, using a fresh sample each time. Thermograms show very similar transition temperatures and heats of transitions in both cases. Furthermore, these runs were carried out at slower heating rates, 5 $Kmin^{-1}$ and 2 $Kmin^{-1}$. Here, endothermic transitions are observed at -131.2°C/141.0K and -131.7°C/141.5K at heating rates of 5°C min^{-1} and 2°C min^{-1}, respectively. Entropy change, ΔS, shows a heating rate dependence as described in Figure 2.7. When approximated to zero heating rate, its value is 0.24 J K^{-1} mol^{-1}, and should be assumed as the approximate thermodynamic equilibrium ΔS for this transition.

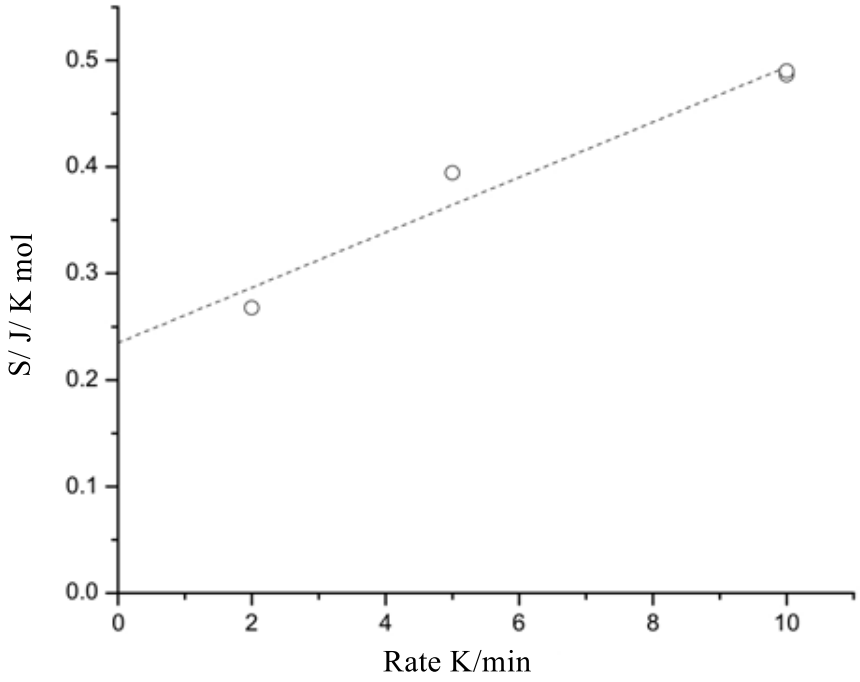

Fig. 2.7. Approximation of experimental entropy change values, ΔS, to zero heating rate.

Thermal analysis for $Mn(acac)_3$

Four Mn samples were crystallized from a variety of solvents as follows:

$Mn(acac)_3$ VWR ethyl acetate in space group $P2_1/n$

$Mn(acac)_3$ Baxter acetonitrile in space group $P2_1/n$

$Mn(acac)_3$ Pharmco Aaper methanol in space group $P2_1/n$

$Mn(acac)_3$ VWR ethyl acetate in space group Pbca

Thermal analyses were initially performed with a series of preliminary measurements to establish optimum experimental conditions; e.g., to maximize signal-to-noise ratio and to avoid shifting the transition temperatures to higher values due to overheating. In that way, it was determined that the heating and cooling rate of 30 K min^{-1} is the best value

and this was used in the final measurements. A fresh sample of material was used for each final experiment.

DSC data for all samples are presented in two ways as shown in Figures 2.8 and 2.9. In Figure 2.8, a collection of curves for all four samples is given for easy comparison of signals produced by each sample.

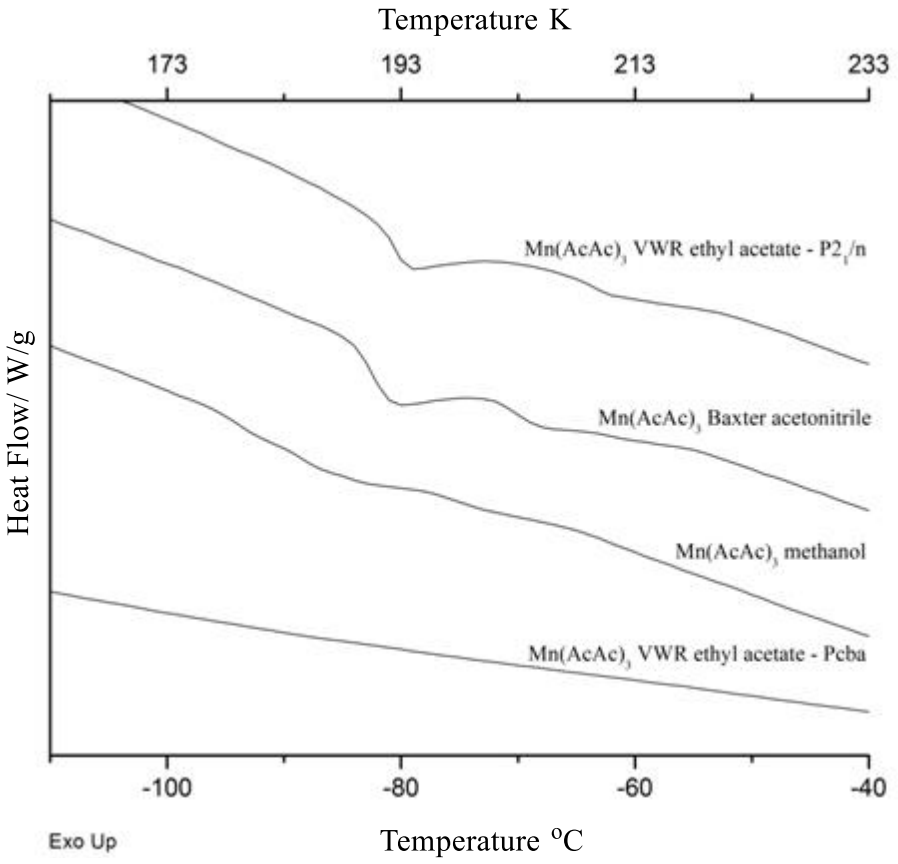

Fig. 2.8. Collection of DSC curves for all four samples listed earlier as a-d.

The presence of endothermic peaks on the DSC curves indicates multiple transitions in the temperature range of approximately -100 to -60ºC or 173 to 213K.

a) $Mn(acac)_3$ from VWR ethyl acetate: $P2_1/n$ has two transitions relatively well-separated with peak temperatures around -79ºC/194K and -62ºC/211K.

b) $Mn(acac)_3$ from Baxter acetonitrile: shows a dominant peak at -80ºC/193K, and a smaller one at -68ºC/205K, as well as a shoulder extending towards higher temperatures with a small, but detectable, peak at -62ºC/211K.

c) Pharmco Aaper methanol $Mn(acac)_3$ samples: DSC detected one broad transition resulting from the overlap of up-to-four transitions showing peak temperatures at -93ºC/180K, 87ºC/186K, -83ºC/190K and -73ºC/200K.

d) $Mn(acac)_3$ from VWR ethyl acetate: Pbca has one smooth, broad endotherm, gradually developing between -130ºC/143K and -50ºC/223K, without signs of discrete transitions within it.

A magnification of the region where these events occur is shown in Figure 2.9 below.

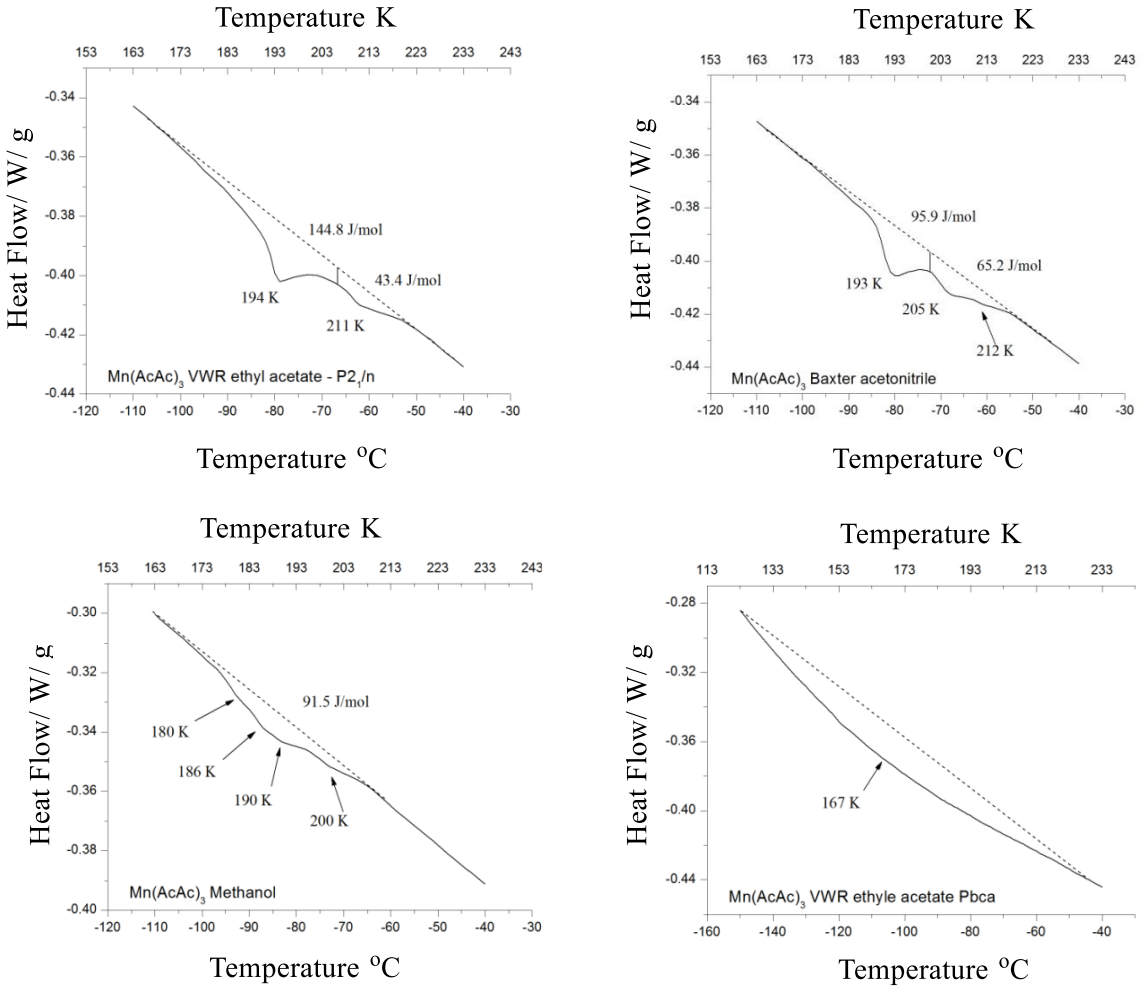

Fig. 2.9. Expanded curves for the DSC measurements for the $Mn(acac)_3$ samples discussed above in Fig. 2.8.

Numerical values for temperatures and heats of transitions are given in Table 2.3.

Table 2.3. Peak temperatures of complexes of $Mn(acac)_3$ with different crystallization solvents. Fixed heating rate of 30°C min^{-1}.

Compound	**Peak Temp/°C/K**	**ΔH_{tot}/J mol^{-1}**	**ΔS_{tot}/J K^{-1} mol^{-1}**
$Mn(acac)_3$ VWR, ethyl acetate, $P2_1/n$	-79.2/193.9 -62.3/210.8	188.2	1.0
$Mn(acac)_3$ Baxter, acetonitrile, $P2_1/n$	-80.5/192.7 -68.5/204.7 -61.2/212.0	161.1	0.8
$Mn(acac)_3$ Pharmco Aaper, methanol, $P2_1/n$	-92.8/180.4 -87.0/186.2 -83.0/190.2 -72.9/200.3	91.5	0.5
$Mn(acac)_3$ VWR, ethyl acetate, Pbca	N/A	N/A	N/A

Calculations of transition parameters for $Mn(acac)_3$ from VWR ethyl acetate, Pbca, were not attempted since it seemed too speculative due to the extreme broadness and smoothness of the peak, and hence the difficulty of assessing its features.

We also measured the heat capacity for one of the $Mn(acac)_3$ samples. The heat capacity measurements were conducted on a Quantum Design Physical Property Measurements system on cooling and warming (Figure 2.10) using the standard relaxation method. The data were collected in 1K steps and measured three times at each temperature. The individual measurements at each temperature were averaged. A fourth order polynomial was used to determine the "background" heat capacity, and the fit was subtracted from the data and is shown in the figure insets. For the cooling curve, the data in the three main features were integrated to give $\Delta H = \int \Delta C_p dT$ ~15 J mol^{-1}.

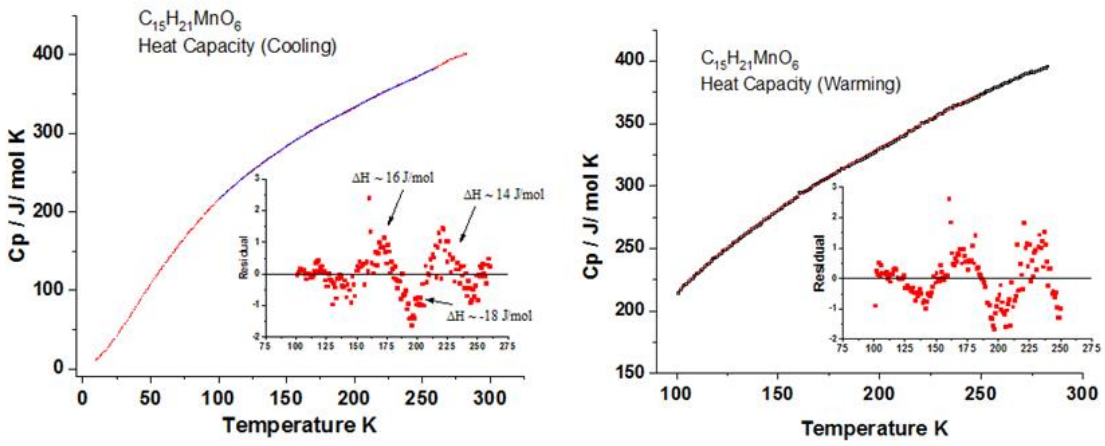

Fig. 2.10. Heat Capacity measurements for $Mn(acac)_3$. Note the very small energy changes associated with the "phase transitions" at ~175K and 225K.

Compound Syntheses and X-Ray Crystal Structure Analyses

1. The syntheses of $M(acac)_3$

The $Al(acac)_3$ complex was prepared according to the procedures in "Inorganic Experiments," Chap. 3.1, by C. Glidewell, p. 109–123 without any modifications.[14] The $Mn(acac)_3$ complex was purchased from Alfa Aesar.

2. Crystallization procedures

Crystals of the aluminum compound, Al(acac), were grown from acetone, acetonitrile, benzene, cyclohexane, dimethylformamide (DMF), ethyl alcohol (EtOH), ethyl acetate, diethyl ether, methyl alcohol (MeOH), 2,4-pentanedione, 2-propyl alcohol, and water.[3] In addition, $Mn(acac)_3$ complex was dissolved and crystallized from acetone, acetonitrile, benzene/diethyl ether (1:1 v/v), ethyl acetate, MeOH, and 2-propyl alcohol.[3]

The crystals used in this study were prepared by slow evaporation of various solutions (up to 12 different solvents were used) in vials covered with Parafilm through which several small holes were pierced.[3]

3. X-Ray diffraction studies

For all the samples, a suitable crystal of each compound was mounted on a Bruker-AXS SMART APEXII CCD diffractometer at 100(1)K. The cell dimensions and intensities were all collected with CuKα radiation (λ = 1.54178 Å). Data processing, Lorentz-polarization, and face-indexed numerical absorption corrections were performed using SAINT, APEX, and SADABS computer programs.[15-16] The structures were solved by direct methods and refined by full-matrix least-squares methods on F^2, using the SHELXTL V6.14 program package.[17-19]

Non-hydrogen atoms were refined anisotropically. All H atoms were found in electron-density difference maps, and allowed to ride on their respective C atoms. The methyl H atoms were constrained to ride with C---H distances of 0.98 Å and $U_{iso}(H) = 1.5U_{eq}(C)$. The methine H atoms were constrained to ride on their parent C atoms with C---H distances of 0.95 Å and $U_{iso}(H) = 1.2U_{eq}(C)$. For all structures, the numbers in parentheses are the errors in the least significant digit. Each crystal was allowed to warm up to room temperature (or a new one mounted), and the cell dimensions and a new dataset were collected to verify that the material was invariant (at least as far as space group) at the different temperatures.

All X-ray crystallographic files in CIF format have been deposited with the Cambridge Structural Database.[4] These materials can be obtained, free of charge, on application to CCDC, 12 Union Road, Cambridge CB2 1EZ, UK. (fax: +44 1223 336033 or e-mail: deposit@ccdc.cam.ac.uk).

X-Ray diffraction results

A summary of the data collection and refinement of the X-ray diffraction measurements appears in Table 2.4, below.

Table 2.4. Summary of X-ray diffraction data for crystals of Al and Mn.

Compound Formula	**$C_{15}H_{21}AlO_6$**	**$C_{15}H_{21}MnO_6$**
Formula weight	324.3	352.26
T/K	100	100
Crystal system	monoclinic	monoclinic
Space group	$P2_1/c$	$P2_1/n$
a/Å	13.7418(2)	16.1123(7)
b/Å	7.4159(1)	7.4939(4)
c/Å	16.1217(2)	29.6014(12)
α/deg	90	90
β/deg	98.883(1)	112.320(2)
γ/deg	90	90
Volume/Å^3	1623.22(4)	3306.4(3)
Z	4	8
Calc. density/ g cm^{-3}	1.327	1.415
Absorption coefficient/ mm^{-3}	1.332	6.723
F/000	688	1472
Crystal size/mm	0.120x0.187x0.372	0.100x0.330x0.510
θ range/deg	3.255-67.500	2.965-69.266
Refl. Collected/unique	14854/2963	29712/6017
Absorption correction	numerical	numerical
Refinement method	Full-matrix least-squares on F^2	
Data/restraints/parameters	2448/0/205	5550/0/409
Goodness-of-fit on F^2	1.068	1.046
Final R indices[I>2σ(I)] R_1/wR_2	0.0433/0.0965	0.0323/0.0838
R indices/all data R_1/wR_2	0.0554/0.1028	0.0358/0.0863

References

1. Von Dreele, R.B.; Fay, R.C., *J. Am. Chem. Soc*, **1971**, *93*, 4936-4938.
2. Kannan R. M.; Jaiswal, P.; Sundaram, N.; Shivashankar, S. A., *Polyhedron*, **2014**, *70*, 188-193.
3. Arslan E.; Lalancette, R.A.; Bernal, I., *Struct. Chem*, **2017**, *28*, 201-212.
4. CSD = Cambridge Crystallographic Structural Database CCSD, Cambridge Crystallographic Data Centre, 12 Union Road, Cambridge CB2 1EZ, UK, release 1.19 (2017). They can be contacted at http://www.ccdc.cam.ac.uk.
5. von Chrzanowski, L.S.; Lutz, M.; Spek, A.L., *Acta Crystallogr*, **2006**, *62*, 3318-3320.
6. von Chrzanowski, L.S.; Lutz, M.; Spek, A.L., *Cryst. Struct. Commun*, **2007**, C *63*, 129-134.
7. Kabak, M.; Elmali, A.; Ozbey, S.; Atakol, O.; Kenar, A., *Z. Kristallogr*, **1996**, 211, 831-832.
8. Spek, A.L., *J. Appl. Crystallogr*, **2003**, *36*, 7-13.
9. Saha, M.K.; Fronczek, F.; Rees, L.H.; Bernal, I., *Inorg. Chem. Commun*, **2003**, *6*, 983-988.
10. Lonsdale, K., *Mathematical, Physical and Engineering Sciences*, **1929**, *123*, 494-515.
11. Hamilton, W.C.; Edmonds, J.W.; Tippe, A., *Disc. Faraday Soc*, **1969**, *48*, 192-204.
12. Rush, J.J., *J. Chem. Physics*, **1967**, *47*, 3936-3943.
13. Nelson, R.; Pierce, L., *Journal of Molecular Spectroscopy*, **1965**, *18*, 344-352.
14. Glidewell, C., in "*Inorganic Experiments*", Edited by J. Derek Woollins, 3rd Revised Edition, Wiley-VCH Verlag GmbH & Co., KGaA, **2010**, Chap. 3.2, 109-123.
15. Bruker, *SAINT*, **2009**, Version 7.23a. Bruker AXS Inc., Madison, Wisconsin, USA.
16. Bruker, *APEX 2*, **2009**, Version 2.0-2. Bruker AXS Inc., Madison, Wisconsin, USA.
17. Sheldrick, G.M., *SHELXT, Acta Crystallogr*, **2015**, A-71, 3-8.
18. Sheldrick, G.M., *SHELXTL, Acta Crystallogr*, **2008**, A-64, 112-122.
19. Sheldrick, G.M., *SHELXL2014, Acta Crystallogr*, **2015**, C-71, 3-8.

Chapter 3

The Results of Efforts to Add Ligands to the Sixth (Axial) Position of Vanadyl Bis-Acetylacetonate--Unexpected Chemical Products, Their Structures, and Magnetic Behavior.

Introduction

In the early 1960's, there was considerable interest in compounds having S = ½ because of the introduction of electron spin resonance into the field of chemistry. Specifically, natural free radicals or man-created radical anions or cations were studied in great numbers because of the vast amount of information one could derive from such studies, both experimental and theoretical.[1]

Likewise, in the field of coordination chemistry, the same considerations were applied and one can readily learn the extent to which all these fields were brought to bear on learning the fundamentals of coordination chemistry by reference to Ballhausen's book on the subject.[2] In this pioneering treatise, one can learn that vanadyl compounds [V=O species] were considered to be very useful because of the simplicity of the electronic and spin states – the topics of greatest interest are the size of the g-factor, the hyperfine splitting by the (I = 7/2) nucleus, and the relationship to metal-electron-to-ligand delocalization, and vice-versa.

As a result of the observations made on the effect of solvent perturbations on the esr results, it was postulated at that time that the sixth position of the [$(acac)_2V{=}O$] could be occupied by molecules which were good electron donors, either on a temporary or on

a permanent basis.[3] Such a prediction was verified many years later; a few references, accessible from the Cambridge Structural Database, are listed below.[4,5]

Later, realizing that molecules having more than one binding site that act as electron donors could link two (or more) such vanadyl derivatives, a variety of groups studied these phenomena. Some examples of such studies are **ADAHOC and ADAHUI**, listed in CSD; unfortunately, these two structures contain a considerable amount of disorder in the peripheral $–CF_3$ fragments, not that this makes any difference for the structural and/or magnetic arguments in question.[4,6]

Results and Discussion

As part of one of our attempts to prepare a compound of $V{=}O(acac)_2$ using 1,3-diazine (pyrimidine), the substance isolated turned out, unexpectedly, to have structure (I), depicted below as Figure 3.1:

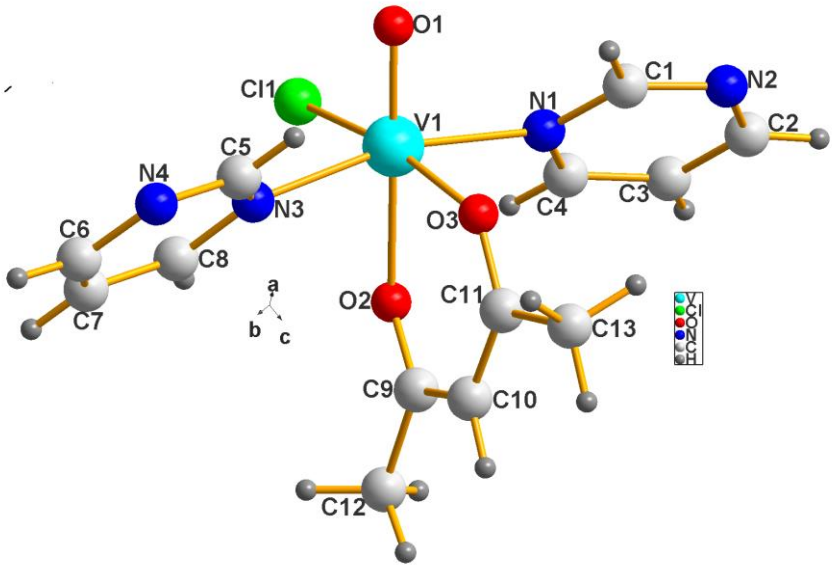

Fig. 3.1. Vanadyl(acac)(1,3-diazine)$_2$ chloride (**I**) $C_{13}H_{15}ClN_4O_3V$

One acac ligand was displaced while two pyrimidine rings (1,3-diazine) and a chloride anion replaced it. The resulting species is now hexa-coordinated, which indicates we succeeded in (a) adding a sixth ligand to the V=O(acac)$_2$ entity while, unexpectedly, displacing one of the acac ligands. This species is a very welcomed one because it helps us to characterize the mechanism in the formation of some of the multinuclear compounds described in what follows.

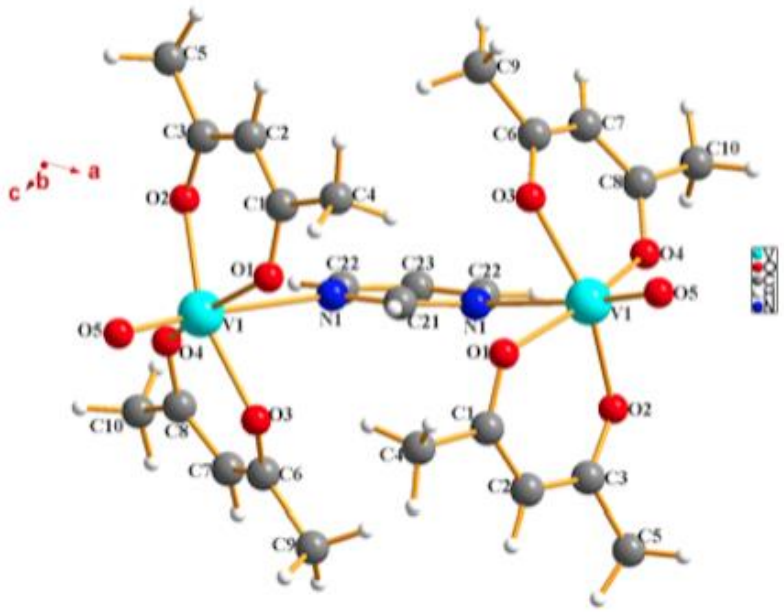

Fig. 3.2. [Vanadyl(acac)$_2$(1,3-diazine)]**(II)** $C_{15.5}H_{20}NO_5V$ (with disordered toluene removed by the program SQUEEZE[7]).

Note that the pyramidal nature of the vanadyl cations is more pronounced in this case (**II**), the (acac)$_2$V=O fragments being more buckled. There is also a toluene of crystallization which is not shown in this structure since it was disordered—e.g., the vanadyl complex and the toluene co-crystallized.

Continuing in our quest for vanadyl acetylacetonate bridged by diazines, we obtained the compound [V=O(acac)$_2$-1,4-diazine-V=O(acac)$_2$], (**III**), shown below as Figure 3.3:

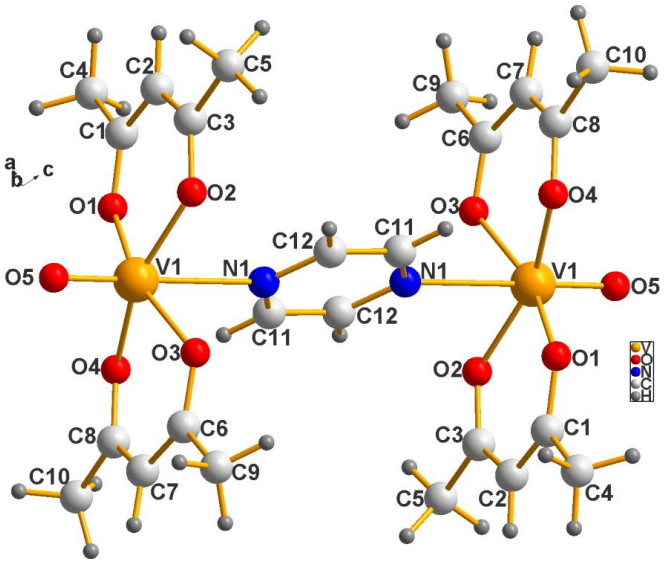

Fig. 3.3. Bis-vanadyl- μ-1,4-diazine (pyrazine) (**III**) $C_{12}H_{16}NO_5V$

This compound contains two vanadyl moieties linked by 1,4-diazine (pyrazine). As is obvious from the numbering system, the molecule lies at an inversion center and is perfectly ordered; we found all of the hydrogen atoms experimentally and refined them using a riding model.

Next, we come to a totally unexpected compound exemplified by Figure 3.4, below. This species is tetranuclear, being constituted of two pairs of vanadyl cations,

related to one another by an inversion center. The outer ones retain their acac ligands and add a 1,3-diazine (pyrimidine) at the sixth position as we intended; but, the inner pair each lost one acac ligand and substituted those two coordination sites by the disordered Cl(OH) bridging moieties. The hydrogens of the OH^- were placed there because charge balance considerations require this neutral species to have only mono-anionic bridges at those sites. Had the oxygens been bare O^{2-}, the whole vanadyl species would be negatively charged, which it is not.

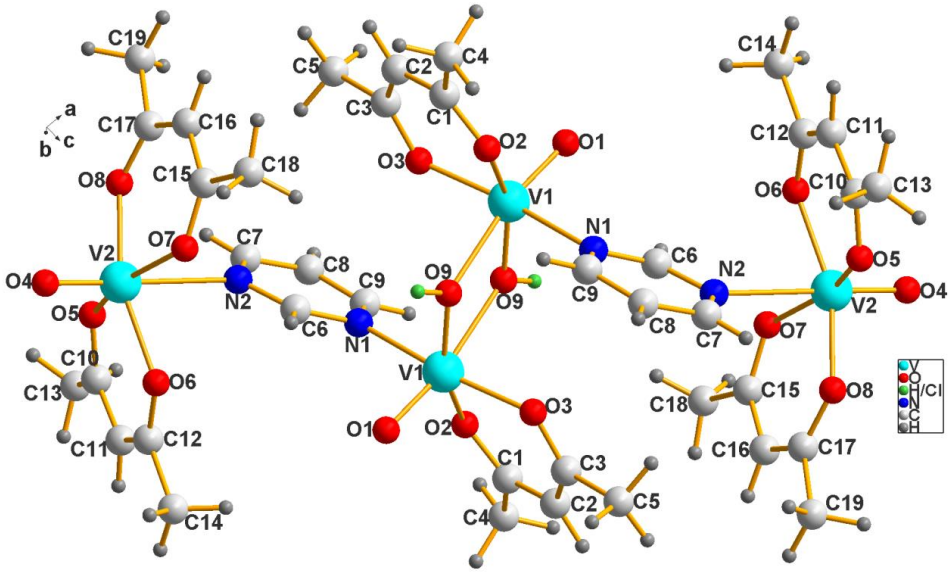

Fig. 3.4. Vanadyl $(acac)_2$ chloro-hydroxo bridge dimer with 1,3-diazine

$C_{38}H_{51.24}Cl_{0.76}N_4O_{17.24}V_4$

The Cl (OH) bridge between the central vanadyls is disordered.

Attack of the fragment at the center of the above molecule, via N_2 of 1,3-diazine, upon unreacted (acac)V=O produces this mixed chloro-hydroxo bridge complex.

The bridges linking the two V(1) atoms consist of a mixture of OH^- [62.0(6)%] as determined by refinement (see above) and of Cl^- [38.0(6)%] (not shown) and accepted by CheckCIF. This is a completely new tetranuclear cluster for the vanadyl ion. Next, we report on one of the results obtained upon reacting $V{=}O(acac)_2$ with 1,3,5-triazine, (**V**), displayed below as Figure 3.5:

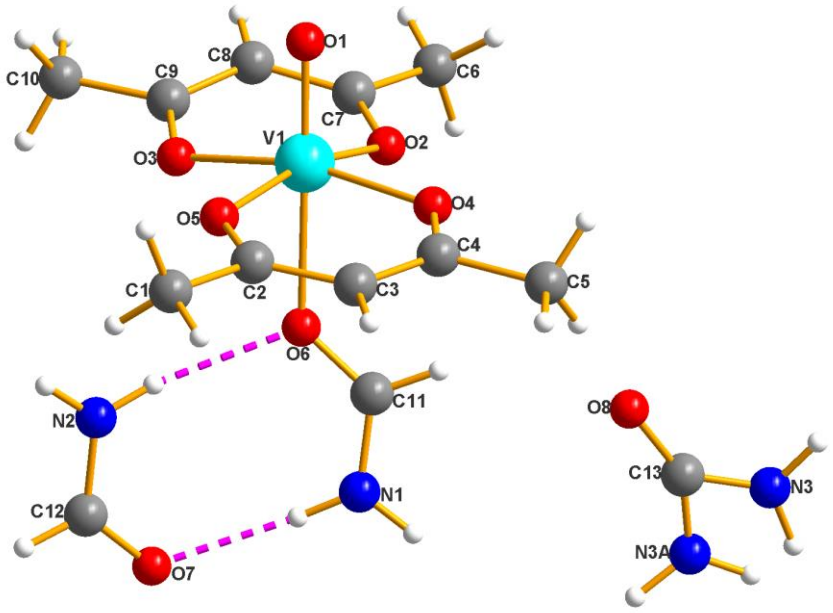

Fig. 3.5. Vanadyl(acac)$_2$formamide · 2 formamide (**V**)

Amazingly, this species shows that the triazine ligand was cleaved and produced formamide; one of the formamides (N1-C11-O6) became a ligand to the vanadyl cation while two others are molecules of crystallization (one of them is disordered, as seen in this figure). The only way such a reaction product can be rationalized is that

1,3,5-triazine (a trimer of HCN) was hydrolyzed under the influence of the $V{=}O(acac)_2$ to produce formamide. That formamide acts as a ligand is interesting; but, it is not a new observation, having been recorded numerous times in CSD and with different metal substrates, such as chromium, cobalt, copper, etc. What is of interest to us is the reaction which led to the formation of our compound and the fact that formamide has, thus far, never been observed as a ligand to the vanadyl cation. We do not know the mechanism whereby the three formamides were generated; however, since the triazine was not protected from air and moisture, we speculate that it was the source of the formamide molecule complexed to the vanadyl and also trapped as molecules of crystallization in the crystals.

This product was obtained by reaction with cyanuric acid which is, in reality, a trimer of composition $[C(O)NH]_3$ derived from the thermal decomposition of urea which can be cleaved into its components. Moreover, the closely related species, imidoformic acid, has been trapped in platinum compounds **VOCLIJ** and **VOCLOP** listed in the CSD database.[8,4]

The packing of the lattice of the above compound is quite complex in its hydrogen-bonded arrangement, a portion of which is shown in Figure 3.6.

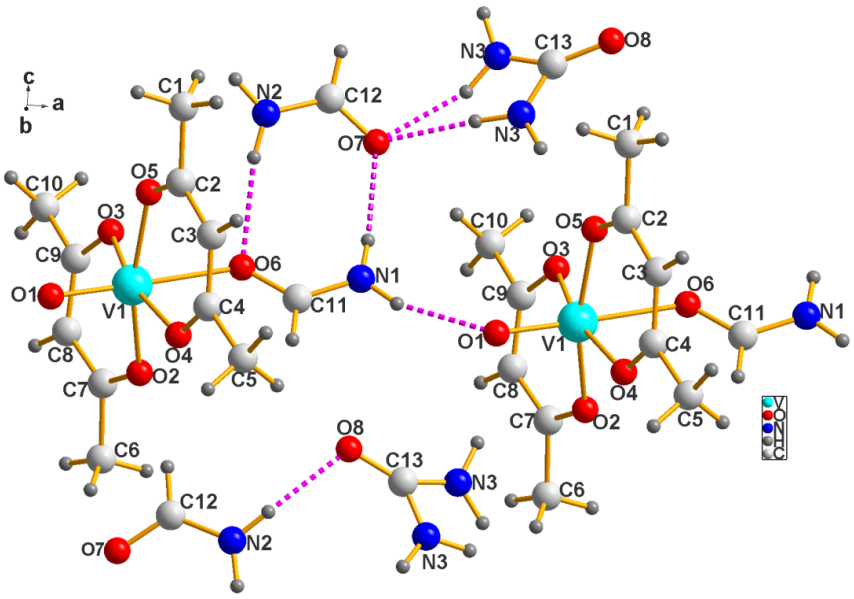

Fig. 3.6. Packing of the complex formed between vanadyl(acac)$_2$ and formamide.

Conclusion

In an effort to prepare aromatic amine adducts of vanadyl bis-acetylacetonate, we encountered products which were those expected, as well as some not planned. Among the unplanned products are mononuclear species containing the $(acac)_2V{=}O$ moiety unchanged and exchanged [e.g., V(IV), $3d^1$, S = ½] while others are multinuclear and contain V=O [e.g., V(IV), $3d^1$, S = ½] and/or V(V) [e.g., $3d^0$, S = 0]. Exchanged means that one of the acetylacetone ligands may have been displaced in the course of the reaction. Their structures were determined using full spheres of X-ray data, collected at 100 K, and confirmed with elemental CHN analysis. Results for both 1,3-diazine and for 1,4 diazine, structures (**II**) and (**III**) are supported by elemental analysis.

Experimental Information

1. Synthetic Studies

Preparation of (I & II): $C_{13}H_{15}ClN_4O_3V$: Vanadyl(acac)(1,3-diazine)$_2$ chloride

1.000 g (3.8 mmoles) of vanadyl(acac)$_2$ ($C_{10}H_{14}O_5V$; MW = 265.157 g/mol) and 0.600 g (7.5 mmoles) of pyrimidine (1,3-diazine) ($C_4H_4N_2$; MW = 80.09 g/mol) [2:1 mole ratio of vanadyl(acac)$_2$ to ligand] were added to 45 mL of toluene in a sealed glass pressure cell and heated at 130ºC in a silicone oil bath for 1.5 hours with stirring. The mixture was allowed to cool slowly, filtered through a sintered-glass funnel, and the filtrate was transferred to three 20-mL vials, whose openings were sealed with Parafilm

through which was poked a number of small holes. The solutions were allowed to evaporate slowly.

Preparation of (III): $C_{15.5}H_{20}NO_5V$: [Vanadyl(acac)$_2$]$_2$(1,4-diazine)

0.500 g (1.89 mmoles) of vanadyl(acac)$_2$ ($C_{10}H_{14}O_5V$; MW = 265.157 g/mol) and 0.300 g (3.8 mmoles) of pyrazine (1,4-diazine) ($C_4H_4N_2$; MW = 80.09 g/mol) [2:1 mole ratio of vanadyl(acac)$_2$ to ligand] were added to 45 mL of toluene in a sealed glass pressure cell and heated at 130^{o}C in a silicone oil bath for 1.5 hours with stirring. The mixture was allowed to cool slowly, filtered through a sintered-glass funnel, and the filtrate was transferred to three 20-mL vials, whose openings were sealed with Parafilm through which was poked a number of small holes. The solutions were allowed to evaporate slowly. After a few days, the vanadyl 1,4-diazine complex crystals (III) formed.

Preparation of (IV): $C_{38}H_{51.24}Cl_{0.76}N_4O_{17.24}V_4$: Vanadyl(acac)$_2$ chloro-hydroxo bridge dimer with 1,3-diazine

The same procedure as used to prepare (I) and (II) above, but with the addition of 2 mL of concentrated HCl, gave the mixed hydroxo-chloride bridged complex with 4 vanadyls and 1,3-diazine **(II)**.

Preparation of (V): $C_{11}H_{17}NO_6V \cdot 2(CH_3NO)$: Vanadyl formamide complex · 2 formamides of crystallization

0.500 g (1.89 mmoles) of vanadyl(acac)$_2$ ($C_{10}H_{14}O_5V$; MW = 265.157 g/mol) and 0.308 g (3.8 mmoles) of 1,3,5-triazine ($C_3H_3N_3$; MW = 81.08 g/mol)) [2:1 mole ratio of vanadyl(acac)$_2$ to ligand] were added to 45 mL of toluene in a sealed glass pressure cell and heated at 130^{o}C in a silicone oil bath for 1.5 hours with stirring. The mixture was allowed to cool slowly, filtered through a sintered-glass funnel, and the filtrate was transferred to three 20-mL vials, whose openings were sealed with Parafilm through which was poked a number of small holes. The solutions were allowed to evaporate slowly. After a few days, the complex containing two formamides of crystallization and a bound formamide (from 1,3,5-triazine) were formed, $C_{11}H_{17}NO_6V \cdot 2(CH_3NO)$.

2. Elemental Analyses

Elemental analyses were completed for both 1,3-diazine and for 1,4 diazine, structures (**II**) and (**III**). For 1,3-diazine: calculated: C 52.99, H 5.74, N 3.99; found: C 52.34, H 5.73, N 4.89. For 1,4-diazine, calculated: C 47.22, H 5.28, N 4.59; found: C 47.0, H 5.35, N 4.68.

Elemental analyses were carried out by Robertson Microlit Laboratories located in Ledgewood, NJ.

3. X-Ray Data Collection and Processing

Data collection and refinement procedures were uniform for all five compounds described herein. Crystals were taken directly from their mother liquor and immediately mounted on a Bruker-AXS SMART APEXII CCD diffractometer in a stream of nitrogen gas cooled to 100(1)K. The cell dimensions and the intensities were collected with CuKα radiation (λ = 1.54178 Å). Data processing, Lorentz-polarization, and face-indexed numerical absorption corrections were performed using SAINT, APEX, and SADABS computer programs.[9,10] After acquiring the 100K datasets, the temperature of the crystal was slowly allowed to warm to room temperature and cell constants were determined at ca. 296 K. In all cases, the cell dimensions were the same as the 100K cell dimensions (except for very slight elongations due to the higher temperatures); therefore, a new dataset was not collected since the original solution of the structure was deemed to be sufficient.

4. Solution and Refinement of the Structures

The structures were solved by direct methods and refined by full-matrix least-squares methods on F^2, using the SHELXTL V6.14 program package.[11-13] All non-hydrogen atoms were refined anisotropically. All the H atoms were found in electron-density difference maps, but were placed as riding models on their respective C atoms, as follows: the methyl H atoms were put in ideally staggered positions with C---H distances of 0.98 Å and $U_{iso}(H) = 1.5U_{eq}(C)$; the methine and aromatic Hs were all placed in geometrically idealized positions and constrained to ride on their parent C atoms with

C---H distances of 1.00 and 0.95 Å, respectively, and $U_{iso}(H) = 1.2U_{eq}(C)$. The diazine and amine Hs were constrained to ride on their N atoms with N---H distances of 0.88 Å and $U_{iso}(H) = 1.2U_{eq}(N)$.

References

1. Bernal, I.; Rieger, P.H.; Fraenkel, G.K., *J. Chem. Phys.*, **1962**, *37*, 1489.
2. Introduction to Ligand Field Theory, *Carl* J. *Ballhausen*, McGraw-Hill, NewYork, 1962.
3. Bernal, I.; Rieger, P. H. *Inorg. Chem.*, 1963, *2*, 256-262.
4. CSD = Cambridge Crystallographic Structural Database CCSD, Cambridge Crystallographic Data Centre, 12 Union Road, Cambridge CB2 1EZ, UK, release 1.19 (2017). They can be contacted at http://www.ccdc.cam.ac.uk.
5. a) Caira, M.R; Haigh, J. M.; Nassimbeni, L. R., *Inorg. Nucl. Chem. Lett.*,**1972**, *8*, 109-112. b) Oughtred, R. E.; Raper, E. S.; Shearer, H. M., *Acta Crystallogr.,Sect.B: Struct. Crystallogr. Cryst. Chem.*,**1976**, *32*, 82-87.
6. Ishida, T.; Mitsubori, S.; Nogami, T.; Takeda, N.; Ishikawa, M.; Iwamura, H. *Inorg. Chem.*, **2001**, *40*, 7059-7064.
7. a) Spek, A.L., *J Appl. Cryst.*,**2003,** *36*, 7-13. b) Spek, A.L., *Acta Cryst.***, 2009**, *D65*, 148-155.
8. Baranovsky, I. B.; Surazhskaya, M. D.; Gulubnichaya, M. A. *Zh. Neorg. Khim. (Russ.)(Russ. J. Inorg. Chem.)*, **2007**, *52(12)*, 1983-1991.
9. Bruker, *SAINT*, **2009**, Version 7.23a. Bruker AXS Inc., Madison, Wisconsin, USA.
10. Bruker, *APEX 2*, **2009**, Version 2.0-2. Bruker AXS Inc., Madison, Wisconsin, USA.
11. Sheldrick, G.M., *SHELXTL, Acta Crystallogr*, **2008**, A-64, 112-122.
12. Sheldrick, G.M., *SHELXT, Acta Crystallogr*, **2015**, A-71, 3-8.
13. Sheldrick, G.M., *SHELXL2014, Acta Crystallogr*, **2015**, C-71, 3-8.

Overall Conclusion

Our results indicate that many of the older published data were correct in space group, cell constants, and general description of the molecular structure. However, whereas the older data were almost always only determined at RT, and always with very limited data sets, our data were always determined at both RT and 100K, AND always with at least a full sphere of data, using CuKα radiation.

We found that there were (a) phase changes caused by changes of solvent(s) (b) there were thermally-induced phase transitions as well. More important, though, is the fact that we were unable to verify the existence of some of the phase transitions described in some of the previous work even in the case of those in which we crystallized our samples from the same solvent as specified in the published reports. This was possible only in a few cases inasmuch as the majority of the data available was rarely explicit concerning the provenance of their crystals.

In a few cases, we are certain that the samples said to be new polymorphic forms are incorrect since the space groups reported are incorrect by the following information: (a) the Niggli matrix of the reported reduced cell(s) show that the material belongs to higher symmetry space groups (such as we found), and (b) the center of mass of the contents of the asymmetric unit of those reported in Sohncke space groups correspond precisely at special positions such as 0,0,0, ¼, ¼, ½, etc., clearly indicating that the space group was incorrectly described as belonging in the Sohncke class.

Finally, we have seen evidence that the crystals of Ti(III), V(III) and Mn(III) display the expected Jahn-Teller distortions of those having an electronic degenerate ground state. That, no doubt, is the result of the quality of the crystal used because the

effect is rather subtle and small, in terms of differences in bond lengths (in some instances) and is also dependent on the magnitude of the esd's. However, it was observed at the level of 21 esds in one case and 10 esds in another. Thus, we feel vindicated in saying that we recorded the Jahn-Teller effect in the appropriate cases. There is no Jahn-Teller Effect in closed shell (or closed half-shell) situations, such as in the Cr(III), Fe(III) and Co(III) derivatives.

Our results indicate that only in the case of V(III) crystals, derived from an ethyl acetate solution, did we observe a thermally-induced change in space group in going, directly, from 100K to 296K, when the space group changed slightly from Pbca to $Pna2_1$. Unfortunately, we cannot comment further because the V(III) crystals are very sensitive to oxidation and we could not rely on DSC measurements for this metal.

Most importantly, given the magnitude of the methyl groups' behavior in our $M(acac)_3$ studies, it is obvious that they do not correspond to the hindered rotational energies found in other studies. It is likely that these small energies are associated with librational motions of the acac methyl groups.

In a separate project, we were successful in filling the sixth position of the $[(acac)_2V{=}O]$ by nitrogenous molecules which were good electron donors. We have made bridged compounds with 1,3-diazine and 1,4-diazine and these results were supported by elemental analyses.

List of Publications

1. **Arslan, E**.; Lalancette, R.A.; Bernal, I., *Struct. Chem.*, **2017**, *28*, 201-212.
2. Lalancette, R.A.; **Arslan, E**.; Bernal, I.; Willhelm, D.; Grebowicz, J.; Pluta, M., *Jour. Therm Anal Calorim*., **2018**, *131*, 2809-2819.
3. Lalancette, R.A.; Syzdek, D.; Grebowicz, J.; **Arslan, E**.; Bernal, I., *Jour. Therm Anal Calorim.*, **2018**, 1-8.

APPENDIX A

An Unexpected and Unusual $V(5+)_{10}$ Cluster Containing Oxygen Bridges as well as Six Bidentate Acetylacetonates

Introduction

Many years ago, Bernal and Rieger described spectroscopic properties of vanadyl acetylacetonate, $(acac)_2V{=}O$, and noted that the visible-UV and esr spectra showed clear evidence of perturbations of the energy levels of the metal caused by changes in solvents.[1] It was then suggested that this was caused by perturbations at the open, sixth position of the vanadium, the reason offered was that such perturbations were clearly associated with the ability of the solvent to form a sixth bond, even if temporarily.[1] That suggestion was later proven to be correct; and, now there are a number (six) of structures in the Cambridge Crystallographic Database (CSD) proving the perturbing species can become permanently attached to the metal, which therefore becomes six-bonded.[2]

Here, we wanted to prepare cluster species containing two, or more, vanadyl acetylacetonate fragments which may, or may not, be magnetically coupled; and, if so, we wanted to know how. There already was one such study in the literature which, unfortunately, reported severe disorder in the structure.[3] In the process of trying to synthesize and characterize additional examples of multi-vanadyl species, we obtained a cluster containing ten metal atoms displaying some unusual structural characteristics.

Results and Discussion

It is known that molecules with non-bonded pairs of electrons can readily become attached to the empty position of vanadyl bis-acetylacetonate.[1-3] The fact that one can be permanently affixed is amply documented; more interesting, however, is the fact that more than one vanadyl bis-acetylacetonate can do so.[2,3] Therefore, we attempted to attach vanadyl bis-acetylacetonate to 1,3,5-triazine in hopes of getting three of them to bind to the organic substrate. That it could happen seemed not so far-fetched inasmuch as 1,3-diazine can readily accommodate two of them, and 1,3,5 triazine can preserve a similar geometry of the vanadyl attachments. So far, all attempts to obtain a product suitable for additional studies have failed with this triazine.

Next, we attempted to obtain well-defined products using cyanuric acid (2,4,6-trihydroxy-1,3,5-triazine), the premise being that the hydroxides could act as ligands to the vanadyl moiety, as well as the nitrogens. This concept is given some validity by the existence of the compound listed in CSD as BAFQOO (see Figure A.1), where an isopropyl alcohol is acting as a ligand to a related vanadyl species as to what we had in mind (see Figure A.1).[2]

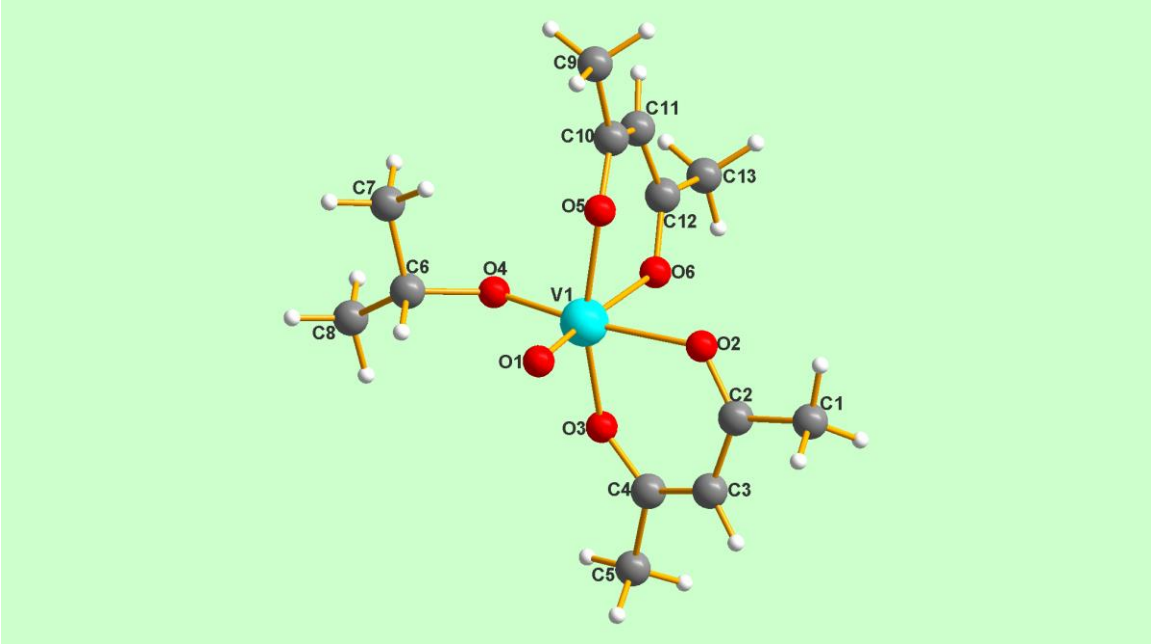

Fig. A.1. This is an example from the literature (see BAFCOO in CSD) that shows a neutral, mono-nuclear $(acac)_2V{=}O$ species containing V(5+) .[2,4] The 6th coordination site is the anion of isopropyl alcohol, playing a role related to that of the –O-V- fragment that is found in this structure (see below).

To our great surprise, we obtained beautiful black crystals that bear no relationship to what we had expected; the resulting species turned out to be a $V(5+)_{10}$ cluster, which we describe here. The cluster material crystallizes in monoclinic space group $P2_1/c$ with 4 molecules per cell and one toluene of crystallization per cluster. Figure A.2 shows the inner part of the cluster.

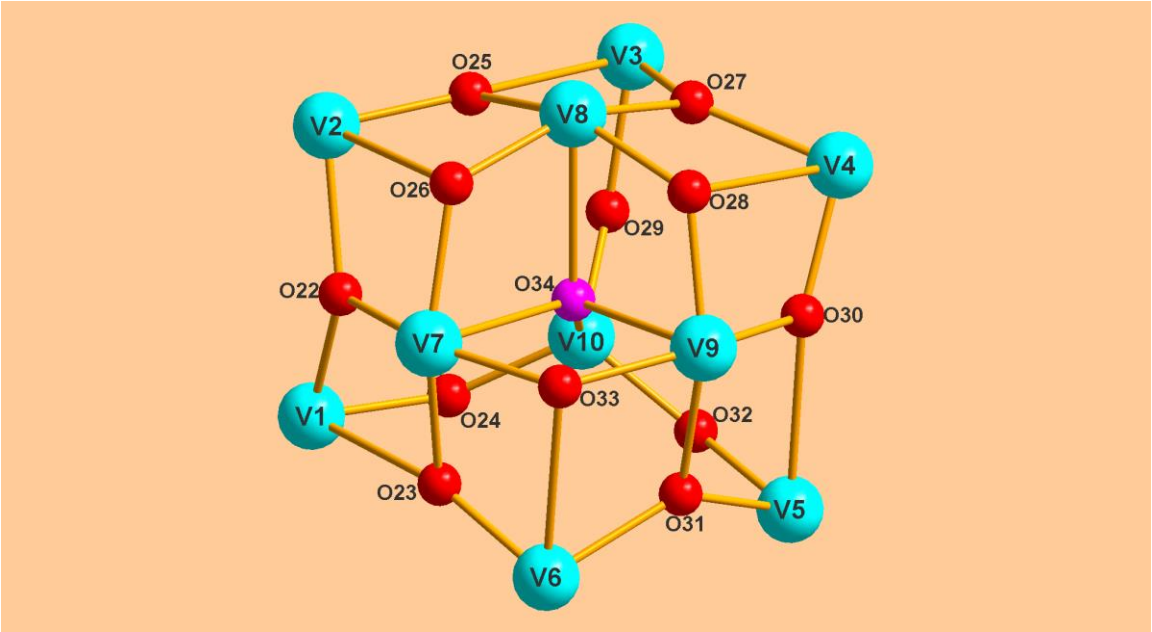

Fig. A.2. For clarity, the six peripheral acetylacetone ligands bonded to V1 through V6 were removed to show the inner cluster. Selected bond lengths are: V=O (not shown) for V1-V9 range from 1.578 to 1.593 Å, (however, the unique V10 has no multiple vanadium-oxygen bond at all); the V-O distances to the acac ligands (V1 through V6) range from 1.912 to 1.989 Å. V1-V5 each has one "long" V-O-V bond inside the cluster (ranging from 2.400 to 2.490 Å) and two other shorter bonds ranging from 1.770 to 1.957 Å; V7 throughV9 make "long" V-O-V bonds to O34 ranging from 2.387-2.415 Å, but V10-O34 is only 1.669 Å. All the vanadium atoms are six-coordinate except for V10. Note that V10 and O34 at the center of the cluster are each tetrahedral, with angles ranging from 107-113^{o} for O-V10-O and 82-131^{o} for V-O34-V; these central atoms are shown in more detail in Figure A.4. A typical fragment containing one entire acetylacetonate is shown in Figure A.3.

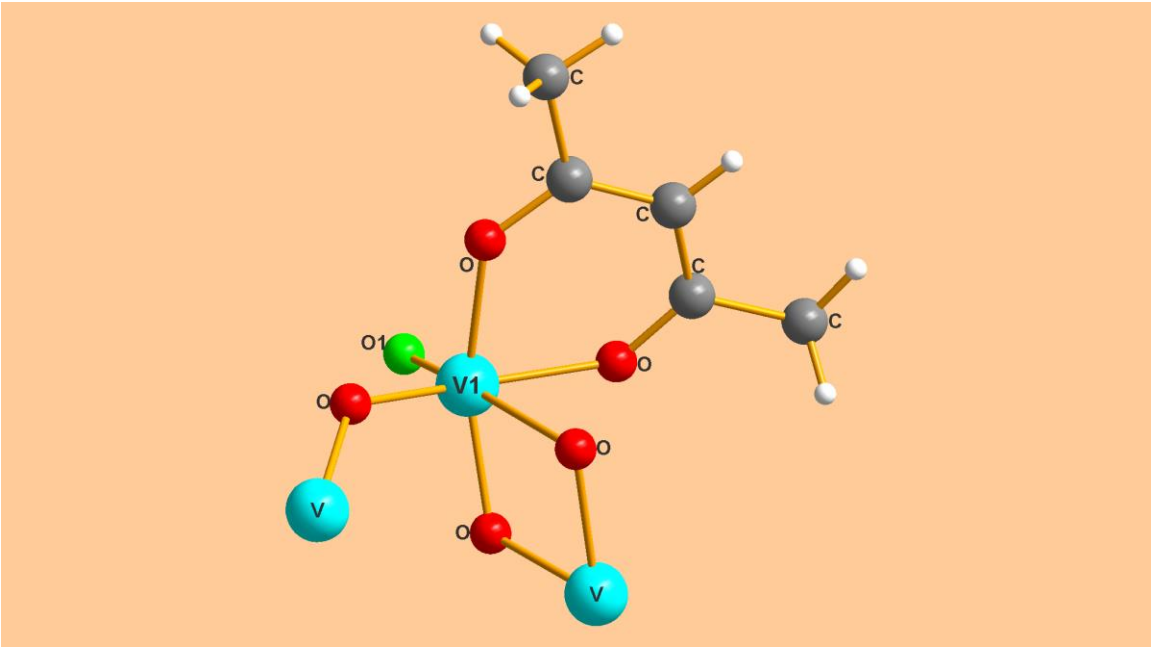

Fig. A.3. Note that this type of peripheral vanadyl species is six-bonded by the V=O oxygen(green), the bidentate acetylacetonate (shown in full), a bidentate VO_2 fragment, as well as by a monodentate V-O-V ligand. Despite the fact there are ten vanadium atoms in the cluster, all 36 hydrogens of the six V(acac) fragments present in the cluster were found in electron density difference maps at the positions reported, and then allowed to ride on their respective C atoms during refinement.

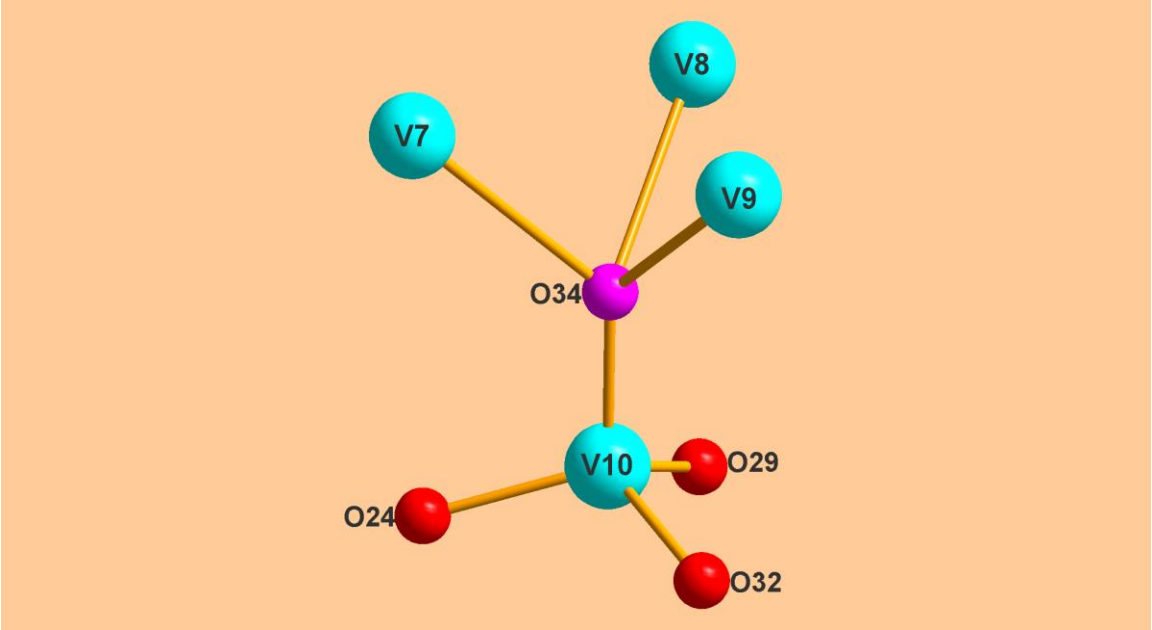

Fig. A.4. This is the central portion of the cluster. Note its resemblance to species such as hexamethylethane or hexathionate anion. Despite the marked difference in coordination, all ten vanadium atoms are in charge state (5+), as required by charge balance; see following text for additional information.

As far as charges in the cluster are concerned: the cluster has 10 vanadium atoms, a total of 34 oxygen atoms, and six acetylacetonates. These latter account for 12 of the oxygens, which leaves 22 inorganic (or bare) oxygens with a charge of 2- each (-44). Each of the six acetylacetones has a charge of -1, giving a total charge of -50 for the cluster. Since there are 10 vanadium atoms, they each have a charge of +5 (for charge compensation). Therefore, this molecule has no unpaired electrons, since V(5+) is $3d^o$.

The structure has a toluene of crystallization which is very well-behaved and sits in channels between the vanadium clusters (see Figure A.5 for a packing of the toluene molecules at 100 K).

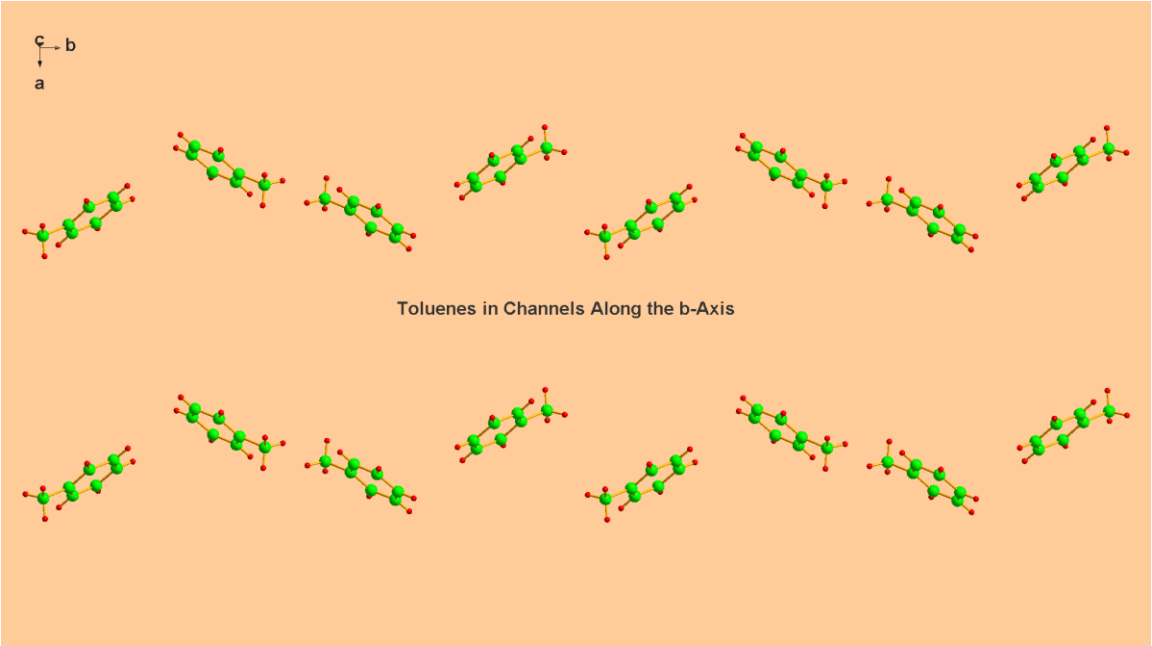

Fig. A.5. This is a c-axis projection showing that the toluene molecules lie in channels extending along the b-axis; the contact interactions of the solvent with the cluster atoms are largely confined to extremely weak van der Waals forces.

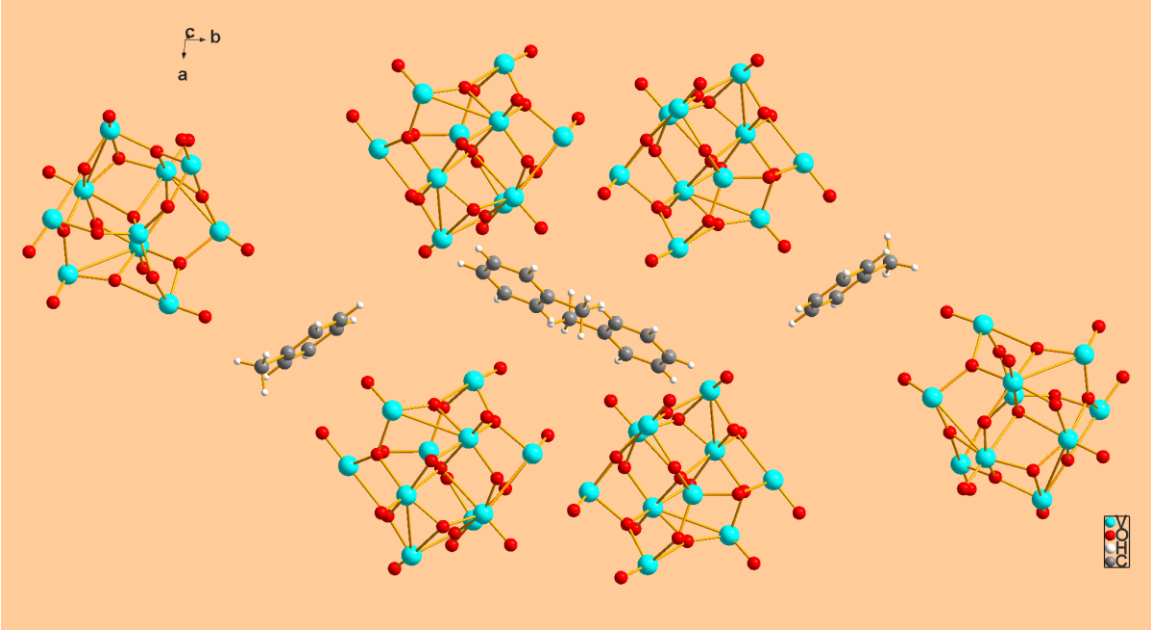

Fig. A.6 is a packing diagram of the cluster (no acetylacetonates shown) as well as the toluene molecules of crystallization.

Conclusions

In attempting to attach three vanadyl bis-acetylacetonates to 1,3,5-triazine, we were surprised by the appearance of a ten vanadium cluster, internally linked by bare oxygens while retaining one acetylacetonate ligand on each of the six peripheral vanadium cations. Part of the surprise, to say the least, was the breaking of the $(acac)_2V{=}O$ in such a fashion, and this is unprecedented, so far as we are able to ascertain. The closely-related molecules 1,3-diazine and 1,4-diazine are known to simply attach themselves to the sixth position of the $(acac)_2V{=}O$ molecule and these have been isolated and documented magnetically and crystallographically.[3,5]

Among other factors that we found puzzling are: what is the origin of the oxygens linking all of the V(5+) cations? A) One source could be the decomposition of the acetylacetone ligands (initially, there were two ligands per vanadyl). B) Another possible source is the cyanuric acid; this is under investigation at the moment; cyanuric acid is, in reality, a trimer of composition $[C(O)NH]_3$, derived from the thermal decomposition of urea, which can be cleaved into its components and can be the source of CNOH, which decomposes into $NCO^- + H^+$ in coordination chemical reactions. Moreover, the closely related species, imidoformic acid, has been trapped in platinum compounds VOCLIJ and VOCLOP, listed in the CSD database.[6,2] Unfortunately, we see no trace of any of these fragments. Therefore, we are at a loss to provide a mechanism for this reaction. However, given the fact that the process of documenting such a reaction may be long, we describe now the empirically most important fact, which is the formation of the cluster, documented by the determination of its structure.

We have found two decavanadate $V_{10}(5+)$ clusters in the literature.[7,8] However, they differ from ours in that (a) they have no peripheral organic ligands as our cluster does at V1 through V6; (b) they do not have a central, unique oxygen, as is the case with O34 in this species; and, (c) those clusters contain OH bridges between vanadium atoms which our complex does not have.

For convenience to the readers, below we list the distances between vanadiums and oxygens in our cluster. Those in the two other cited clusters are available in their respective publications.[7,8] Furthermore, interested readers are referred to our Figure A.2 in order to more clearly visualize the meaning of the tabular material given below (Table A.1).

Table A.1: VO Distances in the Cluster†

V=O: V1=O1 1.584(3) [all the distances listed below have (3) as errors]
V2=O2 1.588 V3=O3 1.578 V4=O4 1.585
V5=O5 1.578
V6=O6 1.580 V7=O7 1.591* V8=O8 1.593*
V9=O9 1.592*
V10 = no V=O bonding
*(The last 3 [V7-V9] have no acac on them, and have longer V=O distances).

V-O Distances to acac oxygens:

V1-O10	1.940	V1-O11	1.951	V2-O12	1.978	V2-O13	1.955
V3-O14	1.948	V3-O15	1.920	V4-O16	1.972	V4-O17	1.918
V5-O18	1.912	V5-O19	1.985	V6-O20	1.989	V6-O21	1.958

Internal Oxygen Distances:

O22–V1	1.842	O22-V2	1.945	O22-V7	2.000	essentially a planar triangle
O23–V1	2.404	O23-V6	1.796	O23-V7	1.928	planar distorted triangle
O24–V1	1.868	O24-V10	1.733			angle = ~131deg
O25–V2	1.770	O25-V2	1.957	O25-V3	2.454	planar distorted triangle
O26–V8	1.813	O26-V7	1.872	O26-V2	2.454	pyramidal
O27–V3	1.837	O27-V4	1.956	O27-V8	1.995	planar distorted triangle
O28–V4	2.490	O28–V9	1.818	O28-V8	1.860	pyramidal
O29–V10	1.730	O29-V3	1.871			angle = ~132deg
O30–V4	1.785	O30-V9	1.931	O30-V5	2.400	planar distorted triangle
O31–V5	1.858	O31-V6	1.927	O31-V9	1.995	planar distorted triangle
O32–V10	1.727	O32-V5	1.876			angle = ~132deg
O33–V6	2.483	O33–V7	1.807	O33-V9	1.864	pyramidal
O34-V10	1.669	O34-V8	2.387	O34-V9	2.407	O34-V7 2.415 distorted tetrahedron

†The reader is advised to look at the CIF to get the respective bond angles in this complex.

Experimental

1. Synthesis of the Complex:

0.500 g (1.89 mmoles) of vanadyl(acac)$_2$ ($C_{10}H_{14}O_5V$; MW = 265.157 g/mol) [Alfa Aesar] and 0.490 g (3.80 mmoles) of cyanuric acid (1,3,5-triazinane-2,4,6-trione) ($C_3H_3N_3O_3$; MW = 129.07 g/mol) [Alfa Aesar] [2:1 mole ratio of vanadyl(acac)$_2$ to ligand] were added to 45 mL of toluene in a sealed glass pressure cell and heated at 130^{o}C in a silicone oil [Fisher Scientific] bath for 1-1/2 hours with stirring. The mixture was allowed to cool slowly, filtered through a medium sintered-glass funnel, and the filtrate transferred to three 20-mL vials, whose openings were sealed with Parafilm through which was poked a number of small holes. The solutions were allowed to evaporate slowly. After 4 days, one of the vials was capped completely. In about 3-4 weeks, jet-black crystals of the cluster were found in the bottom of the capped solution [as well as bright blue crystals of vanadyl(acac)$_2$ on the sides of the container]. The non-capped vials did not yield the cluster, and went to dryness, yielding only the starting material, vanadyl(acac)$_2$.

2. X-Ray Data Collection and Processing:

Crystals of the cluster compound (I) [$C_{30}H_{42}O_{34}V_{10}$, C_7H_8] were taken directly from the toluene solution and immediately mounted in Paratone-N oil on a Bruker-AXS SMART APEXII CCD diffractometer at 100(1)K. Crystal data for [$C_{30}H_{42}O_{34}V_{10}$, C_7H_8]: M = 1548.17, monoclinic, a = 13.1403(5), b = 25.7679(8), c = 20.4875(7) Å,

β = 126.987°, U = 5541.1(3) Å^3, T = 100K, space group P2$_1$/c (no. 14), Z = 4, 9479 reflections measured, 6255 unique which were used in all calculations. The final $wR(F^2)$ was 0.1170 (all data) and R_1 was 0.0516; GOOF = 0.991. The cell dimensions and the intensities were collected with Cu-Kα radiation (λ = 1.54178 Å). Data processing, Lorentz-polarization, and face-indexed numerical absorption corrections were performed using SAINT, APEX, and SADABS computer programs.[9,10] After acquisition of the 100K dataset, the crystal was allowed to slowly warm to room temperature and a new set of data was collected for space group and cell constant determination at ca. 296 K. Since the cell dimensions were the same as the 100K cell dimensions (except for very slight elongations due to the higher temperatures), a new dataset was not collected since the original solution of the structure was deemed to be very good.

3. Solution and Refinement of the Structure:

The structure was solved by direct methods and refined by full-matrix least-squares methods on F^2, using the SHELXTL V6.14 program package.[11-13] All non-hydrogen atoms were refined anisotropically. All the H atoms were found in electron-density difference maps, but were placed as riding models on their respective C atoms, as follows: the methyl H atoms were put in ideally staggered positions with C---H distances of 0.98 Å and U_{iso}(H) = 1.5U_{eq}(C); the methine and aromatic Hs were all placed in geometrically idealized positions and constrained to ride on their parent C atoms with C---H distances of 1.00 and 0.95 Å, respectively, and U_{iso}(H) = 1.2U_{eq}(C).

References

1. Bernal, I.; Rieger, P. H. *Inorg. Chem.*, **1963**, *2*, 256-262.
1. CSD = Cambridge Crystallographic Structural Database CCSD, Cambridge Crystallographic Data Centre, 12 Union Road, Cambridge CB2 1EZ, UK, release 1.19 (2017). They can be contacted at http://www.ccdc.cam.ac.uk.
2. Ishida, T.; Mitsubori, S.; Nogami, T.; Takeda, N.; Ishikawa, M.; Iwamura, H. *Inorg. Chem*., **2001**, *40*, 7059-7064.
3. Jiang, Feilong; Anderson, O. P.; Miller, S. M.; Chen, J.; Mahroof-Tahir, M.; Crans, D. C., *Inorg.Chem.*, **1998**, *37(21)*, 5439-5451.
4. Arslan, E.; Bernal, I.; Lalancette, R. *Struct. Chem.*, **2017**, *28*, 201–212.
5. Baranovsky, I. B.; Surazhskaya, M. D.; Gulubnichaya, M. A. *Zh. Neorg. Khim. (Russ.)(Russ. J. Inorg. Chem.)*, **2007**, *52(12)*, 1983-1991.
6. Zhai, H.; Liu, S.; Peng, J.; Hu, N.; Jia, H., *J. Chem. Crystal*., **2004**, *34*, 541-548.
7. Ferreira da Silva, J. L.; Fátima Minas da Piedade, M.; Teresa Duarte, M. *Inorg. Chim. Acta*, **2003**, *356*, 222-242.
8. Bruker, *SAINT*, **2009**, Version 7.23a. Bruker AXS Inc., Madison, Wisconsin, USA.
9. Bruker, *APEX 2*, **2009**, Version 2.0-2. Bruker AXS Inc., Madison, Wisconsin, USA.
10. Sheldrick, G.M., *SHELXTL, Acta Crystallogr*, **2008**, A-64, 112-122.
11. Sheldrick, G.M., *SHELXT, Acta Crystallogr*, **2015**, A-71, 3-8.
12. Sheldrick, G.M., *SHELXL2014. Acta Crystallogr*, **2015**, C-71, 3-8.

APPENDIX B

Overall report of metal(III) tris-acetylacetonates compiled from CSD

APPENDIX B METAL (III) ACETYLACETONATES PUBLISHED IN THE PAST

	Solvent	Refcode*	Year	Space Group	Temp.	Z	Z'	a,b, c	Alpha, Beta, Gamma	Volume	R-Factor	Comments
ALUMINUM	Acetone	ALACAC11	2001	P21/c	298K	4	1	14.002(3), 7.534(2), 16.325(3)	90, 98.81(3), 90	1701.823	7.25	
		ALACAC12	2001	P21/c	298K	4	1	13.998(3), 7.542(2), 16.315(3)	90, 98.78(3), 90	1702.238	10.84	
		ALACAC18	1959	Pnam	295K	16	2	15.72(3), 13.35(3), 32.80(5)	90, 90, 90	6883.474	NA	
	Benzene	ALACAC17	1956	P21/c	295K	4	1	14.25(5), 7.68(2), 16.17(3)	90, 99.35, 90	1746.134	NA	Isomorphous with Cr analogue
	DMF	ALACAC25	2010	P21/c	170K	4	1	13.848(1), 7.465(4), 16.202(1)	90, 98.99(9), 90	1654.2(2)	3.73	
	Ethyl Acetate	ALACAC19	2006	Pna21	110K	16	4	15.517(1), 31.96(7), 13.23(2)	90, 90, 90	6561.125	3.13	
		ALACAC20	2007	P21/c	240K	4	1	13.9140(7), 7.50076(17), 16.2547(6)	90, 98.806(2), 90	1676.44(11)	4.11	Phase transition between 150K and 110K
		ALACAC21	2007	P21/c	210K	4	1	13.8640(6), 7.4755(3), 16.2080(11)	90, 98.821(2), 90	1659.94(15)	3.92	Phase transition between 150K and 110K
		ALACAC22	2007	P21/c	180K	4	1	13.8385(7), 7.4614(3), 16.1873(11)	90, 98.871(2), 90	1651.42(16)	3.67	Phase transition between 150K and 110K
		ALACAC23	2007	P21/c	150K	4	1	13.7961(5), 7.44012(17), 16.1488(5)	90, 98.914(3), 90	1637.57(9)	3.41	Phase transition between 150K and 110K
		ALACAC24	2007	P21/c	110K	12	3	22.7424(11), 7.4467(2), 29.6165(13)	90, 103.221(2), 90	4882.8(3)	3.83	Phase transition between 150K and 110K
	Unknown Solvent	ALACAC16	2001	P21/c	298K	4	1	13.990(4), 7.543(2), 16.320(5)	90, 98.791(16), 90	1702.0(8)	4.9	Isomorphous with Cr analogue
		ALACAC01	1973	P21/c	298K	4	1	14.069(10), 7.568(5), 16.377(11)	90, 99.00(8), 90	1722.26	7	
		ALACAC02	1990	P21/c	298K	4	1	13.972(3), 7.527(2), 16.307(5)	90, 98.88(2), 90	1694.406	5	
		ALACAC10	1975	Pna21	298K	16	4	15.699(3), 32.546(7), 13.369(2)	90, 90, 90	6830.752	9.2	
MANGANESE	Acetone	ACACMN	1964	P21/c	298K	4	1	13.87(15), 7.467(7), 16.20(25)	90, 98.42(20), 90	1660.569	9	It is suggested that this data is for the Co analogue
	Acetonitrile or Methanol	ACACMN2	1979	P21/n	298K	4	1	7.786(1), 27.975(4), 8.020(1)	90, 100.34(1), 90	1718.494	4.5	
	Benzene/ether	ACACMN0	1974	P21/c	298K	4	1	14.013(1), 7.600(1), 16.373(1)	90, 99.33(1), 90	1720.6	8.4	
	Cyclohexane and Petroleum ether	ACACMN2	2005	P21/n	100K	8	2	16.117, 7.511, 27.831	90, 100.03, 90	3317.585	5.31	Phase transition between 180K and 190K
		ACACMN2	2005	P21	293K	8	4	19.799, 7.618, 23.288	90, 99.134, 90	3468	7.66	Phase transition between 180K and 190K
	Unknown Solvent	ACACMN2	2008	P21	223K	8	4	19.67, 7.563, 23.179	90, 99.23, 90	3403.591	4.61	

COBALT	Acetone	COACAC03	1974	P21/c	298K	4	1	13.90(7), 7.47(4), 16.21(7)	90, 98.4(1), 90	1665.077	3.8	
		COACAC05	1959	P21/c	295K	4	1	14.25(3), 7.5(2), 16.38(3)	90, 99.00(1), 90	1729.06	NA	
	Benzene-Petroleum Ether	COACAC02	1973	P21/c	298K	4	1	13.951(9), 7.470(5), 16.222(11)	90, 98.48(8), 90	1672.077	8	
	Ethyl Acetate	COACAC06	2007	P21/c	240K	4	1	13.809, 7.433, 16.148	90, 98.43, 90	1639.67	3.98	Isomorphous with the Al analogue
		COACAC07	2007	P21/c	210K	4	1	13.771, 7.420, 16.124	90, 98.45, 90	1629.544	3.88	Isomorphous with the Al analogue
		COACAC08	2007	P21/c	180K	4	1	13.734, 7.407, 16.096	90, 98.47, 90	1619.53	3.6	Isomorphous with the Al analogue
		COACAC09	2007	P21/c	150K	4	1	13.693, 7.392, 16.064	90, 98.5, 90	1608.096	3.45	Isomorphous with the Al analogue
		COACAC10	2007	P21/c	110K	4	1	13.638, 7.376, 16.045	90, 98.59, 90	1595.777	2.88	Isomorphous with the Al analogue
	Hexane Benzene	COACAC04	1971	P21	298K	4	2	11.31, 12.47, 12.5	90, 101.04, 90	1730.321	NA	
	Unknown Solvent	COACAC	1961	NA	NA			NA	NA	NA	NA	Crystal data were taken from COACAC01
		COACAC01	1958	P21/c	298K	4	1	14.160, 7.480, 16.430	90, 98.68, 90	1720.282	18	
CHROMIUM	Acetone	ACACCR	1965	P21/c	298K	4	1	14.031, 7.551, 16.379	90, 99.06, 90	1713.674	6.6	
	Choloroform/Acetone	ACACCR06	1956	P21/c	295K	4	1	13.8(5), 7.58(2), 16.44(3)	90, 99.5, 90	1696.105	NA	Isomorphous with the Al analogue
	Ethyl Acetate	ACACCR07	2007	P21/c	290K	4	1	13.9970(8), 7.5441(4), 16.3590(12)	90, 99.031(2), 90	1706.01(18)	4.24	Isomorphous with the Al analogue, Phase transition between 150K and 110K
		ACACCR08	2007	P21/c	110K	24	6	27.5823(2), 7.4656(1), 48.6012(4)	90, 99.2731(3), 90	9877.09(17)	4	Isomorphous with the Al analogue, Phase transition between 150K and 110K
	Unknown Solvent	ACACCR01	1969	P21/c	298K	4	1	14.035(4), 7.559(1), 16.404(4)	90, 98.91(2), 90	1719.309	NA	
		ACACCR02	1982	P21/c	298K	4	1	14.012(2), 7.548(1), 16.364(1)	90, 99, 90	1709.4	4.7	
		ACACCR05	2001	P21/c	298K	4	1	14.022(4), 7.546(2), 16.364(5)	90, 99.0(1), 90	1710.158	4.9	Isomorphous with the Al analogue
		ACACCR10	2010	P21/c	150K	4	1	13.803(5), 7.478(3), 16.243(6)	90, 99.155(6), 90	1655.2(1)	4.94	
		ACACCR11	2009	P21/c	293K	4	1	13.826(3), 7.457(1), 16.15(3)	90, 99.02(3), 90	1644.394	7.63	
		ACACCR12	2009	P21/c	150K	4	1	13.805, 7.467, 16.212	90, 99.2, 90	1649.698	3.45	
IRON	Acetone	FEACAC06	1959	Pbca	295K	8	1	15.48(3), 13.55(3), 16.55(3)	90, 90, 90	3471.429	NA	
	Alcohol	FEACAC01	1981	NA	358K			15.51, 33.10, 13.62	90, 90, 90	6992.249	NA	
	Benzene	FEACAC	1967	Pbca	298K	8	1	15.471, 13.577, 16.565	90, 90, 90	3479.474	7.9	
	DCM	FEACAC09	2011	Pbca	200K	8	1	15.313, 13.496, 16.481	90, 90, 90	3406.072	5	Light sensitive
	Ether	FEACAC04	1956	Pbca	298K	8	1	15.471, 13.577, 16.565	90, 90, 90	3479.474	23	
	Unknown Solvent	FEACAC02	1996	P212121	298K	8	2	13.585(1), 15.458(1), 16.563(1)	90, 90, 90	3478.179	3.8	Re-interpretation of FEACAC and FEACAC04
		FEACAC03	2001	Pbca	200K	8	1	16.561(3), 15.434(4), 13.578(3)	90, 90, 90	3470.57	5.3	
		FEACAC05	2001	Pbca	298K	8	1	15.463(4), 13.594(3), 16.579(4)	90, 90, 90	3484.972	3.1	
		FEACAC07	2007	Pbca	295K	8	1	15.452, 13.588, 16.573	90, 90, 90	3479.663	3.77	Melting point at 456K
		FEACAC08	2007	Pbca	150K	8	1	15.254, 13.445, 16.426	90, 90, 90	3368.774	3.15	Melting point at 456K
VANADIUM	Benzene, Methanol, or 2,4-Pentanedione	VAACAC	1969	Pcab	298K	8	1	15.43(2), 16.6(2), 13.53(1)	90, 90, 90	3465.547	6.6	Air sensitive
		VAACAC01	1969	P21/n	298K	4	1	16.34(1), 13.06(1), 8.108(5)	90, 90, 90	1730.25	10.2	Air sensitive
	Hexane	VAACAC02	2001	Pcab	298K	8	1	15.447, 16.623, 13.502	90, 90, 90	3466.748	4.4	Air sensitive, melting point 460-461K
	Unknown Solvent	VAACAC12	1970	P21/n	298K	4	1	8.07(1), 13.04(1), 16.38(1)	90, 90.33(8), 90	1723.685	11.5	Air sensitive
		VAACAC13	2005	Pbca	120K	8	1	13.392, 16.404, 15.19	90, 90, 90	3337.058	5.75	Air sensitive, melting point 457K
		VAACAC14	2009	Pbca	153K	8	1	15.247, 13.406, 16.438	90, 90, 90	3360.013	3.83	Air sensitive
		VAACAC15	2013	P21/c	150K	4	1	13.915, 7.478, 16.241	90, 99.53, 90	1666.692	4.85	Air sensitive
		VAACAC16	2013	P21/c	100K	4	1	13.878, 7.446, 16.194	90, 99.74, 90	1649.343	3.92	Air sensitive
TITANIUM	Hexane	QAMCAI	1999	P21/c	298K	4	1	14.187(4), 7.576(3), 16.574(7)	90, 99.34(2), 90	1757.769	5.8	Air sensitive

*REFCODES are from CCDC

APPENDIX C

Complete report of our metal (III) tris-acetylacetonates

APPENDIX C METAL(III) ACETYLACETONATES										
	Solvent	Space Group	Temp.	Z	Z'	a,b, c	Alpha, Beta, Gamma	Volume	R-Factor	Comments*
ALUMINUM	Acetone	P21/c	296K	4	1	13.9908(5), 7.5446(2), 16.3237(5)	90, 98.8090(16), 90	1702.72(9)	4.10	1484898
		P21/c	100K	4	1	13.7244(3), 7.4444(2), 16.0544(4)	90, 99.0260(9), 90	1619.97(7)	5.03	1499051
	Acetonitrile	P21/c	296K	4	1	13.9867(7), 7.5435(3), 16.3288(7)	90, 98.812(2), 90	1702.49(13)	4.10	1499142
		P21/c	100K	4	1	13.7243(2), 7.4409(1), 16.0558(3)	90, 99.037(1), 90	1619.28(4)	5.58	1499136
	Benzene	P21/c	296K	4	1	13.9968(4), 7.5417(2), 16.3245(4)	90, 98.790(2), 90	1702.97(8)	4.50	1499052
		P21/c	100K	4	1	13.7284(3), 7.4398(1), 16.0554(3)	90, 99.0390(8), 90	1619.48(5)	4.89	1499139
	Cyclohexane	P21/c	296K	4	1	13.9930(5), 7.5407(3), 16.3243(5)	90, 98.7920(19), 90	1702.2(1)	4.16	1499137
		P21/c	100K	4	1	13.7205(3), 7.4416(2), 16.0620(3)	90, 99.0330(11), 90	1619.63(6)	4.93	1499053
	DMF	P21/c	296K	4	1	13.975(8), 7.531(4), 16.315(9)	90, 98.790(14), 90	1696.9(16)	4.89	1499054
		P21/c	100K	4	1	13.7418(2), 7.4159(1), 16.1217(2)	90, 98.883(1), 90	1623.22(4)	4.33	1499055
	Ethanol	P21/c	296K	4	1	13.9940(19), 7.552(1), 16.318(2)	90, 98.790(6), 90	1696.9(16)	4.23	1499056
		P21/c	100K	4	1	13.7263(7), 7.4389(4), 16.0643(8)	90, 99.055(2), 90	1696.9(14)	5.03	1499057
	Ethyl Acetate	P21/c	296K	4	1	13.9960(8), 7.5402(4), 16.3166(9)	90, 98.825(3), 90	1701.55(16)	4.09	1499143
		P21/c	100K	4	1	13.7305(2), 7.4407(1), 16.0544(3)	90, 99.062(7), 90	1619.72(5)	4.81	1499058
	Diethyl Ether	P21/c	296K	4	1	13.9930(4), 7.5412(2), 16.3229(4)	90, 98.8320(13), 90	1702.03(8)	4.89	1499144
		P21/c	100K	4	1	13.7311(5), 7.4456(3), 16.0533(6)	90, 99.0510(14), 90	1620.79(11)	4.69	1499145
	Methanol	P21/c	296K	4	1	13.9877(4), 7.5412(2), 16.3159(4)	90, 98.7940(13), 90	1700.83(8)	3.99	1499146
		P21/c	100K	4	1	13.7314(2), 7.4429(1), 16.0507(2)	90, 99.0325(6), 90	1620.06(4)	4.93	1499147
	2,4 -Pentanedione	P21/c	296K	4	1	14.0006(9), 7.5412(5), 16.308(1)	90, 98.849(3), 90	1701.33(19)	4.45	1505749
		P21/c	100K	4	1	13.7277(7), 7.4386(4), 16.0627(8)	90, 99.061(2), 90	1619.77(14)	5.09	1499148
	Propanol	P21/c	296K	4	1	13.9857(5), 7.5406(3), 16.3139(5)	90, 98.7800(19), 90	1700.3(1)	4.63	1499059
		P21/c	100K	4	1	13.7302(2), 7.4414(1), 16.0535(2)	90, 99.033(1), 90	1619.87(4)	4.84	1499149
	Water	P21/c	296K	4	1	13.9956(6), 7.5429(3), 16.3174(6)	90, 98.809(3), 90	1702.27(12)	5.30	1499150
		P21/c	100K	4	1	13.7268(2), 7.4423(1), 16.0566(2)	90, 99.0235(7), 90	1620.02(4)	4.86	1499151

MANGANESE	Acetone	P21/c	296K	4	1	14.0448(4), 7.6084(2), 16.4341(4)	90, 99.3190(14), 90	1732.95(8)	4.29	Disorder in one ring	1499084
		P21/n	100K	8	2	16.1263(4), 7.4869(2), 27.7763(6)	90, 99.9337(11), 90	3303.32(14)	4.70		1499085
	Acetonitrile	Pbca	296K	8	1	15.4517(9), 13.4583(9), 16.736(1)	90, 90, 90	3480.3(4)	3.95		1499086
		Pbca	100K	8	1	15.0556(3), 13.2378(3), 16.6101(4)	90, 90, 90	3310.44(13)	2.43		1484899
	Benzene/ether	P21/c	296K	4	1	14.0348(4), 7.6103(2), 16.4246(5)	90, 99.3790(17), 90	1730.84(9)	4.41	Disorder in one ring	1499087
		P21/n	100K	8	2	16.1125(5), 7.4965(2), 27.7771(8)	90, 99.9362(15), 90	3304.80(17)	3.73		1499088
	Ethyl Acetate	P21/c	296K	4	1	14.0270(4), 7.6023(2), 16.4196(4)	90, 99.3650(16), 90	1727.61(8)	4.48	Disorder in one ring	1484901
		P21/n	100K	8	2	16.1123(7), 7.4939(4), 27.8133(13)	90, 100.085(2), 90	3306.4(3)	3.23		1484900
	Methanol	P21/c	296K	4	1	14.0380(2), 7.6035(1), 16.4203(3)	90, 99.3600(9), 90	1729.33(5)	4.83	Disorder in one ring	1499089
		P21/n	100K	8	2	16.1254(2), 7.4875(1), 27.7652(4)	90, 99.9790(7), 90	3301.62(8)	4.91		1499090
	Propanol	P21/c	296K	4	1	14.0260(15), 7.6060(9), 16.4205(17)	90, 99.392(6), 90	1728.3(3)	4.85	Disorder in one ring	1499140
		P21/n	100K	8	2	16.1209(2), 7.4923(1), 27.7796(4)	90, 100.0186(7), 90	3304.13(8)	3.80		1499141
COBALT	Acetone	P21/c	296K	4	1	13.8878(3), 7.4687(1), 16.2131(3)	90, 98.4340(11), 90	1663.50(5)	3.64		1499339
		P21/c	100K	4	1	13.620(1), 7.3726(5), 16.0138(12)	90, 98.564(3), 90	1590.1(2)	3.00		1499246
	Acetonitrile	P21/c	296K	4	1	13.8960(12), 7.4756(7), 16.2007(13)	90, 98.477(5), 90	1664.6(3)	3.52		1499247
		P21/c	100K	4	1	13.6151(3), 7.3721(2) c 16.0274(3)	90, 98.5510(11), 90	1590.82(6)	2.81		1484902
	Ethyl Acetate	P21/c	296K	4	1	13.8825(5), 7.4673(3), 16.2076(5)	90, 98.4190(17), 90	1662.0(1)	3.58		1499248
		P21/c	100K	4	1	13.61440(15), 7.37010(8), 16.02950(18)	90, 98.5760(5), 90	1590.41	2.50		1499759
	Hexane Benzene	P21/c	296K	4	1	13.8885(5), 7.4705(2), 16.2126(5)	90, 98.410(2), 90	1664.03(9)	3.53		1499245
		P21/c	100K	4	1	13.6215(2), 7.3678(1), 16.0327(2)	90, 98.5430(7), 90	1591.2(4)	2.76		1499249
	Methanol	P21/c	296K	4	1	13.8866(4), 7.4733(2), 16.2046(5)	90, 98.4370(16), 90	1663.49(8)	3.75		1499250
		P21/c	100K	4	1	13.6180(2), 7.3703(1), 16.0307(2)	90, 98.5700(7), 90	1591.02(4)	3.39		1499305
	2,4 -Pentanedione	P21/c	296K	4	1	13.8925(4), 7.4668(2), 16.2131(4)	90, 98.4270(14), 90	1663.67(8)	3.43		1500098
		P21/c	100K	4	1	13.640(6), 7.372(4), 16.031(6)	90, 98.622(11), 90	1593.7(13)	2.68		1500078
	Propanol	P21/c	296K	4	1	13.8939(4), 7.4706(2), 16.2056(4)	90, 98.4510(17), 90	1663.81(8)	3.59		1499252
		P21/c	100K	4	1	13.6221(2), 7.3704(1), 16.0348(2)	90, 98.581(1), 90	1591.88(4)	2.52		1499306
	Water	P21/c	296K	4	1	13.8857(3), 7.4694(2), 16.2062(3)	90, 98.4290(13), 90	1662.72(7)	3.57		1499307
		P21/c	100K	4	1	13.6061(4), 7.3761(2), 16.0320(5)	90, 98.551(1), 90	1591.09(8)	3.35		1499253

CHROMIUM	Acetone	P21/c	296K	4	1	14.015(1), 7.5530(5), 16.370(1)	90, 99.024(3), 90	1711.5(2)	3.40	Disorder in one ring	1499575
		P21/c	100K	4	1	13.7598(6), 7.4551(3), 16.1499(7)	90, 99.297(2), 90	1634.91	2.70	Disorder in one ring	1484903
	Acetonitrile	P21/c	296K	4	1	14.021(6), 7.597(3), 16.350(7)	90, 98.20(2), 90	1723.7(12)	4.26	Disorder in one ring	1499576
		P21/c	100K	4	1	13.7552(6), 7.4501(3), 16.1497(6)	90, 99.337(2), 90	1633.06(11)	4.18	Disorder in one ring	1499577
	Cyclohexane	P21/c	296K	4	1	14.0221(5), 7.5489(3), 16.3758(5)	90, 98.999(2), 90	1712.07(11)	4.82	Disorder in one ring	1499578
		P21/c	100K	4	1	13.7549(2), 7.4467(1), 16.1658(2)	90, 99.2740(9), 90	1634.20(4)	3.37	Disorder in one ring	1499594
	DMF	P21/c	296K	4	1	14.049(3), 7.5468(15), 16.333(3)	90, 99.046(12), 90	1710.1(6)	3.96	Disorder in one ring	1505750
		P21/c	100K	4	1	13.7578(4), 7.4500(2), 16.1554(5)	90, 99.267(2), 90	1634.25(8)	2.75	Disorder in one ring	1505807
	Ethanol	P21/c	296K	4	1	14.0141(3), 7.5484(2), 16.3643(4)	90, 99.0280(12), 90	1709.64(7)	3.64	Disorder in one ring	1500093
		P21/c	100K	4	1	13.7595(2), 7.4479(1), 16.1589(3)	90, 99.332(1), 90	1634.04(4)	3.41	Disorder in one ring	1500094
	Ethyl Acetate	P21/c	296K	4	1	14.0166(3), 7.5493(2), 16.3633(4)	90, 98.9930(11), 90	1710.21(7)	3.43	Disorder in one ring	1500095
		P21/c	100K	4	1	13.7536(3), 7.4498(1), 16.1605(3)	90, 99.2710(9), 90	1634.20(5)	2.77	Disorder in one ring	1500097
	Heptane	P21/c	296K	4	1	14.0381(13), 7.5579(8), 16.3445(15)	90, 99.079(4), 90	1712.4(3)	3.50	Disorder in one ring	1500052
		P21/c	100K	4	1	13.756(3), 7.449(2), 16.157(3)	90, 99.28(3), 90	1633.9(7)	2.99	Disorder in one ring	1505812
	Hexane/Benzene	P21/c	296K	4	1	14.0192(3), 7.5500(2), 16.3673(4)	90, 98.988(1), 90	1711.12	3.50	Disorder in one ring	1505813
		P21/c	100K	4	1	13.766(3), 7.455(2), 16.168(3)	90, 99.29(3), 90	1637.4(7)	2.88	Disorder in one ring	1505751
	Propanol	P21/c	296K	4	1	14.0138(3), 7.5525(2), 16.3645(3)	90, 99.0210(11), 90	1710.58(7)	3.93	Disorder in one ring	1499978
		P21/c	100K	4	1	13.7576(3), 7.4492(1), 16.1602(3)	90, 99.2970(7), 90	1634.39(5)	2.66	Disorder in one ring	1499977
	Toluene	P21/c	296K	4	1	14.013(2), 7.5385(11), 16.411(2)	90, 99.031(6), 90	1712.1(4)	3.39	Disorder in one ring	1499933
		P21/c	100K	4	1	13.7573(6), 7.4503(3), 16.1631(6)	90, 99.269(2), 90	1635.02(11)	4.37	Disorder in one ring	1499976
	Water	P21/c	296K	4	1	14.0107(8), 7.5506(4), 16.365(1)	90, 99.046(3), 90	1709.75	3.80	Disorder in one ring	1499975
		P21/c	100K	4	1	13.7565(3), 7.4512(2), 16.1564(3)	90, 99.288(1), 90	1634.36(6)	3.27	Disorder in one ring	1499932
IRON	Acetone	Pbca	296K	8	1	15.4554(6), 13.5928(5), 16.5786(7)	90, 90, 90	3482.9(2)	4.79		1499398
		Pbca	100K	8	1	15.1988(4), 13.3944(3), 16.3600(4)	90, 90, 90	3330.55(14)	2.44		1499399
	Acetonitrile	Pbca	296K	8	1	15.4665(12), 13.5815(11), 16.5724(14)	90, 90, 90	3481.2(5)	3.36		1499400
		Pbca	100K	8	1	15.1909(6), 13.3879(6), 16.3724(7)	90, 90, 90	3329.7(2)	2.60		1499401
	Benzene	Pbca	296K	8	1	15.4675(9), 13.599(1), 16.5692(11)	90, 90, 90	3485.2(4)	3.36		1499402
		Pbca	100K	8	1	15.1907(12), 13.3947(11), 16.3585(13)	90, 90, 90	3328.5(5)	2.82		1499403
	DMF	Pbca	296K	8	1	15.4576(8), 13.5775(7), 16.5713(9)	90, 90, 90	3477.9(3)	5.26		1499419
		Pbca	100K	8	1	15.1910(2), 13.3889(2), 16.3595(2)	90, 90, 90	3327.37(8)	2.55		1499420
	Diethyl Ether	Pbca	296K	8	1	15.473(3), 13.593(3), 16.590(3)	90, 90, 90	3489.3(11)	3.46		1499421
		Pbca	100K	8	1	15.1898(3), 13.3897(2), 16.3685(3)	90, 90, 90	3329.1(1)	2.55		1499479
	Ethyl Acetate	Pbca	296K	8	1	15.449(3), 13.599(3), 16.611(4)	90, 90, 90	3489.6(12)	3.35		1499422
		Pbca	100K	8	1	15.1941(9), 13.3852(8), 16.356(1)	90, 90, 90	3326.3(3)	2.47		1499480
	Methanol	Pbca	296K	8	1	15.4724(3), 13.5955(3), 16.5688(4)	90, 90, 90	3485.33(13)	4.07		1499517
		Pbca	100K	8	1	15.1858(2), 13.3898(2), 16.3641(2)	90, 90, 90	3327.39(8)	2.45		1484904
	Propanol	Pbca	296K	8	1	15.4562(9), 13.5896(8), 16.5723(9)	90, 90, 90	3480.9(3)	3.65		1499518
		Pbca	100K	8	1	15.1881(2), 13.3876(2), 16.3685(3)	90, 90, 90	3328.24(9)	2.88		1499519
	Water	Pbca	296K	8	1	15.4609(6), 13.5828(6), 16.5744(8)	90, 90, 90	3480.7(3)	3.82		1499520
		Pbca	100K	8	1	15.1958(4), 13.3781(4), 16.3679(5)	90, 90, 90	3327.45(17)	2.70		1488515

VANADIUM	Methanol	Pbca	296K	8	1	15.4649(19), 13.5395(16), 16.679(2)	90, 90, 90	3492.3(7)	4.37	Air sensitive	1499048
		Pbca	100K	8	1	15.1626(3), 13.3781(3), 16.3676(4)	90, 90, 90	3320.11	2.53	Air sensitive	1484905
	THF	P21/c	296K	4	1	14.1490(11), 7.5578(6), 16.5077(13)	90, 99.284(4), 90	1742.13	5.83	Air sensitive, disorder in one ring	1484907
		P21/c	100K	8	2	27.7770(9), 7.4670(2), 16.3073(5)	90, 99.660(2), 90	3334.35	4.07	Air sensitive	1484906
	Toluene	P21/c	296K	4	1	14.113(3), 7.5769(18), 16.396(3)	90, 99.486(11), 90	1729.4(7)	4.85	Air sensitive, disorder in one ring	1499049
		P21/c	100K	4	1	13.9049(7), 7.4781(4), 16.1429(7)	90, 99.963(2), 90	1653.26(14)	3.40	Disorder in one ring	1499050
TITANIUM	DCM	Pbca	296K	8	1	15.547(2), 13.4456(19), 16.795(2)	90, 90, 90	3510.7(9)	3.83	Air sensitive	1498984
		Pbca	100K	8	1	15.2506(3), 13.2713(2), 16.5882(3)	90, 90, 90	3357.37	2.70	Air sensitive	1484908
	2,4 -Pentanedione	P21/n	296K	4	1	8.1295(3), 13.1030(6), 16.4078(7)	90, 90.593(2), 90	1747.68(13)	3.19	Air sensitive	1498985
		P21/n	100K	4	1	8.0136(1), 13.0078(2), 16.0010(2)	90, 90.79(6), 90	1667.77	2.43	Air sensitive	1484909
	Toluene	P21/c	296K	4	1	14.1775(5), 7.5614(3), 16.5275(6)	90, 99.452(2), 90	1747.72(11)	4.91	Air sensitive	1498986
		P21/c	100K	4	1	13.901(1), 7.4686(5), 16.3360(11)	90, 99.843(4), 90	1671.0(2)	4.41	Air sensitive, disorder in one ring	1498987

* CCDC numbers, REFCODES will be available after paper has been accepted